What makes the simple and crucial lipids lysophosphatidic acid and phosphatidic acid so special?

Wat maakt de simpele en essentiële lipiden lysofosfatide zuur en fosfatide zuur zo bijzonder?

(met een samenvatting in het Nederlands)

Proefschrift

ter verkrijging van de graad van doctor
aan de Universiteit Utrecht
op gezag van de rector magnificus, prof. dr. W.H. Gispen,
ingevolge het besluit van het college voor promoties
in het openbaar te verdedigen op
woensdag 30 augustus 2006 te 12.45 uur

door

Edgar Eduard Kooijman

geboren op 19 januari 1974 te Nieuwegein

Promotor: Prof. Dr. B. de Kruijff

Co-promotor: Dr. K.N.J. Burger

Het in dit proefschrift beschreven onderzoek werd mogelijk gemaakt met financiële steun van de Nederlandse organisatie voor Wetenschappelijk Onderzoek (NWO), gebied Aard en Levens Wetenschappen (ALW), en de stichting Fundamenteel Onderzoek der Materie (FOM), via het fysische biologie programma.

Het drukken van dit proefschrift werd mogelijk gemaakt met financiële steun van Mrs. Jessie Brown (Beavercreek, USA) en Dhr. Kees Kooijman (de Glind, Nederland).

aan Deña, Arijana
en Aron

Beoordelings commissie:

Prof. Dr. S. McLaughlin (Department of Physiology and Biophysics Stony Brook State University of New York, New York, USA)
Prof. Dr. W.H. Moolenaar (Universiteit van Leiden Medical Center en het Nederlands Kanker Instituut)
Prof. Dr. G. van Meer (Membraan Enzymologie, Universiteit Utrecht)
Prof. Dr. P. Gros (Kristal en Structuur Chemie, Universiteit Utrecht)
Prof. Dr. J.A. Killian Biochemie van Membranen, universiteit Utrecht)

Paranimfen:

Els van den Brink – van der Laan
Edith Hendriks – Kooijman

Omslag: AV-dienst faculteit Scheikunde, Universiteit Utrecht
Drukker: Febodruk b.v., Enschede

ISBN-10: 90-393-4296-2
ISBN-13: 978-90-393-4296-1

Contents

Abbreviations

ARF	ADP-ribosylation factor
BARS	brefeldin A ribosylated substrate
CL	cardiolipin
CS	chemical shift
CSA	chemical shift anisotropy
CtBP	C-terminal binding protein
DAG	diacylglycerol
DAGK	diacylglycerol kinase
dehydroxy-LPA	1-oleoyl-3-(phosphoryl)propanediol
DEPE	dielaidoylphosphatidylethanolamine
DOPA	dioleoylphsophatidic acid
DOPE	dioleoylphosphatidylethanolamine
DOPS	dioleoylphosphatidylserine
δ	chemical shift
H_{II}	inverted hexagonal
LPA	lysophosphatidic acid
LPAAT	LPA acyl transferase
LPC	lysophosphatidylcholine
MAS	magic angle spinning
NMR	nuclear magnetic resonance
PA	phosphatidic acid
PAP	phosphatidic acid phosphatase
PC	phosphatidylcholine
PE	phosphatidylethanolamine
PI	phosphatidylinositol
PI(Px)	phosphatidylinositol(phosphates)
PL	phospholipid
PS	phosphatidylserine
PLA	phospholipase A
PLC	phospholipase C
PLD	phospholipase D
R_{0p}	spontaneous radius of curvature
TC	transport carrier
T_H	lamellar to H_{II} phase transition temperature
type I lipids	micelle-forming lipids (positive, *convex*, curvature)
type II lipid	lipids capable of forming inverted no-bilayer lipid structures (negative, *concave*, curvature)

CHAPTER 1

Introduction

Biological membranes are dynamic structures composed of proteins and lipids

Biological membranes enclose cells, and their main function is to serve as a barrier for molecules dissolved in the aqueous phase. They therefore protect the cell from its environment and at the same time prevent the cellular content from diffusing into the surroundings. Biomembranes are thus essential for the vitality of a cell.

A biological membrane is made up of fatty molecules, lipids, that form a fluid lipid bilayer which contains two distinct classes of membrane associated proteins. One class consists of proteins that completely span the lipid bilayer and these are called trans-(or intrinsic) membrane proteins, while the second class consists of proteins that are more loosely associated with the lipid bilayer, the so-called peripheral membrane proteins (*1*). Eukaryotic cells are surrounded by a single limiting membrane, the plasma membrane (PM), and contain highly specialized intracellular compartments (organelles) that are also surrounded by a biological membrane (two in the case of the nucleus, mitochondria and chloroplasts). These organelles carry out distinct and specific functions. The nucleus, for example, contains DNA, which encodes for most of the proteins synthesized in the cell. Another organelle in mammalian cells that contains a small fraction of cellular DNA is the mitochondrion; mitochondria are involved in such processes as ATP synthesis and apoptosis (*2*). Other organelles (schematically shown in Figure 1) such as the endoplasmic reticulum (ER), the Golgi, and the endosomal/lysosomal compartments house functions such as, protein and lipid synthesis and sorting (ER), glycosylation (Golgi), and receptor recycling (endosomes). The ER, Golgi and PM make up what is called the secretory pathway (Figure 1).

These different organelles do not stand-alone but are in constant communication through the intracellular transport of proteins, lipids, and other bioactive molecules. One example of organelle communication is the exchange of membrane bound transport carriers (TC's). At any point in time these TCs are busy picking up specific lipid and protein cargo for delivery elsewhere in the cell. For example, transmembrane proteins and most membrane lipids, destined for the PM, are synthesized in the ER and thus need to be transported, usually along the secretory pathway (see Figure 1), to the PM (*2*). These TCs appear to be either small (spherical) vesicles or, more often, large pleiomorphic structures. In either case, membrane transport requires two specific membrane events i.e. the fission of a TC from a donor membrane and the subsequent fusion of the TC with an acceptor membrane (see Figure 2). During fission, the neck region of the TC constricts, the inner leaflets of the bilayer merge, and eventually the neck is destabilized leading to the release of the TC (see Figure 2, also see (*3*)). Membrane fusion is a related process, however here the two outer leaflets of apposing membranes are brought into close contact, leading to the initial merger of these outer leaflets and the formation of a hemi-fusion intermediate (*4-6*). From this hemi-fusion intermediate a pore is formed, which usually expands resulting in a complete merger of the TC with the acceptor membrane (see Figure 2). Membrane

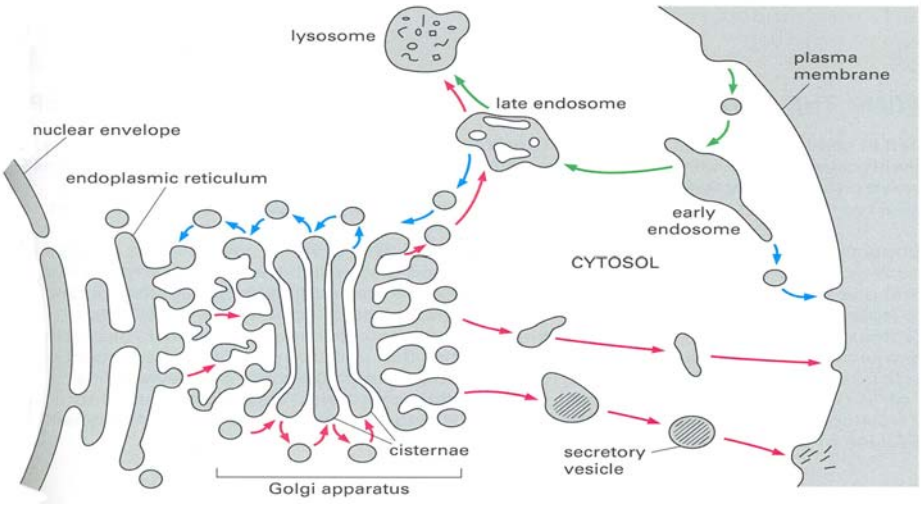

Figure 1: Schematic overview of the compartmentalization of a eukaryotic cell. Shown in this figure are the nuclear membrane, the endosomal/lysosomal compartments, and the secretory pathway. The secretory pathway consists of the endoplasmic reticulum ER, Golgi and plasma membrane. The figure is taken from (*2*).

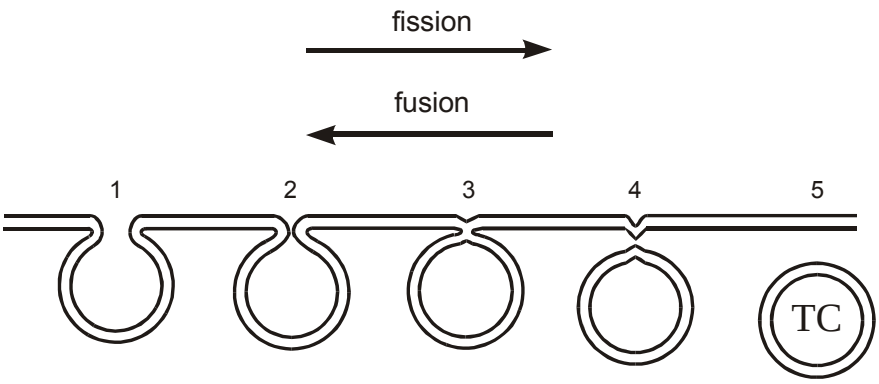

Figure 2: Formation and pinching off of a transport carrier from a donor membrane (1-5) and subsequent fusion of the transport carrier to an acceptor membrane (5-1) involve similar stages organized in opposite order. During fission a bud is formed from the donor membrane (1), followed by the constriction of the neck region (2), which may lead to the fusion of the inner monolayers and formation of a hemi-fission intermediate (3). Scission of the neck takes place in (4), leading to the release of the TC (5). In fusion, this process is reversed and the outer leaflets of the membranes come into a localized contact (4), leading to the merger of the outer monolayers and formation of the hemi-fusion intermediate (3). After opening of the fusion pore (2), the TC may then completely merge with the accepting membrane. For convenience a spherical vesicle is shown.

fission and fusion are energetically unfavorable processes, do not occur spontaneously inside cells, and are highly regulated in time and space. They are therefore under the strict control of (membrane) proteins. Membrane lipids are also crucial to these processes, since it is the lipid bilayer that eventually undergoes the fission and fusion process. However, aside from this "passive" role, specific membrane lipids are known to play additional roles (*7-11*). These membrane lipids may either bind (simply recruit or activate/inactivate) specific proteins required for fission and fusion or alternatively change the biophysical properties of the membrane, such as its curvature, and thereby facilitate fission or fusion processes (*6*).

The aim of the work described in this thesis was to improve our understanding of the molecular processes that underlie membrane fission. The major focus has been on two membrane lipids, namely phosphatidic acid (PA) and the related lipid lysophosphatidic acid (LPA), which have been proposed to play important roles in the regulation of membrane fission. Before discussing LPA and PA in more detail, membrane lipids will be introduced more generally below.

Membrane lipids are versatile components of biomembranes

Membrane lipids are molecules that contain a hydrophobic (apolar) and hydrophilic (polar) part and this amphiphilic character is the main reason why several lipids extracted from biological membranes self-assemble in a fluid bilayer (called the liquid crystalline or L_α phase) upon hydration. Membrane lipids are a diverse group of molecules, and a single biological membrane can contain well over a 100 different types of lipids (*1*). The reason for this diversity is not yet fully understood, but because this diversity is not needed to maintain a simple barrier function membrane lipids must have additional roles (*12*). For example, the interaction between the hydrophilic headgroups of certain membrane lipids with proteins has been suggested to be crucial for the proper folding, integration and/or translocation of polypeptide chains at the membrane/water interface (*13-15*). Membrane lipids can also function as co-factors, where in larger multi-protein complexes they may bind between α-helices of adjacent polypeptide chains and play an important role in the structural integrity of these complexes (*16-18*). Additionally, packing of membrane lipids between α-helices may function as a wedge keeping them apart and thus affecting protein function (*19*). Alternatively, membrane lipids may affect the activity of trans- and peripheral membrane proteins by virtue of their molecular shape, which affects the physical properties (such as lateral tension and curvature) of the membrane (*20*). Still other membrane lipids carry out special signaling functions in the cell (*21, 22*). These signaling lipids result from the controlled breakdown of other membrane lipids, and are present at only minute amounts. They can recruit, activate and/or inactivate numerous proteins and thereby regulate many cellular processes (*21-23*). Signaling lipids can also be secreted or formed extracellularly where they can activate

plasma membrane receptors and trigger numerous intracellular signaling cascades, controlling for example cell growth and differentiation (*24-27*). Clearly, membrane lipids are versatile components of biomembranes with distinct and unique functions.

Membrane lipids may be subdivided into three main classes, namely the glycerol based lipids, such as phosphatidylcholine (PC), sphingolipids, such as sphingomyelin (SM), and the sterols, of which cholesterol is, perhaps, the best-known example (*1*). Phosphatidic acid and lysophosphatidic acid (see Figure 3 B and A respectively) belong to the former class, the glycerol based membrane lipids, which make up a large percentage (>70 %, see (*28*)) of the membrane lipids found in mammalian cells. The glycero-(phospho-)lipids (Figure 3) are therefore of crucial importance to a cell and are discussed in more detail below.

PA and LPA are among the simplest of the glycero-(phospho-)lipids

The glycero-(phospho-)lipids contain a glycerol "backbone" with typically two of the hydroxyl groups esterified to long chain fatty acids, which are usually located at the *sn*-1 and -2 positions in eukaryotes (Figure 3 B). When only one fatty acid is present, as is found in a small (< 1%) fraction of glycero-(phospho-)lipids in biological membranes, the lipid is referred to as a lyso-lipid (Figure 3 A). The fatty acids esterified to the glycerol backbone show enormous diversity, but some general trends can be identified. They are often long (14 carbons or longer) and can carry one or more (cis) double bonds. In mammalian cells the fatty acid esterified to the *sn*-1 position is usually saturated, whereas the fatty acid at the *sn*-2 position is usually unsaturated. Occasionally, one of the fatty acids (at the *sn*-1 position) is attached via a vinyl ether linkage, instead of an ester bond, these glycero-(phospho-)lipids are called plasmalogens.

In the case of glycerophospholipids (PLs) the third hydroxyl of the glycerol backbone is esterified to a phosphate, which in turn can be esterified to a base (Figure 3), forming a phosphodiester. Many different types of phosphate containing headgroup exist, but the most common of these, found in mammalian cells, are phosphocholine, phosphoethanolamine, phosphoserine, and (poly)phosphoinositol (Figure 3). Phosphatidic acid (Figure 3 B), containing just a phosphate is unique among the PLs in that its headgroup is attached to the glycerol backbone as a phosphomonoester. An example of a glycerol-based lipid that does not contain a phosphate is diacylglycerol (DAG, see Figure 3 C). The lipid headgroups differ in size, charge and ability to form hydrogen bonds. The most abundant class of glycerophospholipids carries a net neutral charge at physiologically relevant pH (~5<pH<~8), i.e. they are zwitterionic, namely phosphatidylcholine (PC) and phosphatidylethanolamine (PE). The second most abundant group are the negatively charged glycerophospholipids, phosphatidylserine (PS), phosphatidylinositol (phosphates; PI(P_x)), and

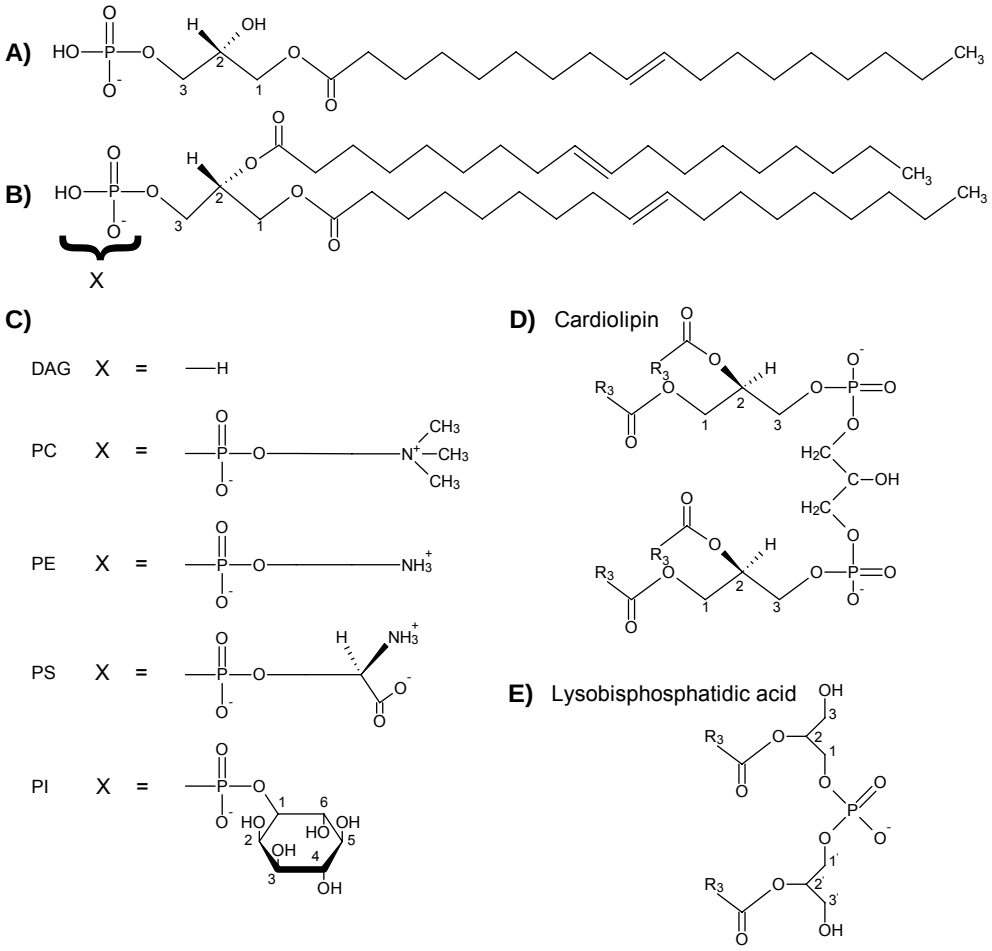

Figure 3: Molecular structures of membrane glycero(phospho)lipids. The structure of 1-oleoyl-LPA is shown in (A), followed by the structure of di-oleoyl-PA in (B). In (C) the headgroups of other glycerophospholipids most relevant to this thesis are shown together with the name of the corresponding diacyl-lipid; DAG, diacylglycerol; PA, phosphatidic acid; PC, phosphatidylcholine; PE, phosphatidylethanolamine; PS, phosphatidylserine; PI, phosphatidylinosition. In (D), and (E) the structures of cardiolipin and lysobisphosphatidic acid are shown, R_3 denotes an acylchain.

phosphatidic acid (PA). Diacylglycerol is uncharged and only found in small amounts in biological membranes.

Two less common PL's that are nonetheless present at high concentrations in certain organelles of mammalian cells are cardiolipin (CL) and lysobisphosphatidic acid (LBPA, see Figure 3 C and D). Cardiolipin is exclusively localized to the mitochondria where it is an important lipid of the inner membrane with a role in the respiratory functions of the mitochondrion (*29-31*). LBPA is only found in late

endosomes and lysosomes, and appears to regulate the transport of lipids and proteins through the endosomal-lysosomal system (*32-39*).

Structurally, LPA and PA are thus the simplest of the glycerol based PL's present in a cell (see Figure 3). However, they are crucial to the survival of a cell despite being present in only small amounts (1-4 %, in living cells). One reason is that they are key intermediates in the de novo biosynthesis of all other glycero-(phospho-)lipids, which make up a large percentage of lipids in mammalian cells, as well as of triglycerides which are important energy stores (*28, 40, 41*). Another important reason is that LPA and PA appear to play a key regulatory role in many vital intracellular processes.

LPA and PA are formed via multiple biosynthetic pathways

The de novo synthesis of LPA and PA can occur via two different acylation pathways (Figure 4). The first and main synthesis route, present in both pro- and eukaryotes, is the glycerol 3-phosphate (Gro3P) pathway. Gro3P is acylated by a glycerol 3-phosphate acyl transferase specific for either the *sn*-1 or 2 position to form LPA (*42-44*). The 2nd pathway to LPA formation, present only in yeast and mammals, involves the acylation of dihydroxyacetone phosphate (DHAP), via DHAP acyltransferase (*45*) and 1-acyl-DHAP reductase (*46*). LPA can be further acylated by a LPA acyltransferase (LPAAT) specific for the *sn*-1 or 2 position to form PA (*47*). This PA is the major substrate for the de novo synthesis of all other glycero-(phospho-)lipids and triacylglycerols (*41*). The enzymes required for the de novo synthesis of LPA and PA localize to the ER, with some minor pools present in other intracellular compartments, such as the mitochondria and peroxisomes in mammalian cells, and lipid droplets in yeast (*41*).

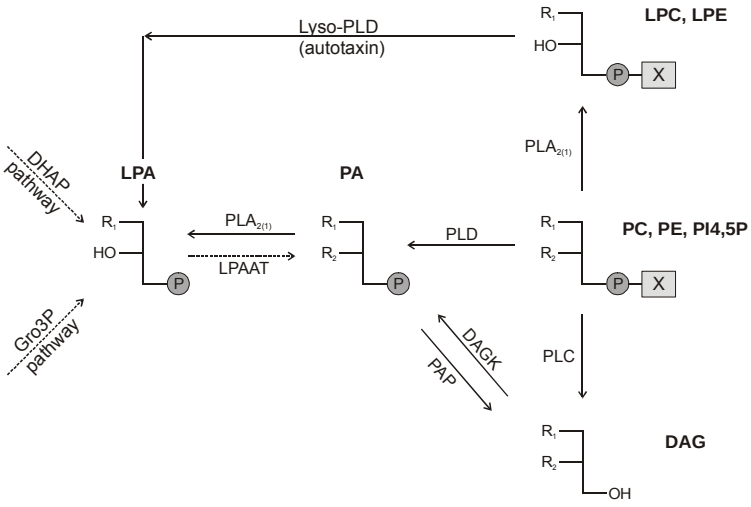

Figure 4: Biosynthetic pathways for the formation of LPA and PA. The *de novo* synthesis routes to the formation of (L)PA are shown by dashed arrows. Solid arrows represent those synthesis routes most often involved in signaling processes. X represents diverse lipid headgroups, as shown in Figure 3. However, PLD enzymes preferentially use PC and PE as substrates, whereas PLC is often specific for PI4,5P.

Aside from the de novo biosynthesis of (L)PA there are several additional routes for the formation of LPA and PA in a cell (Figure 4). This (L)PA originates from the breakdown of other glycero-(phospho-)lipids such as PC, and forms a unique pool of (L)PA, which is involved in all of the additional roles that LPA and PA play in a cell. LPA can be formed via at least two additional routes, namely via the sequential action of phospholipase A_1 or A_2 ($PLA_{1/2}$) and lysoPLD (recently identified as the cytokine autotaxin, see (*48, 49*)), which acts on extracellular lysophospholipids such as LPC and LPE, or via the action of PLD and $PLA_{1/2}$ (for recent reviews, see (*50, 51*)). Two distinct signaling pathways generate PA. PA can be formed directly by phospholipase D (PLD) via the hydrolysis of the ester linkage between the primary alcohol and the phosphate of other membrane phospholipids, mainly PC (*21*). Alternatively, PA may be formed by the sequential action of phospholipase C (PLC), which forms DAG, and diacylglycerol kinase (DGK), which forms PA (*21*). Another, distinct (from de novo synthesis) route to PA formation may be via novel LPAATs (*52, 53*). Note that PA formed via either of these pathways may be rapidly dephosphorylated by PA-specific phosphatases (*54*), and that, thus, PA and DAG are often found to be in a dynamic equilibrium.

LPA and PA fulfill diverse (intra)cellular roles

LPA elicits numerous cellular responses in a cell type dependent fashion, such as cellular proliferation and prevention of apoptosis (*55-61*), increase in cell motility (*62*), cytokine and chemokine secretion (*63*), and smooth muscle contraction (*64, 65*). Most of the responses attributable to LPA are initiated by the binding of LPA to specific G protein-coupled receptors (GPCRs) in the plasma membrane of the cell. Four plasma membrane GPCRs specific for LPA have been identified and recently an intracellular receptor specific for LPA has been localized at the nuclear membrane (*26, 66-71*). This last finding shows that LPA is likely to play direct intracellular roles as well.

PA, like LPA, has been implicated in numerous cellular responses as diverse as actin polymerisation (*72*), respiratory burst (*73*), Ca^{2+} signaling (*21, 74*), and the activation of various signaling networks (*75-80*). Unlike LPA however these effects are not mediated by the binding of extracellular PA to GPCRs specific for PA (*74*). Exactly how PA exerts its effects is unclear, but local intracellular production of PA via any of the above-mentioned pathways appears to be responsible for these cellular responses.

A recurring theme in PA signaling is the involvement of PA in membrane trafficking events particularly along the secretory pathway. For example PLD activity and PA synthesis were proposed to be involved in the formation of transport carriers at the Golgi complex (*7, 8, 81, 82*). Also, PLD activity was shown to activate PI4 kinases (*83*), and a recent study showed that PA specifically activates PI4, 5 kinase and thus stimulates the formation of $PI4,5P_2$ (*84*), which is required for exocytosis (*85*). Manifava and coworkers have recently shown that

several proteins involved in vesicle trafficking bind to PA, *in vitro* (*23*). Furthermore, in *in vitro* studies, the conversion of LPA into PA by the putative LPAATs, CtBP3/BARS and the unrelated enzyme endophilin, correlated with fission of Golgi tubules and endocytic vesicles respectively (*52, 53*).

LPA and PA are the simplest phospholipids present in the cell and it is unclear exactly how (L)PA functions in these processes. A key question, addressed in this thesis, is how (L)PA might mediate such effects. One possibility is that LPA and PA themselves are involved, via for example their molecular shape. Another possibility is that (L)PA recruit proteins through their negatively charged headgroup that then carry out the required functions. Membrane transport involves bending of a flat membrane into highly curved intermediates as shown in Figure 2, and lipids with a molecular shape fitting these high regions of curvature may potentially facilitate membrane bending. Furthermore, the negative charge of (L)PA is likely to be important for (L)PA/protein interactions as well. Thus, detailed knowledge of the molecular shape and ionization properties of PA and LPA is crucial in order to evaluate the potential role of these lipids in membrane dynamics. Before discussing membrane electrostatics and lipid ionization the general concepts of lipid molecular shape and those factors that influence it will be introduced.

Membrane lipids come in different shapes

The effective molecular shape of a lipid and the organization it adopts upon hydration can be conveniently described according to the shape-structure model of lipid polymorphism (Figure 5, (*86*)). Lipids in biomembranes are usually organized in fluid liquid crystalline bilayers (L_α phase), but surprisingly single lipid species often adopt other structures as well, such as micelles or a hexagonal phase (H_{II}, see Figure 5). Lipids that upon isolation and hydration form bilayer structures (e.g. a gel, L_β, or fluid, L_α, phase), such as PC are very common and have an effective headgroup area that is comparable to the area occupied by their hydrocarbon chains, and therefore have an overall cylindrical shape (Figure 5). Lipids with a headgroup area larger than the hydrocarbon area, such as lyso-PC, form a minor group of lipids found in biomembranes, and will self-assemble in convex structures with positive curvature, for example micelles (so called type I lipids, Figure 5). Lipids with a small headgroup area compared to the hydrocarbon area, such as unsaturated-PE's, are much more common than the type I lipids and form concave structures with negative curvature, such as the inverted hexagonal (H_{II}) phase (so called type II lipids, Figure 5). In this phase the lipid headgroups line an aqueous channel of long lipid tubes, which are organized in a hexagonal array.

It is interesting to note that both fission and fusion processes involve highly curved intermediates (see Figure 2), and membrane lipids with a type I or type II shape might be ideally suited to facilitate different steps in these processes (*6, 87*). This hypothesis is supported by model membrane studies where it was shown that

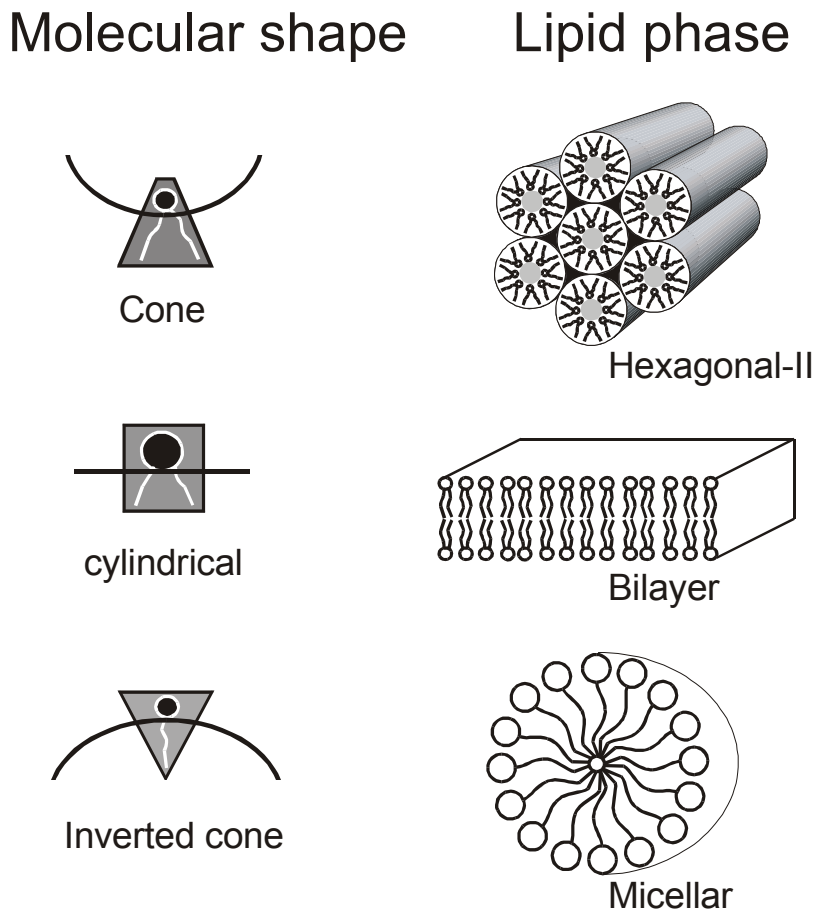

Figure 5: Lipid polymorphism. Lipids with a cone like shape, such as phosphatidylethanolamine, can form negatively curved (concave) structures as the inverted hexagonal phase (top), and lipids with an overall cylindrical shape, such as phosphatidylcholine, form bilayer structures (middle). Finally lipids with an inverted cone shape, such as lyso-phosphatidylcholine, form positively curved (convex) structures as micelles (bottom).

type II lipids such as DAG facilitate fusion, whereas type I lipids inhibit this process (*88, 89*). Furthermore, recent modeling of membrane fission events predicts an opposite dependence on lipid molecular shape than that of membrane fusion (*3*). Also, lipid metabolism, potentially changing the shape of membrane lipids, was shown to be involved in transport carrier formation and or fission (*52, 53, 90, 91*).

The effective molecular shape of a lipid is not only determined by its chemical structure but also depends on intermolecular interactions with neighboring lipids and other molecules, and is modulated by such factors as hydration, temperature,

the presence of mono and divalent cations and pH (*86, 92*). For example, the association of water molecules increases the effective size of a lipid headgroup. At full hydration PC for example has a "hydration shell" of about 25 water molecules, whereas PE has only ~11 (*93*). The headgroup of PC is thus not only structurally larger than that of PE, but this difference is further enhanced by a difference in the relative hydration of the headgroups. Temperature increases the disorder of the acyl-chains and thus increases the area occupied by the acyl-chains, resulting in a more pronounced type II shape. Indeed, PE with a structurally small headgroup undergoes a thermotropic phase transition from a bilayer (cylindrical lipid shape) to a hexagonal H_{II} phase (conical lipid shape) (*94, 95*), depending on the acyl-chain composition, i.e. chain length and degree of unsaturation. Mono- and divalent cations screen the negative charge of the anionic lipids and thus have the tendency to decrease the effective area occupied by a negatively charged headgroup, and thus induce a more pronounced type II shape.

PA and LPA are both anionic phospholipids and their molecular shape but also the interaction with other lipids and proteins is likely to depend on their negative charge. The charge properties of PA and LPA can thus be expected to be crucial for their function in biological membranes, such as fission or fusion. Before discussing the methods used in this thesis to determine the molecular shape and ionization of LPA and PA, membrane electrostatics and in particular the factors influencing membrane lipid ionization will be introduced below.

Lipid charge is affected by bilayer organization and local lipid environment

Biomembranes are generally negatively charged, as is illustrated by the inner leaflet of the PM, which contains well over 30% of anionic phospholipids (*28, 96*), mainly PS and PI in mammalian cells. Negative charge carried by membrane lipids is an important determinant of biomembrane structure and function. It is, for example, well established that negatively charged membranes act as a site of attraction for positively charged (basic) protein domains (*97, 98*). For example, the cytosolic protein myristoylated alanine-rich C-kinase substrate (MARCKS) is recruited to anionic lipid membranes by an unstructured domain containing 13 basic amino acid residues (*99*). Positively charged residues in transmembrane proteins can similarly interact with the negatively charged lipids in the membrane (*100*), and may guide the membrane insertion and orientation of these proteins (*14*). Membrane insertion, orientation and other biophysical aspects of transmembrane protein/lipid bilayer interaction have been probed by the use of synthetic transmembrane α-helical peptides (*101-104*).

Given that membrane charge has important functional implications, what factors influence the charge of membrane lipids in a bilayer? Ionization behavior of lipids is different for a membrane embedded lipid as compared to a lipid free in solution. The reason for this is the interface between the hydrophobic interior and hydrophilic lipid headgroups in a membrane system. The dielectric constant

undergoes an abrupt change from about 80 in bulk water to about 2 for the hydrocarbon region. As a result, a charge (as in PO_4^-, COO^-, and NH_3^+ groups for example) in the interface produces an electrostatic potential in the aqueous phase that is nearly twice that for the same (point) charge free in solution (the so-called mirror effect (*105*)). This electrostatic potential affects the potential and charge of nearby (point) charges in the membrane and adjacent aqueous phase. These effects can be approximated surprisingly well by the classical Gouy-Chapman theory of the diffuse double layer (*106*). The diffuse double layer is composed of the charged lipid headgroups and adjacent counter ions in the aqueous phase that are able to freely diffuse into the bulk solution. A detailed theoretical description is beyond the scope of this general introduction, and the interested reader is referred to the following excellent reviews (*105-107*). However, some main points relevant for this thesis can be derived from this theory and these will be briefly discussed below.

One well known effect is that the surface potential (Ψ) of the membrane is proportional to the surface charge density (σ), and an increase in the negative surface charge thus results in an increase in the negative electrostatic potential of the membrane. In addition, the negative surface potential of a membrane containing acidic lipids is decreased by an increase in the salt concentration (c, ionic strength) of the aqueous phase (Ψ is proportional to $1/\sqrt{c}$) due to adsorption of counter ions in the diffuse double layer. A consequence of the adsorption of positive charges is that the interfacial pH of an anionic membrane will be lower than the bulk pH, since protons will also be attracted by the negative charge of the membrane into the diffuse double layer. Interestingly, changes in ionic conditions at constant bulk pH, for example due to Ca^{2+} fluxes, lead to changes in the surface pH, since cations like Ca^{2+} will displace protons from the interface into the bulk solution thereby decreasing the proton concentration when compared to the situation prior to the increase in ionic strength (*107*). Thus the interfacial pH, and the ionic equilibria that control it greatly influence the charge of membrane lipids.

At physiological pH values ($5<pH<8$) the charge of most PLs will not be affected since their ionization equilibria (pKs) fall outside this pH range. However, the charge of ionizable groups with pK values in the physiological pH range will be affected. Apart from the interfacial pH, the charge of ionizable groups can also be influenced by the formation of hydrogen bonds. Hydrogen atoms (of –OH and –COOH groups for example) that participate in a hydrogen bond will be stabilized against dissociation, i.e. it will take a lower proton concentration (higher interfacial pH) to cause their dissociation. Hydrogen bonds thus result in an increase in the pK of the ionizable group (*108-110*).

Both the molecular shape and charge of (L)PA are likely to be important for their biological functions as described above. Before coming to the scope of this thesis, the methods by which the shape and charge properties of LPA and PA were determined will be discussed below.

Methods

In order to gain insight into the molecular mechanisms underlying the cellular roles of PA and LPA we set out to determine lipid molecular shape, charge, and in the case of PA studied the interaction of PA with membrane interacting peptides. These studies were performed using lipid model membrane systems and biophysical techniques such as NMR and x-ray diffraction, explained in more detail below.

Model lipid membranes form an ideal experimental system

The molecular shape of lipids cannot be determined in complex biological systems such as a native cell membrane. The biological membrane is simply too complex, containing over 100 different types of lipids and trans- and peripheral membrane proteins, and current technologies do not allow one to extract structural information on individual lipids. Therefore simplified systems in the form of model membranes, consisting of one or a few membrane lipids, have to be used. The experiments described in this thesis all employ such model membranes studied at physiologically relevant pH, ion concentrations and temperature. The use of physiological conditions is of crucial importance because the biophysical properties of lipids and their interaction with proteins are very sensitive to such factors as divalent cations and temperature (see e.g. (*111, 112*)).

Model membranes can be investigated using a wide variety of techniques. The main techniques used in this thesis to determine the molecular shape of LPA and PA are (solid state) ^{31}P-NMR and small angle x-ray diffraction. In order to determine the charge of (L)PA and the interaction of PA with membrane interacting peptides we used a special solid state NMR technique, namely magic angle spinning (MAS) ^{31}P-NMR. These three techniques will be discussed briefly below.

Lipid molecular shape can be conveniently determined by ^{31}P-NMR

^{31}P-NMR is a convenient technique to determine the organization of a lipid dispersion. Unlike solution NMR, which yields isotropic spectra, (solid state) ^{31}P-NMR spectra of large multilamellar aggregates (multilamellar vesicles MLV's) are characterized by a large residual chemical shift anisotropy (Figure 6 curve 2). The chemical shift (CS) of the phosphorus nucleus of a PL is determined by the asymmetric distribution of electrons in the electron cloud surrounding the nucleus, which depends on the chemical bond pattern. Different orientations of the phosphate with respect to the external magnetic field result in a different shielding (local magnetic field) of the phosphorus nucleus by the surrounding electrons and hence in a different resonance frequency. Phospholipids in a dry powder will be randomly oriented in the magnetic field and display a ^{31}P-NMR spectrum (see Figure 6, curve 1) that is the sum of the CS of all the individual PLs present in the

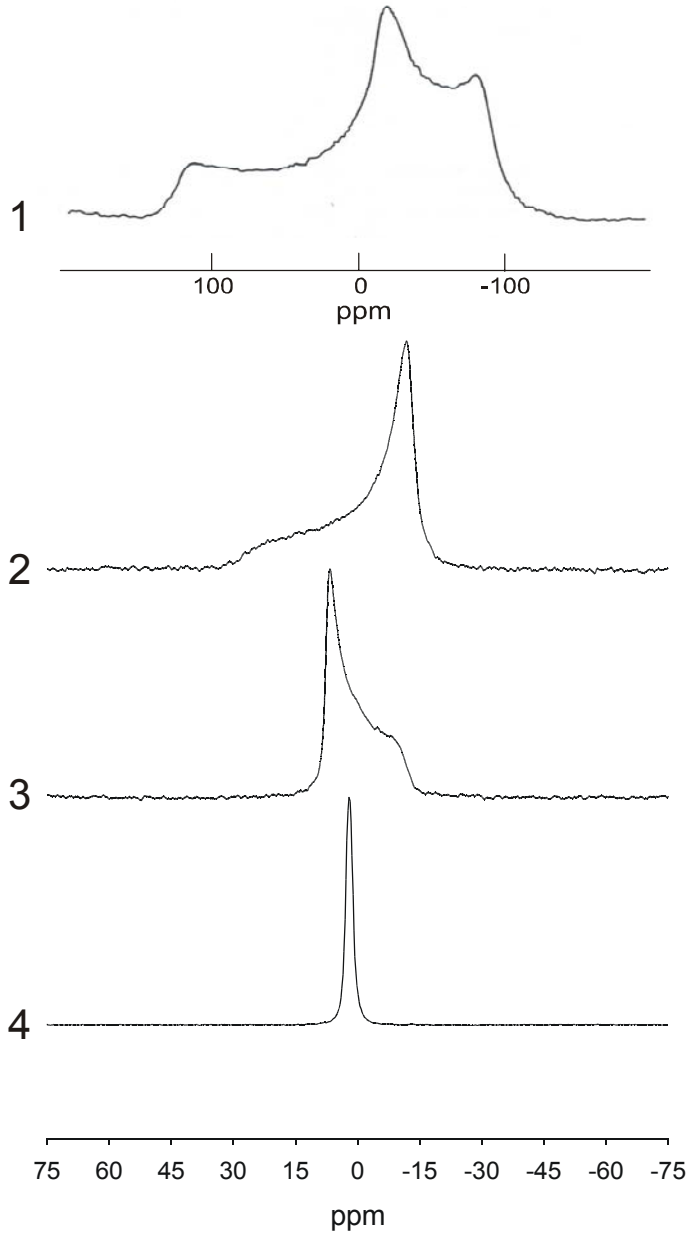

Figure 6: Representative ^{31}P-NMR spectra. Curve 1 is an example of a dry phospholipid powder, in which the lipid phosphate is immobilized. Curve 2 is an example of a phospholipid bilayer in the liquid crystalline phase; here hydrated DEPE at 42°C. Curve 3 shows the ^{31}P-NMR spectrum from the same sample as curve 2 but now at 63°C, where DEPE forms an inverted hexagonal phase. Curve 4 is an example of a lipid dispersion undergoing isotropic averaging; here LPA micelles at room T.

sample. This spectrum has the largest, so-called, chemical shift anisotropy (CSA). The CSA will be partially averaged if the lipids move with respect to the magnetic field, if this motion is fast on the NMR time scale (~100 µs to ~1 ms). This is the case when PL's become hydrated and are able to quickly rotate around their long axis (i.e. around the bilayer normal), and thus reorient with respect to the magnetic field. An example of such a ^{31}P-NMR spectrum is shown in Figure 6, curve 2 for a lipid dispersion in the fluid or L_α phase. A high field peak and low field shoulder characterize the axially symmetric, anisotropic ^{31}P-NMR spectrum of the L_α phase, and is representative for lipids organized in large (multilamellar) vesicles. Additional motional averaging can result in a further reduction of the CSA. This is the case for the hexagonal H_{II} phase, where fast (with respect to the NMR time scale) reorientation of lipids around the hexagonally packed cylinders results in a reduction of the residual CSA by a factor of 2 (Figure 6, curve 3). A high field shoulder and a low field peak characterize the H_{II} spectrum, opposite to that observed for large (multilamellar) vesicles. Further reorientation of the lipids with respect to the magnetic field (such as fast tumbling of vesicles) can result in a nearly complete averaging of the CSA, if this reorientation is fast with respect to the NMR time scale, as is the case for micelles, small unilamellar vesicles and the various cubic phases (Figure 6, curve 4). The spectral shape of the ^{31}P-NMR spectrum can therefore provide a signature of the lipid organization.

The effective molecular shape of a particular lipid can be determined relative to a specific (usually unsaturated) PE species by studying the effect of the lipid on the liquid crystalline L_α to hexagonal H_{II} phase transition temperature of this PE (*113-115*). For example, lipids with a type I shape will stabilize the bilayer phase of the PE matrix reflecting the complementary shapes of type I and type II lipids. Contrary, lipids with a more pronounced type II behavior than the PE matrix destabilize the bilayer phase.

Spontaneous curvature can be determined by small angle x-ray diffraction

A more quantitative description of the effective molecular shape of a lipid is given by the spontaneous (or intrinsic) radius of curvature (R_{0p}, (*116*)). Briefly, R_{0p} is defined in the H_{II} phase as the radius of curvature from the center of the aqueous pore to a plane in the lipid volume (see Figure 7 B), in the case where the lipid monolayer is elastically relaxed (*117, 118*). By definition R_{0p} is negative for type II and positive for type I lipids, whereas bilayer lipids will have a (very) large R_{0p} that can either be positive or negative. R_{0p} can be determined from the measurement of the H_{II} phase dimension, d_{hex}, (see Figure 7 B) and knowledge of such parameters as specific lipid volume and water content in the fully hydrated H_{II} phase (for further experimental details see chapter 3). The spontaneous radius of curvature can also be determined for lipids that do not by themselves adopt a H_{II} phase. Here, R_{0p} is determined from the effect the lipid of interest has on the R_{0p} of a (unsaturated) PE matrix. These lipids will either increase R_{0p} (if they are less negatively curved than the matrix PE) or decrease R_{0p} (are more negatively curved)

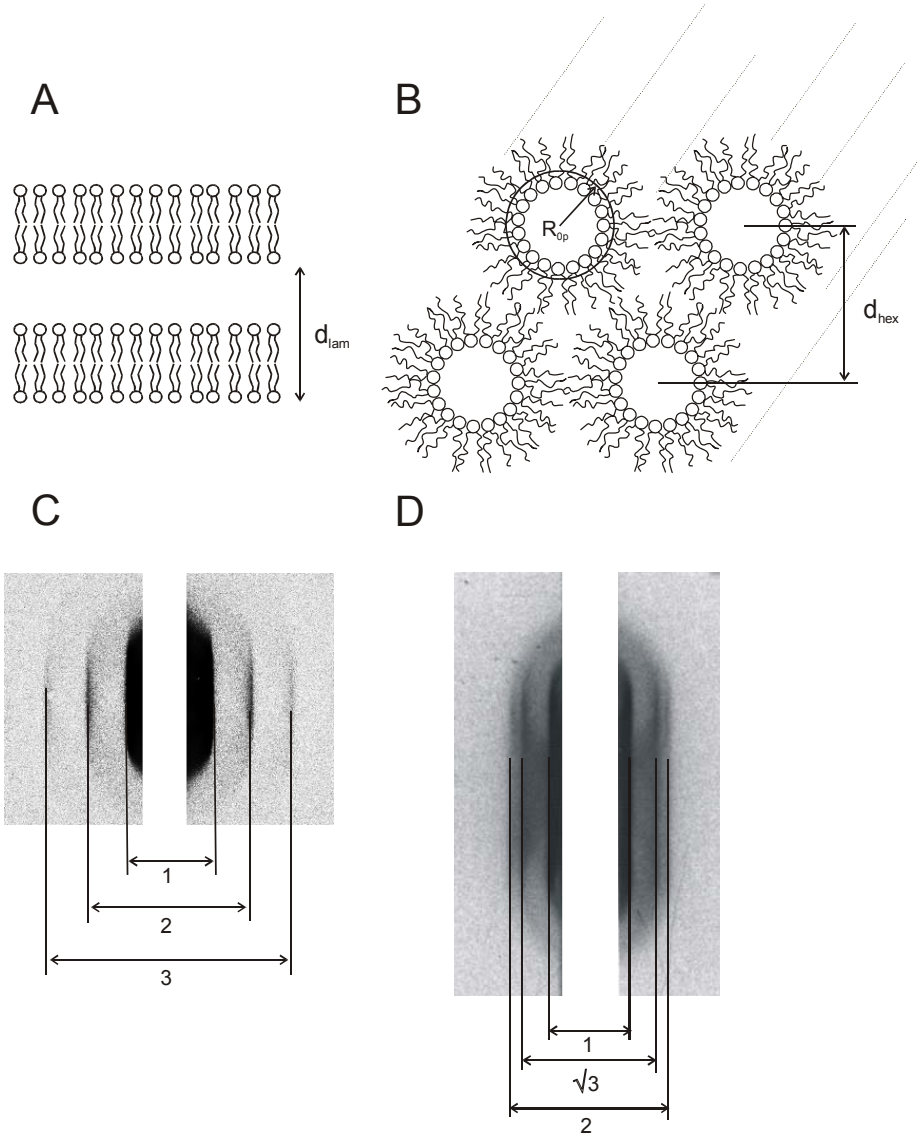

Figure 7: Structure and corresponding x-ray diffraction patterns of a bilayer and H_{II} phase. Sketch of stacked lipid bilayers (A) and corresponding x-ray diffraction pattern (C) of such a multilamellar array of bilayers. The regular, integer, repeat spacing, d_{lam}, is the sum of the bilayer thickness and inter-bilayer distance. In (B) a sketch of the cross section of a hexagonal H_{II} phase is shown, together with the spontaneous curvature R_{0p}, as discussed in the text, and the hexagonal phase repeat distance d_{hex}. The resulting diffraction pattern is shown in (D).

depending on the unsaturated PE used as the matrix. If this effect is linear for increasing concentrations of the lipid of interest then $R_{0p}^{lipid\ X}$ can be determined.

The hexagonal phase dimension(s), d_{hex}, needed to calculate the spontaneous radius of curvature, can be measured by small angle x-ray diffraction (SAXD). SAXD can be used in the case of highly concentrated and particularly well-organized lipid samples, and allows for the unambiguous determination of lipid phase and dimension (i.e. bilayer and H_{II} phase repeat distance, see Figure 7 A and B). Lipids organized in a bilayer configuration yield diffraction patterns with regularly spaced (n = 1, 2, 3, 4, etc.) Bragg peaks as shown in Figure 7 C. The H_{II} phase gives Bragg peak spacings of 1, $\sqrt{3}$, 2, $\sqrt{7}$, 3, $\sqrt{15}$, $\sqrt{17}$, etc., reflecting the hexagonal packing of the lipid tubes (Figure 7 D).

Ionization state of LPA and PA can be measured using MAS-^{31}P-NMR

The pKa's of small concentrations of LPA and PA in a flat, extended, lipid bilayer cannot easily be determined by such techniques as acid-base titration, pH dependent phase transition studies, or surface potential measurements, since these methods are either indirect or hampered by difficulties/uncertainties in data analysis (*106, 107*). However, since the hydroxyls of the phosphomonoester headgroup of (L)PA are located close to the phosphorus nucleus, their ionization will influence the magnetic properties of this nucleus. Changes in the electron distribution, due to (de)protonation of the phosphate, will affect the chemical shielding and thus the chemical shift of the phosphorus nucleus. This chemical shift can be readily determined using magic angle spinning ^{31}P-NMR (*119, 120*). The MAS technique averages orientation dependent magnetic interactions, such as homonuclear and heteronuclear dipolar interactions, and chemical shift anisotropy and yields isotropic (solution type) values of both chemical shifts and spin-spin couplings for the phosphorus nucleus of lipids in a flat lipid bilayer (*119-121*). MAS NMR involves placing the samples at a specific angle (the magic angle, 54.7°) with respect to the magnetic field and fast spinning of the sample (kHz) around its long axis (Figure 8). Under these conditions the scalar multiplication factor describing the orientation dependent interactions ($3\cos^2\theta - 1$) equals zero. At 5 kHz this results in an averaging of the residual CSA of the lipid phosphorus nucleus as is exemplified for an extended lipid bilayer composed of 20 mol % LPA in dioleoyl-PC, in Figure 8. Sample spinning at 5kHz is clearly sufficient to yield isotropic values of the CSA of LPA (minor peak near 0 ppm) and PC (major peak near 0 ppm), similar to the isotropic averaging obtained for lipids in highly curved structures as shown in Figure 6, curve 4.

Scope of this thesis

The main aim of the work described in this thesis is to improve our understanding of the molecular processes that underlie membrane fission, and, more specifically,

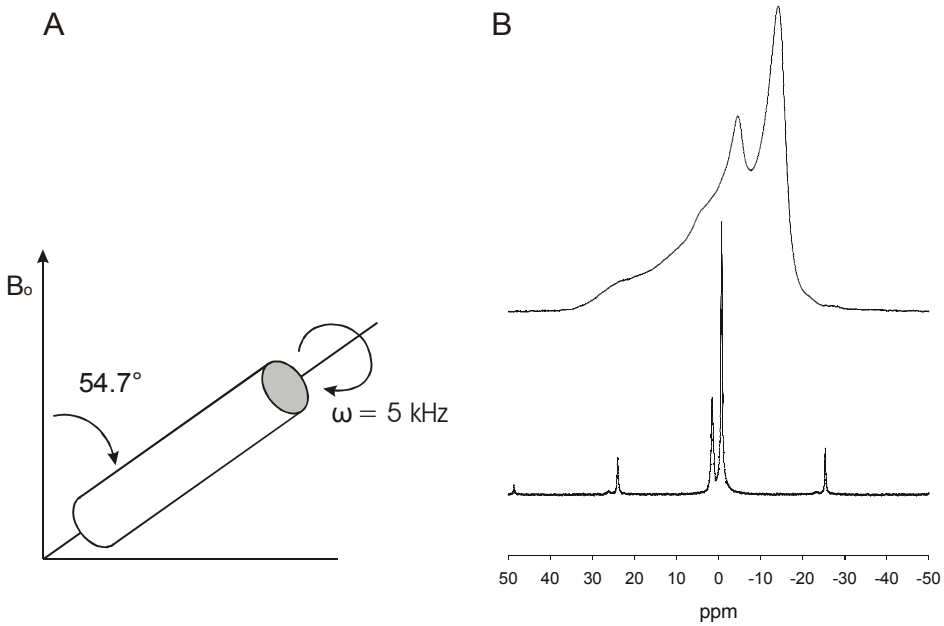

Figure 8: Magic angle spinning ^{31}P-NMR. The experimental set-up of the MAS experiment (A). The MAS rotor is placed at an angle of 54.7° with respect to the magnetic field direction in the laboratory frame. Fast (5kHz) rotation of the sample reduces the large chemical shift anisotropy of the corresponding static spectrum (B, top curve) to the isotropic peaks (B, bottom curve) of the individual lipids making up the liquid crystalline bilayer composed of PC (80 mol%) and LPA (20 mol%).

to explore the role of the phospholipids PA and LPA in the regulation of membrane fission. The role of (L)PA in membrane fission may be either direct or indirect, i.e. (L)PA may directly facilitate membrane bending or (L)PA may recruit and/or activate downstream effector proteins required for membrane fission.

In order to evaluate how PA and LPA may directly affect biomembrane structure, and thus processes such as membrane fission, we used ^{31}P-NMR to estimate the molecular shape of (L)PA, these data are described in chapter 2. This is the first study of the molecular shape of (L)PA at physiologically relevant conditions and sheds important light on the potential role of (L)PA in membrane fission. Chapter 3 describes x-ray diffraction experiments to determine the spontaneous curvature of LPA and PA. These spontaneous curvature measurements provided more quantitative data on the molecular shape of (L)PA, which are essential for the biophysical modeling of processes such as membrane fission and fusion.

Binding of (L)PA to proteins is likely facilitated by the negative charge of the phosphomonoester headgroup, and lipid headgroup charge also affects the molecular shape of (L)PA. Chapter 4 describes MAS-^{31}P-NMR experiments to determine the negative charge of (L)PA in extended membrane systems consisting

of PC and PE. In chapter 5 the interaction of PA with proteins is further explored by determining the effect of basic amino acids in membrane interacting peptides on the negative charge of PA.

Finally in chapter 6 the results are summarized and discussed in light of the recent literature.

References

1. Gennis, R. B. (1989) *Biomembranes: Molecular Structure and Function*, Springer-Verlag, New York.
2. Alberts, B., Bray, D., Lewis, J., Raff, M., Roberts, K., and Watson, J., D. (1994) *Molecular Biology of the Cell*, 3rd ed., Garland Publishing, New York.
3. Kozlovsky, Y., and Kozlov, M. M. (2003) Membrane fission: model for intermediate structures. *Biophys. J. 85*, 85-96.
4. Chernomordik, L. V., Kozlov, M. M., Melikyan, G. B., Abidor, I. G., Markin, V. S., and Chizmadzhev, Y. A. (1985) The shape of lipid molecules and monolayer membrane fusion. *Biochim. Biophys. Acta - Biomembranes 812*, 643.
5. Kozlov, M. M., Leikin, S. L., Chernomordik, L. V., Markin, V. S., and Chizmadzhev, Y. A. (1989) Stalk mechanism of vesicle fusion. Intermixing of aqueous contents. *Eur. Biophys. J. 17*, 121-9.
6. Burger, K. N. J. (2000) Greasing membrane fusion and fission machineries. *Traffic 1*, 605-13.
7. Siddhanta, A., and Shields, D. (1998) Secretory vesicle budding from the trans-Golgi network is mediated by phosphatidic acid levels. *J. Biol. Chem. 273*, 17995-8.
8. Roth, M. G., Bi, K., Ktistakis, N. T., and Yu, S. (1999) Phospholipase D as an effector for ADP-ribosylation factor in the regulation of vesicular traffic. *Chem. Phys. Lipids 98*, 141-52.
9. Cremona, O., and De Camilli, P. (2001) Phosphoinositides in membrane traffic at the synapse. *J. Cell Sci. 114*, 1041-52.
10. Bankaitis, V. A. (2002) Cell biology. Slick recruitment to the Golgi. *Science 295*, 290-1.
11. Baron, C. L., and Malhotra, V. (2002) Role of diacylglycerol in PKD recruitment to the TGN and protein transport to the plasma membrane. *Science 295*, 325-8.
12. Dowhan, W. (1997) Molecular basis for membrane phospholipid diversity: why are there so many lipids? *Annu. Rev. Biochem. 66*, 199-232.
13. de Vrije, T., de Swart, R. L., Dowhan, W., Tommassen, J., and de Kruijff, B. (1988) Phosphatidylglycerol is involved in protein translocation across Escherichia coli inner membranes. *Nature 334*, 173-5.
14. van Klompenburg, W., Nilsson, I., von Heijne, G., and de Kruijff, B. (1997) Anionic phospholipids are determinants of membrane protein topology. *Embo J. 16*, 4261-6.
15. White, S. H., Ladokhin, A. S., Jayasinghe, S., and Hristova, K. (2001) How membranes shape protein structure. *J. Biol. Chem. 276*, 32395-8.
16. Heginbotham, L., Kolmakova-Partensky, L., and Miller, C. (1998) Functional reconstitution of a prokaryotic K+ channel. *J. Gen. Physiol. 111*, 741-9.
17. Zhou, Y., Morais-Cabral, J. H., Kaufman, A., and MacKinnon, R. (2001) Chemistry of ion coordination and hydration revealed by a K+ channel-Fab complex at 2.0 A resolution. *Nature 414*, 43-8.
18. Valiyaveetil, F. I., Zhou, Y., and MacKinnon, R. (2002) Lipids in the structure, folding, and function of the KcsA K+ channel. *Biochemistry 41*, 10771-7.
19. Lee, A. G. (2004) How lipids affect the activities of integral membrane proteins. *Biochim. Biophys. Acta 1666*, 62-87.
20. van den Brink-van der Laan, E., Killian, J. A., and de Kruijff, B. (2004) Nonbilayer lipids affect peripheral and integral membrane proteins via changes in the lateral pressure profile. *Biochim. Biophys. Acta 1666*, 275-88.
21. Munnik, T., Irvine, R. F., and Musgrave, A. (1998) Phospholipid signalling in plants. *Biochim. Biophys. Acta 1389*, 222-72.

22. Cockcroft, S. (2001) Signalling roles of mammalian phospholipase D1 and D2. *Cell Mol. Life Sci. 58*, 1674-87.
23. Manifava, M., Thuring, J. W., Lim, Z. Y., Packman, L., Holmes, A. B., and Ktistakis, N. T. (2001) Differential binding of traffic-related proteins to phosphatidic acid- or phosphatidylinositol (4,5)-bisphosphate-coupled affinity reagents. *J. Biol. Chem. 276*, 8987-94.
24. Moolenaar, W. H. (1999) Bioactive lysophospholipids and their G protein-coupled receptors. *Exp. Cell Res. 253*, 230-8.
25. Pyne, S., and Pyne, N. J. (2000) Sphingosine 1-phosphate signalling in mammalian cells. *Biochem. J. 349*, 385-402.
26. Contos, J. J., Ishii, I., and Chun, J. (2000) Lysophosphatidic acid receptors. *Mol. Pharmacol. 58*, 1188-96.
27. Moolenaar, W. H. (2000) Development of our current understanding of bioactive lysophospholipids. *Ann. N. Y. Acad. Sci. 905*, 1-10.
28. van Meer, G. (1998) Lipids of the Golgi membrane. *Trends Cell Biol. 8*, 29-33.
29. Schlame, M., Rua, D., and Greenberg, M. L. (2000) The biosynthesis and functional role of cardiolipin. *Prog. Lipid Res. 39*, 257-88.
30. Haines, T. H., and Dencher, N. A. (2002) Cardiolipin: a proton trap for oxidative phosphorylation. *FEBS Lett. 528*, 35-9.
31. McMillin, J. B., and Dowhan, W. (2002) Cardiolipin and apoptosis. *Biochim. Biophys. Acta. 1585*, 97-107.
32. Kobayashi, T., Stang, E., Fang, K. S., de Moerloose, P., Parton, R. G., and Gruenberg, J. (1998) A lipid associated with the antiphospholipid syndrome regulates endosome structure and function. *Nature 392*, 193-7.
33. Kobayashi, T., Beuchat, M. H., Lindsay, M., Frias, S., Palmiter, R. D., Sakuraba, H., Parton, R. G., and Gruenberg, J. (1999) Late endosomal membranes rich in lysobisphosphatidic acid regulate cholesterol transport. *Nat. Cell Biol. 1*, 113-8.
34. Galve-de Rochemonteix, B., Kobayashi, T., Rosnoblet, C., Lindsay, M., Parton, R. G., Reber, G., de Maistre, E., Wahl, D., Kruithof, E. K., Gruenberg, J., and de Moerloose, P. (2000) Interaction of anti-phospholipid antibodies with late endosomes of human endothelial cells. *Arterioscler. Thromb. Vasc. Biol. 20*, 563-74.
35. Simons, K., and Gruenberg, J. (2000) Jamming the endosomal system: lipid rafts and lysosomal storage diseases. *Trends Cell Biol. 10*, 459-62.
36. Kobayashi, T., Beuchat, M. H., Chevallier, J., Makino, A., Mayran, N., Escola, J. M., Lebrand, C., Cosson, P., Kobayashi, T., and Gruenberg, J. (2002) Separation and characterization of late endosomal membrane domains. *J. Biol. Chem. 277*, 32157-64.
37. Lebrand, C., Corti, M., Goodson, H., Cosson, P., Cavalli, V., Mayran, N., Faure, J., and Gruenberg, J. (2002) Late endosome motility depends on lipids via the small GTPase Rab7. *Embo J. 21*, 1289-300.
38. Matsuo, H., Chevallier, J., Mayran, N., Le Blanc, I., Ferguson, C., Faure, J., Blanc, N. S., Matile, S., Dubochet, J., Sadoul, R., Parton, R. G., Vilbois, F., and Gruenberg, J. (2004) Role of LBPA and Alix in multivesicular liposome formation and endosome organization. *Science 303*, 531-4.
39. Le Blanc, I., Luyet, P. P., Pons, V., Ferguson, C., Emans, N., Petiot, A., Mayran, N., Demaurex, N., Faure, J., Sadoul, R., Parton, R. G., and Gruenberg, J. (2005) Endosome-to-cytosol transport of viral nucleocapsids. *Nat. Cell Biol. 7*, 653-64.
40. Newsholme, E., and Leech, A. (1992) *Biochemistry for the medical sciences*, 8th ed., John Wiley & Sons, Chichester.
41. Athenstaedt, K., and Daum, G. (1999) Phosphatidic acid, a key intermediate in lipid metabolism. *Eur. J. Biochem. 266*, 1-16.
42. Dircks, L. K., and Sul, H. S. (1997) Mammalian mitochondrial glycerol-3-phosphate acyltransferase. *Biochim. Biophys. Acta 1348*, 17-26.
43. Coleman, R. A., Lewin, T. M., and Muoio, D. M. (2000) Physiological and nutritional regulation of enzymes of triacylglycerol synthesis. *Annu. Rev. Nutr. 20*, 77-103.
44. Zheng, Z., and Zou, J. (2001) The initial step of the glycerolipid pathway: identification of glycerol 3-phosphate/dihydroxyacetone phosphate dual substrate acyltransferases in Saccharomyces cerevisiae. *J. Biol. Chem. 276*, 41710-6.

45. Hajra, A. K. (1997) Dihydroxyacetone phosphate acyltransferase. *Biochim. Biophys. Acta 1348*, 27-34.
46. Datta, S. C., Ghosh, M. K., and Hajra, A. K. (1990) Purification and properties of acyl/alkyl dihydroxyacetone-phosphate reductase from guinea pig liver peroxisomes. *J. Biol. Chem. 265*, 8268-74.
47. Nagiec, M. M., Wells, G. B., Lester, R. L., and Dickson, R. C. (1993) A suppressor gene that enables Saccharomyces cerevisiae to grow without making sphingolipids encodes a protein that resembles an Escherichia coli fatty acyltransferase. *J. Biol. Chem. 268*, 22156-63.
48. Tokumura, A., Majima, E., Kariya, Y., Tominaga, K., Kogure, K., Yasuda, K., and Fukuzawa, K. (2002) Identification of human plasma lysophospholipase D, a lysophosphatidic acid-producing enzyme, as autotaxin, a multifunctional phosphodiesterase. *J. Biol. Chem. 277*, 39436-42.
49. Umezu-Goto, M., Kishi, Y., Taira, A., Hama, K., Dohmae, N., Takio, K., Yamori, T., Mills, G. B., Inoue, K., Aoki, J., and Arai, H. (2002) Autotaxin has lysophospholipase D activity leading to tumor cell growth and motility by lysophosphatidic acid production. *J. Cell Biol. 158*, 227-33.
50. Pages, C., Simon, M. F., Valet, P., and Saulnier-Blache, J. S. (2001) Lysophosphatidic acid synthesis and release. *Prostaglandins Other Lipid Mediat. 64*, 1-10.
51. Aoki, J. (2004) Mechanisms of lysophosphatidic acid production. *Semin. Cell Dev. Biol. 15*, 477-89.
52. Schmidt, A., Wolde, M., Thiele, C., Fest, W., Kratzin, H., Podtelejnikov, A. V., Witke, W., Huttner, W. B., and Soling, H. D. (1999) Endophilin I mediates synaptic vesicle formation by transfer of arachidonate to lysophosphatidic acid. *Nature 401*, 133-41.
53. Weigert, R., Silletta, M. G., Spano, S., Turacchio, G., Cericola, C., Colanzi, A., Senatore, S., Mancini, R., Polishchuk, E. V., Salmona, M., Facchiano, F., Burger, K. N. J., Mironov, A., Luini, A., and Corda, D. (1999) CtBP/BARS induces fission of Golgi membranes by acylating lysophosphatidic acid. *Nature 402*, 429-33.
54. Nanjundan, M., and Possmayer, F. (2003) Pulmonary phosphatidic acid phosphatase and lipid phosphate phosphohydrolase. *Am. J. Physiol. Lung Cell Mol. Physiol. 284*, L1-23.
55. Levine, J. S., Koh, J. S., Triaca, V., and Lieberthal, W. (1997) Lysophosphatidic acid: a novel growth and survival factor for renal proximal tubular cells. *Am. J. Physiol. 273*, F575-85.
56. Umansky, S. R., Shapiro, J. P., Cuenco, G. M., Foehr, M. W., Bathurst, I. C., and Tomei, L. D. (1997) Prevention of rat neonatal cardiomyocyte apoptosis induced by simulated in vitro ischemia and reperfusion. *Cell. Death Differ. 4*, 608-16.
57. Weiner, J. A., and Chun, J. (1999) Schwann cell survival mediated by the signaling phospholipid lysophosphatidic acid. *Proc. Natl. Acad. Sci. U S A 96*, 5233-8.
58. Fang, X., Yu, S., La Pushin, R., Lu, Y., Furui, T., Penn, L. Z., Stokoe, D., Erickson, J. R., Bast, R. C., Jr., and Mills, G. B. (2000) Lysophosphatidic acid prevents apoptosis in fibroblasts via G(i)-protein-mediated activation of mitogen-activated protein kinase. *Biochem. J. 352 Pt 1*, 135-43.
59. Goetzl, E. J., Lee, H., Dolezalova, H., Kalli, K. R., Conover, C. A., Hu, Y. L., Azuma, T., Stossel, T. P., Karliner, J. S., and Jaffe, R. B. (2000) Mechanisms of lysolipid phosphate effects on cellular survival and proliferation. *Ann. N. Y. Acad. Sci. 905*, 177-87.
60. Karliner, J. S., Honbo, N., Summers, K., Gray, M. O., and Goetzl, E. J. (2001) The lysophospholipids sphingosine-1-phosphate and lysophosphatidic acid enhance survival during hypoxia in neonatal rat cardiac myocytes. *J. Mol. Cell Cardiol. 33*, 1713-7.
61. Sautin, Y. Y., Crawford, J. M., and Svetlov, S. I. (2001) Enhancement of survival by LPA via Erk1/Erk2 and PI 3-kinase/Akt pathways in a murine hepatocyte cell line. *Am. J. Physiol. Cell Physiol. 281*, C2010-9.
62. Jalink, K., Moolenaar, W. H., and Van Duijn, B. (1993) Lysophosphatidic acid is a chemoattractant for Dictyostelium discoideum amoebae. *Proc. Natl. Acad. Sci. U S A 90*, 1857-61.
63. Shiono, S., Kawamoto, K., Yoshida, N., Kondo, T., and Inagami, T. (1993) Neurotransmitter release from lysophosphatidic acid stimulated PC12 cells: involvement of lysophosphatidic acid receptors. *Biochem. Biophys. Res. Commun. 193*, 667-73.
64. Vogt, W. (1957) The chemical nature of Darmstoff. *J. Physiol. 137*, 154-67.
65. Vogt, W. (1957) Pharmacologically active lipid soluble acids of natural occurrence. *Nature 179*, 300-4; passim.
66. Hecht, J. H., Weiner, J. A., Post, S. R., and Chun, J. (1996) Ventricular zone gene-1 (vzg-1) encodes a lysophosphatidic acid receptor expressed in neurogenic regions of the developing cerebral cortex. *J. Cell Biol. 135*, 1071-83.

67. An, S., Dickens, M. A., Bleu, T., Hallmark, O. G., and Goetzl, E. J. (1997) Molecular cloning of the human Edg2 protein and its identification as a functional cellular receptor for lysophosphatidic acid. *Biochem. Biophys. Res. Commun. 231*, 619-22.
68. An, S., Bleu, T., Hallmark, O. G., and Goetzl, E. J. (1998) Characterization of a novel subtype of human G protein-coupled receptor for lysophosphatidic acid. *J. Biol. Chem. 273*, 7906-10.
69. Bandoh, K., Aoki, J., Hosono, H., Kobayashi, S., Kobayashi, T., Murakami-Murofushi, K., Tsujimoto, M., Arai, H., and Inoue, K. (1999) Molecular cloning and characterization of a novel human G-protein-coupled receptor, EDG7, for lysophosphatidic acid. *J. Biol. Chem. 274*, 27776-85.
70. McIntyre, T. M., Pontsler, A. V., Silva, A. R., St Hilaire, A., Xu, Y., Hinshaw, J. C., Zimmerman, G. A., Hama, K., Aoki, J., Arai, H., and Prestwich, G. D. (2003) Identification of an intracellular receptor for lysophosphatidic acid (LPA): LPA is a transcellular PPARgamma agonist. *Proc. Natl. Acad. Sci. U S A 100*, 131-6.
71. Noguchi, K., Ishii, S., and Shimizu, T. (2003) Identification of p2y9/GPR23 as a novel G protein-coupled receptor for lysophosphatidic acid, structurally distant from the Edg family. *J. Biol. Chem. 278*, 25600-6.
72. Ha, K. S., and Exton, J. H. (1993) Activation of actin polymerization by phosphatidic acid derived from phosphatidylcholine in IIC9 fibroblasts. *J. Cell. Biol. 123*, 1789-96.
73. McPhail, L. C., Waite, K. A., Regier, D. S., Nixon, J. B., Qualliotine-Mann, D., Zhang, W. X., Wallin, R., and Sergeant, S. (1999) A novel protein kinase target for the lipid second messenger phosphatidic acid. *Biochim. Biophys. Acta 1439*, 277-90.
74. English, D., Cui, Y., and Siddiqui, R. A. (1996) Messenger functions of phosphatidic acid. *Chem. Phys. Lipids 80*, 117-32.
75. Tsai, M. H., Yu, C. L., Wei, F. S., and Stacey, D. W. (1989) The effect of GTPase activating protein upon ras is inhibited by mitogenically responsive lipids. *Science 243*, 522-6.
76. Tsai, M. H., Yu, C. L., and Stacey, D. W. (1990) A cytoplasmic protein inhibits the GTPase activity of H-Ras in a phospholipid-dependent manner. *Science 250*, 982-5.
77. Siddiqui, R. A., and Yang, Y. C. (1995) Interleukin-11 induces phosphatidic acid formation and activates MAP kinase in mouse 3T3-L1 cells. *Cell. Signal. 7*, 247-59.
78. Ghosh, S., Strum, J. C., Sciorra, V. A., Daniel, L., and Bell, R. M. (1996) Raf-1 kinase possesses distinct binding domains for phosphatidylserine and phosphatidic acid. Phosphatidic acid regulates the translocation of Raf-1 in 12-O-tetradecanoylphorbol-13-acetate-stimulated Madin-Darby canine kidney cells. *J. Biol. Chem. 271*, 8472-80.
79. Rizzo, M. A., Shome, K., Vasudevan, C., Stolz, D. B., Sung, T. C., Frohman, M. A., Watkins, S. C., and Romero, G. (1999) Phospholipase D and its product, phosphatidic acid, mediate agonist-dependent raf-1 translocation to the plasma membrane and the activation of the mitogen-activated protein kinase pathway. *J. Biol. Chem. 274*, 1131-9.
80. Rizzo, M. A., Shome, K., Watkins, S. C., and Romero, G. (2000) The recruitment of Raf-1 to membranes is mediated by direct interaction with phosphatidic acid and is independent of association with Ras. *J. Biol. Chem. 275*, 23911-8.
81. Ktistakis, N. T., Brown, H. A., Waters, M. G., Sternweis, P. C., and Roth, M. G. (1996) Evidence that phospholipase D mediates ADP ribosylation factor-dependent formation of Golgi coated vesicles. *J. Cell Biol. 134*, 295-306.
82. Chen, Y. G., Siddhanta, A., Austin, C. D., Hammond, S. M., Sung, T. C., Frohman, M. A., Morris, A. J., and Shields, D. (1997) Phospholipase D stimulates release of nascent secretory vesicles from the trans-Golgi network. *J. Cell Biol. 138*, 495-504.
83. Moritz, A., De Graan, P. N., Gispen, W. H., and Wirtz, K. W. (1992) Phosphatidic acid is a specific activator of phosphatidylinositol-4-phosphate kinase. *J. Biol. Chem. 267*, 7207-10.
84. Honda, A., Nogami, M., Yokozeki, T., Yamazaki, M., Nakamura, H., Watanabe, H., Kawamoto, K., Nakayama, K., Morris, A. J., Frohman, M. A., and Kanaho, Y. (1999) Phosphatidylinositol 4-phosphate 5-kinase alpha is a downstream effector of the small G protein ARF6 in membrane ruffle formation. *Cell 99*, 521-32.
85. De Camilli, P., Emr, S. D., McPherson, P. S., and Novick, P. (1996) Phosphoinositides as regulators in membrane traffic. *Science 271*, 1533-9.
86. Cullis, P. R., and de Kruijff, B. (1979) Lipid polymorphism and the functional roles of lipids in biological membranes. *Biochim. Biophys. Acta 559*, 399-420.

87. Chernomordik, L. V., and Kozlov, M. M. (2003) Protein-lipid interplay in fusion and fission of biological membranes. *Annu. Rev. Biochem. 72*, 175-207.
88. Cullis, P. R., and Hope, M. J. (1978) Effects of fusogenic agent on membrane structure of erythrocyte ghosts and the mechanism of membrane fusion. *Nature 271*, 672-4.
89. Chernomordik, L., Kozlov, M. M., and Zimmerberg, J. (1995) Lipids in biological membrane fusion. *J. Membr. Biol. 146*, 1-14.
90. de Figueiredo, P., Drecktrah, D., Katzenellenbogen, J. A., Strang, M., and Brown, W. J. (1998) Evidence that phospholipase A2 activity is required for Golgi complex and trans Golgi network membrane tubulation. *Proc. Natl. Acad. Sci U S A 95*, 8642-7.
91. de Figueiredo, P., Polizotto, R. S., Drecktrah, D., and Brown, W. J. (1999) Membrane tubule-mediated reassembly and maintenance of the Golgi complex is disrupted by phospholipase A2 antagonists. *Mol. Biol. Cell 10*, 1763-82.
92. Tate, M. W., Eikenberry, E. F., Turner, D. C., Shyamsunder, E., and Gruner, S. M. (1991) Nonbilayer phases of membrane lipids. *Chem. Phys. Lipids 57*, 147-64.
93. Langner, M., and Kubica, K. (1999) The electrostatics of lipid surfaces. *Chem. Phys. Lipids 101*, 3-35.
94. Tate, M. W., and Gruner, S. M. (1987) Lipid polymorphism of mixtures of dioleoylphosphatidylethanolamine and saturated and monounsaturated phosphatidylcholines of various chain lengths. *Biochemistry 26*, 231-6.
95. Toombes, G. E., Finnefrock, A. C., Tate, M. W., and Gruner, S. M. (2002) Determination of L(alpha)-H(II) phase transition temperature for 1,2-dioleoyl-sn-glycero-3-phosphatidylethanolamine. *Biophys. J. 82*, 2504-10.
96. Op den Kamp, J. A. (1979) Lipid asymmetry in membranes. *Annu. Rev. Biochem. 48*, 47-71.
97. Kim, J., Mosior, M., Chung, L. A., Wu, H., and McLaughlin, S. (1991) Binding of peptides with basic residues to membranes containing acidic phospholipids. *Biophys. J. 60*, 135-48.
98. Montich, G., Scarlata, S., McLaughlin, S., Lehrmann, R., and Seelig, J. (1993) Thermodynamic characterization of the association of small basic peptides with membranes containing acidic lipids. *Biochim. Biophys. Acta 1146*, 17-24.
99. Arbuzova, A., Murray, D., and McLaughlin, S. (1998) MARCKS, membranes, and calmodulin: kinetics of their interaction. *Biochim. Biophys. Acta 1376*, 369-79.
100. Killian, J. A., and von Heijne, G. (2000) How proteins adapt to a membrane-water interface. *Trends Biochem. Sci. 25*, 429-34.
101. de Planque, M. R., Goormaghtigh, E., Greathouse, D. V., Koeppe, R. E., 2nd, Kruijtzer, J. A., Liskamp, R. M., de Kruijff, B., and Killian, J. A. (2001) Sensitivity of single membrane-spanning alpha-helical peptides to hydrophobic mismatch with a lipid bilayer: effects on backbone structure, orientation, and extent of membrane incorporation. *Biochemistry 40*, 5000-10.
102. de Planque, M. R., Boots, J. W., Rijkers, D. T., Liskamp, R. M., Greathouse, D. V., and Killian, J. A. (2002) The effects of hydrophobic mismatch between phosphatidylcholine bilayers and transmembrane alpha-helical peptides depend on the nature of interfacially exposed aromatic and charged residues. *Biochemistry 41*, 8396-404.
103. Strandberg, E., Morein, S., Rijkers, D. T., Liskamp, R. M., van der Wel, P. C., and Killian, J. A. (2002) Lipid dependence of membrane anchoring properties and snorkeling behavior of aromatic and charged residues in transmembrane peptides. *Biochemistry 41*, 7190-8.
104. van der Wel, P. C., Strandberg, E., Killian, J. A., and Koeppe, R. E., 2nd. (2002) Geometry and intrinsic tilt of a tryptophan-anchored transmembrane alpha-helix determined by (2)H NMR. *Biophys. J. 83*, 1479-88.
105. McLaughlin, S. (1989) The electrostatic properties of membranes. *Annu. Rev. Biophys. Biophys. Chem. 18*, 113-36.
106. Cevc, G. (1990) Membrane electrostatics. *Biochim. Biophys. Acta. 1031*, 311-82.
107. Tocanne, J. F., and Teissie, J. (1990) Ionization of phospholipids and phospholipid-supported interfacial lateral diffusion of protons in membrane model systems. *Biochim. Biophys. Acta 1031*, 111-42.
108. Boggs, J. M. (1987) Lipid intermolecular hydrogen bonding: influence on structural organization and membrane function. *Biochim. Biophys. Acta 906*, 353-404.
109. Kates, M., Syz, J. Y., Gosser, D., and Haines, T. H. (1993) pH-dissociation characteristics of cardiolipin and its 2'-deoxy analogue. *Lipids 28*, 877-82.

110. Moncelli, M. R., Becucci, L., and Guidelli, R. (1994) The intrinsic pKa values for phosphatidylcholine, phosphatidylethanolamine, and phosphatidylserine in monolayers deposited on mercury electrodes. *Biophys. J. 66*, 1969-80.
111. Rand, R. P., and Sengupta, S. (1972) Cardiolipin forms hexagonal structures with divalent cations. *Biochim. Biophys. Acta 255*, 484-92.
112. Rizo, J., and Sudhof, T. C. (1998) C2-domains, structure and function of a universal Ca2+-binding domain. *J. Biol. Chem. 273*, 15879-82.
113. Madden, T. D., and Cullis, P. R. (1982) Stabilization of bilayer structure for unsaturated phosphatidylethanolamines by detergents. *Biochim. Biophys. Acta 684*, 149-53.
114. Janes, N. (1996) Curvature stress and polymorphism in membranes. *Chem. Phys. Lipids 81*, 133-150.
115. Fuller, N., and Rand, R. P. (2001) The influence of lysolipids on the spontaneous curvature and bending elasticity of phospholipid membranes. *Biophys. J. 81*, 243-54.
116. Gruner, S. M. (1985) Intrinsic curvature hypothesis for biomembrane lipid composition: a role for nonbilayer lipids. *Proc. Natl. Acad. Sci. U S A 82*, 3665-9.
117. Leikin, S., Kozlov, M. M., Fuller, N. L., and Rand, R. P. (1996) Measured effects of diacylglycerol on structural and elastic properties of phospholipid membranes. *Biophys. J. 71*, 2623-32.
118. Rand, R. P., Fuller, N. L., Gruner, S. M., and Parsegian, V. A. (1990) Membrane curvature, lipid segregation, and structural transitions for phospholipids under dual-solvent stress. *Biochemistry 29*, 76-87.
119. Watts, A. (1998) Solid-state NMR approaches for studying the interaction of peptides and proteins with membranes. *Biochim. Biophys. Acta 1376*, 297-318.
120. Traikia, M., Warschawski, D. E., Lambert, O., Rigaud, J. L., and Devaux, P. F. (2002) Asymmetrical membranes and surface tension. *Biophys. J. 83*, 1443-54.
121. Fyfe, C. (1983) *Solid state NMR for chemists*, C.F.C. Press, Guelph, Ontario, Canada.

CHAPTER 2

Modulation of membrane curvature by phosphatidic acid and lysophosphatidic acid

Taken from:
Traffic (2003) *4, 162*-174

Abstract

The local generation of phosphatidic acid plays a key role in the regulation of intracellular membrane transport through mechanisms which are largely unknown. Phosphatidic acid may recruit and activate downstream effectors, or change the biophysical properties of the membrane and directly induce membrane bending and/or destabilization. To evaluate these possibilities, we determined the phase properties of phosphatidic acid and lysophosphatidic acid (LPA) at physiological conditions of pH and ion concentrations. In single-lipid systems, unsaturated phosphatidic acid behaved as a cylindrical, bilayer-preferring lipid at cytosolic conditions (37°C, pH 7.2, 0.5 mM free Mg^{2+}), but acquired a type-II shape at typical intra-Golgi conditions, a mildly acidic pH and submillimolar free Ca^{2+} (pH 6.6-5.9, 0.3 mM Ca^{2+}). Lysophosphatidic acid formed type-I lipid micelles in the absence of divalent cations, but anhydrous cation-lysophosphatidic acid bilayer complexes in their presence. These data suggest a similar molecular shape for phosphatidic acid and lysophosphatidic acid at cytosolic conditions; however, experiments in mixed-lipid systems indicate that their shape is not identical. Lysophosphatidic acid stabilized the bilayer phase of unsaturated phosphatidylethanolamine, while the opposite effect was observed in the presence of phosphatidic acid. These results support the hypothesis that a conversion of lysophosphatidic acid into phosphatidic acid by endophilin or BARS (50 kDa brefeldin A rybosylated substrate) may induce negative spontaneous monolayer curvature and regulate endocytic and Golgi membrane fission. Alternative models for the regulation of membrane fission based on the strong dependence of the molecular shape of (lyso)phosphatidic acid on pH and divalent cations are also discussed.

Introduction

Intracellular membrane transport occurs via membranebound transport containers (TCs) that bud off from a donor compartment and ultimately fuse with an acceptor compartment (1). Formation and consumption of these TCs depends on membrane fission and fusion, respectively. Fusion and fission are mechanistically related events which both involve strong membrane bending and a transient reorganization of the equilibrium bilayer configuration of the membrane into highly curved non-bilayer intermediates (2-4). As such, membrane fission and fusion are energetically unfavorable and do not occur spontaneously *in vivo*, but only under strict control of specialized proteins. Evidence is accumulating that these proteins do not act alone but in concert with particular membrane lipids, i.e. phosphoinositides (5), diacylglycerol (DAG; 6, 7), and phosphatidic acid (PA; 6, 8-10). The role of these lipids in membrane fission and fusion may be two-fold: (i) to allow the localized and intimate interaction of a membrane-destabilizing protein with the membrane; and (ii) to facilitate membrane bending and the formation of

the highly curved intermediates, and thereby effectively reducing the energy barriers to fusion and fission. The latter possibility, a direct role for local lipid metabolism in the regulation of membrane curvature, should relate to special biophysical properties of the lipids formed, and is especially suggestive for PA. Phosphatidic acid is a unique phospholipid because of its small negatively charged headgroup very close to the acyl chain region of the bilayer, its high affinity for divalent cations, and its propensity to form intermolecular hydrogen bonds (11, 12). Experiments in lipid model systems suggest that, depending on local conditions such as pH and divalent cation concentrations, PA may segregate into microdomains (13, 14), or promote negative (concave) membrane curvature (15, 16).

Although in mammalian cells PA only occurs in small amounts, it is a key metabolite in lipid biosynthesis with a very high turnover rate. Besides *de novo* synthesis, in particular, through acylation of glycerol-3-phosphate (17), PA can be formed by three alternative biosynthetic pathways: phosphorylation of DAG by DAG-kinase, hydrolysis of phospholipids by phospholipase D (PLD), and acylation of lyso-PA (LPA) by LPA-acyltransferases (LPAATs). The latter three pathways have all been implicated in the regulation of intracellular membrane traffic (6, 8-10). In particular, the local formation of PA is a recurring theme in signaling pathways regulating Golgi membrane transport (9, 10), and recent data suggest that PA may play a direct role in TC formation which is probably related to the special biophysical properties of PA (2, 8, 18). In the Golgi, PA is either generated by ARF-activated PLD, which converts phosphatidylcholine (PC) into PA and choline (9), by DAG-kinases (6), or by 50 kDa brefeldin A rybosylated substrate (BARS). Brefeldin A rybosylated substrate is an enzyme capable of converting lyso-PA into PA using acyl-CoA as the acyl donor, and this activity is essential for fission of Golgi membrane tubules *in vitro* (8). Strikingly, endophilin I, a protein involved in endocytic membrane fission, has been independently found to display the same enzymatic activity (19), and palmitoyl-CoA activates the fission of TCs from the Golgi (20). Finally, a member of the endophilin family localizes to mitochondria and is implicated in the regulation of mitochondrial membrane fission (van der Bliek, personal communication). Thus, collectively, these findings suggest that the formation of PA from LPA could be part of a universal "lipid machinery" for membrane fission.

Because acylation of LPA selectively increases the cross-sectional area of the tail region, the role of the acyltransferases may be to reduce the spontaneous curvature of the cytosolic membrane leaflet and facilitate the formation of negative (concave) membrane curvature during constriction of the neck region; neck constriction has been proposed to result from the conversion of inverted-cone-shaped LPA into cone-shaped PA (19). Although an attractive hypothesis, the polymorphic phase behavior of LPA has not been studied so far, and it is unclear to what extent a conversion of LPA into PA would reduce the spontaneous monolayer curvature. Some initial characterizations of PA have been performed (15, 16), but the polymorphic phase behavior of PA and LPA has not been studied

at physiological conditions of pH and divalent cation concentrations. In order to evaluate various models for the role of LPA acyltransferases in biomembrane fission, the aim of the current study was to determine the biophysical properties of PA and LPA at conditions relevant to Golgi membrane fission. To this end we considered conditions typical for the cytosol, pH 7.2 and submillimolar concentrations of Mg^{2+}, as well as conditions typical for the Golgi lumen, a mildly acidic pH and submillimolar concentrations of Ca^{2+}. We focus on PA and LPA carrying oleoyl fatty acids because BARS-mediated Golgi membrane fission *in vitro* is most efficient in the presence of unsaturated fatty acyl-CoA (8), and in a lipid acyltransferase assay BARS greatly prefers oleoyl-LPA to lauroyl-, palmitoyl, and stearoyl-LPA (Roberto Weigert, personal communication). Our results indicate that, as proposed, a conversion of LPA into PA may induce negative spontaneous monolayer curvature and membrane bending. In addition, we observed a strong dependence of the polymorphic phase behavior of PA on pH and divalent cation concentration, suggesting that PA may have additional or alternative roles in membrane bending and fission.

Materials and Methods

Sample preparation

Lipids were purchased from Avanti Polar lipids, Inc. (Birmingham, AL, USA), and were > 99% pure as judged by HPTLC. All other chemicals were of analytical grade. Lipid stocks were prepared in chloroform/methanol (2/1) and stored at -20 ^{o}C. Phospholipid phosphorus was determined according to Rouser (57). Dry lipid films were prepared by rotary evaporation, followed by high vacuum desiccation overnight. Lipid films were then hydrated using a Mes-Hepes buffer: 25 mM Mes, 25 mM Hepes-NaOH, 1 mM EGTA, 150 mM NaCl, at pH 7.2/6.8/6.4/6.0 (37^{o}C); pH checked/adjusted after hydration of the dry lipid film. Samples containing DOPE were hydrated just below T_H. Residual lipid aggregates were removed from the wall of the flask using a glass rod or a pipette. Lipid suspensions were then transferred to high-resolution 10-mm NMR tubes.

$MgCl_2$ or $CaCl_2$ was added to get a Me^{2+}/lipid mol ratio of 0.2, 0.5, 1.0, and 2.0. A Ca/Mg ionophore (A23187; Sigma Chemical Co., St. Louis, MO, USA) was present at a final ionophore/lipid mol ratio of 1-to-1000, to allow for rapid and complete equilibration of cations. The ionophore was added from methanol (2 mg/ml) and the samples incubated for at least 30 min before ^{31}P-NMR spectra were recorded. Ionophore addition had no effect on the phase behavior of lipid suspensions (data not shown).

In order to more closely mimic physiological conditions of pH and divalent cation concentrations, dialysis was used (24 Å pore-size; Medicell Int. Ltd., London, UK): "cytosol-dialysis" at pH 7.2 and 0.50 mM free Mg^{2+}, and "intra-Golgi-dialysis" at pH 6.0 and 0.30 mM free Ca^{2+} (Mes-Hepes buffer, 37^{o}C). The 1

ml sample (20-40mM) was placed in the dialysis tube and dialyzed against 100 ml overnight at 20 °C (4 °C for DOPE-containing samples). Free divalent cation concentrations were calculated using the MAXC program (http://www.stanford.edu/~cpatton/maxc.html) (58). The dialysis tube was inserted into a 10-mm NMR-tube and held down by a Teflon stopper.

NMR measurements

^{31}P-NMR spectra of 0.5-1 ml samples (20-40 mM phospholipid) were recorded on MSL 300 WB or on Avance 500 WB spectrometers. NMR spectra were recorded using a high resolution 10 mm broadband-gated proton decoupling. The recycling delay was 1.5 s and the p/4 pulse width 7 ms. Up to 60,000 scans were recorded with the MSL 300, and from 1500 to 3000 scans were recorded with the Avance 500 spectrometer, depending on total amount of lipid. An exponential multiplication with a line-broadening factor of 100 Hz was used before performing the Fourier transformation. Chemical shifts in ^{31}P-NMR spectra were measured relative to the isotropic signal of 85% H_3PO_4.

Temperature-scans were recorded in steps of 2 °C (unless stated otherwise). Samples were allowed to equilibrate for 10 minutes after each temperature increase. At the end of the measurements, samples were cooled down to their initial temperature and reanalyzed; identical spectra were obtained, excluding the possibility of lipid hydrolysis (data not shown). The percentages of different phases present were estimated by comparing the ^{31}P-NMR spectra against a series of calibration graphs. Estimation is accurate to within 5%. This series was constructed by taking the respective percentage of a pure L_α phase just prior to and a pure H_{II} phase just after the phase transition.

The anhydrous Mg-LPA complex was analyzed using the cross-polarization (CP) technique (35). Cross-polarization spectra were recorded by using an 8-mm static probe, on an Avance 500 WB spectrometer, with a contact time of 1ms and 1s recycle delay.

Electron microscopy

Dispersions were visualized by freeze-fracture electron microscopy. Samples were fast frozen by plunging into liquid propane, and fractured and replicated according to standard procedures (59) using a Balzers BAF 400 (BAL-TEC AG, Liechtenstein). Cryoprotectants were not used.

Results

^{31}P-NMR was used to determine the lipid polymorphic properties of PA and LPA at physiological conditions of pH and ion concentrations. Lipid polymorphic phase behavior may be qualitatively understood by considering the molecular shape and packing of the lipid molecules, or the monolayer spontaneous radius of curvature

(21-23). Amphiphilic lipids with equally sized cross-sectional areas of the headgroup and acyl chains have a cylindrical shape and will organize into a lamellar phase. If the lipid headgroup is smaller than the cross-sectional area of the acyl chains, the lipids have a cone shape and will tend to curve toward the water region (negative or concave curvature), favoring the formation of type-II (inverted) nonlamellar phases, such as the inverted hexagonal H_{II} phase. The lipid molecules in the H_{II} phase are organized in hexagonally arranged cylinders, with the polar headgroups lining a central aqueous channel. If the lipid headgroup is larger than the cross-sectional area of the acyl chain(s), the lipids have an inverted cone or wedge shape, and will favor positive or convex curvature and tend to form type-I nonlamellar phases such as type-I lipid micelles. The phase preference or spontaneous curvature depends not only on the molecular structure of the lipid in question, but also on its dynamic properties, the hydration of the lipid headgroup, as well as on intra- and intermolecular interactions. Thus, the curvature preference of lipids such as PA and LPA is greatly influenced by factors such as temperature, pH, salt and cation concentrations.

^{31}P-NMR can distinguish between lamellar, inverted hexagonal H_{II}, and structures allowing isotropic motion (cubic phases, micelles, small vesicles), and is the method of choice to study the polymorphic phase behavior of phospholipids (24). Because most biomembranes appear to contain lateral heterogeneities, microdomains, relatively enriched in particular lipid species, the biophysical properties of PA and LPA were studied in single-lipid as well as mixed-lipid systems. In key experiments, lipid suspensions were dialyzed against buffers mimicking particular cytosolic or intra-Golgi conditions. In these experiments, A23187, a cation-selective ionophore transporting both Ca^{2+} and Mg^{2+} (25), was added to allow full equilibration of ions across all membranes (26, 27).

Polymorphic phase behavior of dioleoyl-phosphatidic acid

A first set of experiments was performed on single-lipid systems, i.e. using pure dioleoyl-PA (DOPA), at 37 ^{o}C. At neutral pH, DOPA formed a lamellar phase, even in the presence of an equimolar amount of Ca^{2+}: broad-line ^{31}P-NMR spectra (Figure 1A) showed a high-field peak and a low-field shoulder typical of phospholipids in the lamellar liquid crystalline (L_{α}) phase (24). Identical results were obtained with a 2-fold molar excess of Ca^{2+} or Mg^{2+} (data not shown). To mimic cytosolic conditions more closely, a DOPA suspension was dialyzed overnight against a buffer of pH 7.2 containing 0.5 mM free Mg^{2+}, and again a pure lamellar phase was observed (data not shown). These data indicate that in a single-lipid system, DOPA behaves as a bilayer-preferring lipid at cytosolic conditions of temperature, pH, and divalent cations.

A lamellar phase was also observed for DOPA at low pH (pH 5) in the absence of divalent cations (Figure 1B). However, at pH 5 and a Ca^{2+}/lipid mol ratio of 0.2 or higher, the lamellar phase was completely converted into a hexagonal H_{II} phase (Figure 1C-E): ^{31}P-NMR spectra were characterized by a high-field shoulder, a low-

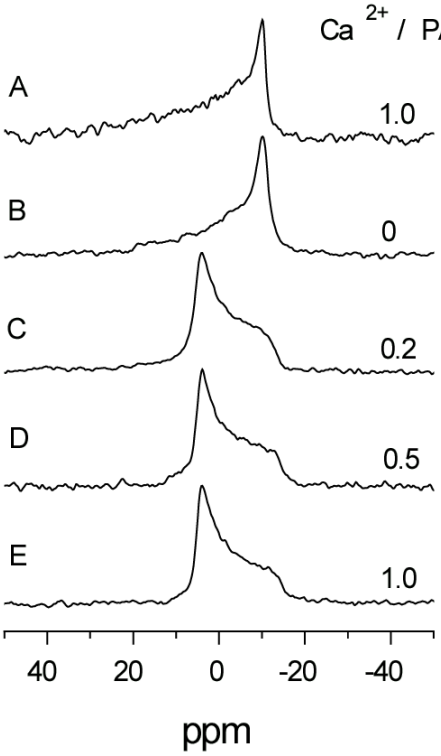

Figure 1: Polymorphic phase behavior of phosphatidic acid (PA). Proton-decoupled ^{31}P-NMR spectra of aqueous dispersions of DOPA recorded at 37°C. (A) at pH 7.2 and a Ca^{2+} to lipid molar ratio of 1. (B-E) at pH 5.0, and a Ca^{2+} to lipid molar ratio of 0 (no Ca^{2+} B), 0.2 (C), 0.5 (D), and 1.0 (E).

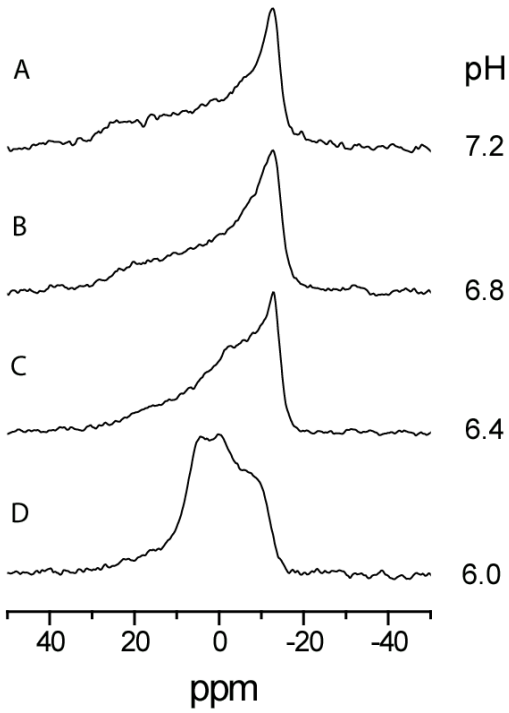

Figure 2: Type-II preference of phosphatidic acid (PA) is extremely pH-sensitive. Proton-decoupled ^{31}P-NMR spectra of aqueous dispersions of DOPA recorded at 37°C after overnight equilibration against a free Ca^{2+} concentration of 0.3 mM, typical for the Golgi lumen, and pH 7.2 (A), pH 6.8 (B), pH 6.4 (C), and pH 6.0 (D).

field peak, and a chemical shift anisotropy (CSA) exactly half of that of the corresponding bilayer phase (24). In view of the pH-dependence of the phase behavior of DOPA and the mild acidic pH of the Golgi lumen, DOPA was studied at intra-Golgi conditions. The lumenal pH of the Golgi decreases down the secretory pathway from pH 6.6 for medial/*trans*-Golgi (28) to pH 5.9-6.2 for the TGN (29, 30). Moreover, the Golgi lumen contains significant amounts of free Ca^{2+}; the lumenal free Ca^{2+} concentration varies around 0.3 mM (31). Therefore, the phase behavior of DOPA was studied at 0.3 mM free Ca^{2+} varying the pH between pH 7.2 and 6.0 (Figure 2). At pH values below pH 6.8, a mixed lamellar-H_{II} phase was observed with a significant fraction, ~5 % and 60 %, of the DOPA in the H_{II} phase at pH 6.4 and pH 6.0, respectively. These results indicate that the phase behavior of DOPA is remarkably pH-sensitive, with the type-II preference of

DOPA clearly being expressed at pH values and divalent cation concentrations typical for the Golgi lumen.

A convenient tool to study the molecular shape of specific lipids in mixed-lipid systems is to examine the influence of these lipids on the polymorphic phase behavior of a type-II lipid such as dioleoyl-phosphatidylethanolamine (DOPE). Adding small amounts of a type-I lipid to a lipid matrix of DOPE results in an increase in the L_α-H_{II} phase transition temperature, i.e. in the stabilization of the bilayer phase (Figure 3A (23, 32, 33)). This is easily explained by considering the shape-structure concept of lipid polymorphism and the complementary shapes of type-I and type-II lipids. It can also be understood in terms of curvature stress: a lipid bilayer containing type-II lipids suffers from considerable curvature stress, this stress will be relieved by incorporating lipids with an opposite shape. Thus, cylindrical, and even more so, inverted cone-shaped (type-I) lipids will decrease curvature stress and stabilize the bilayer (Figure 3A, B). In contrast, cone-shaped

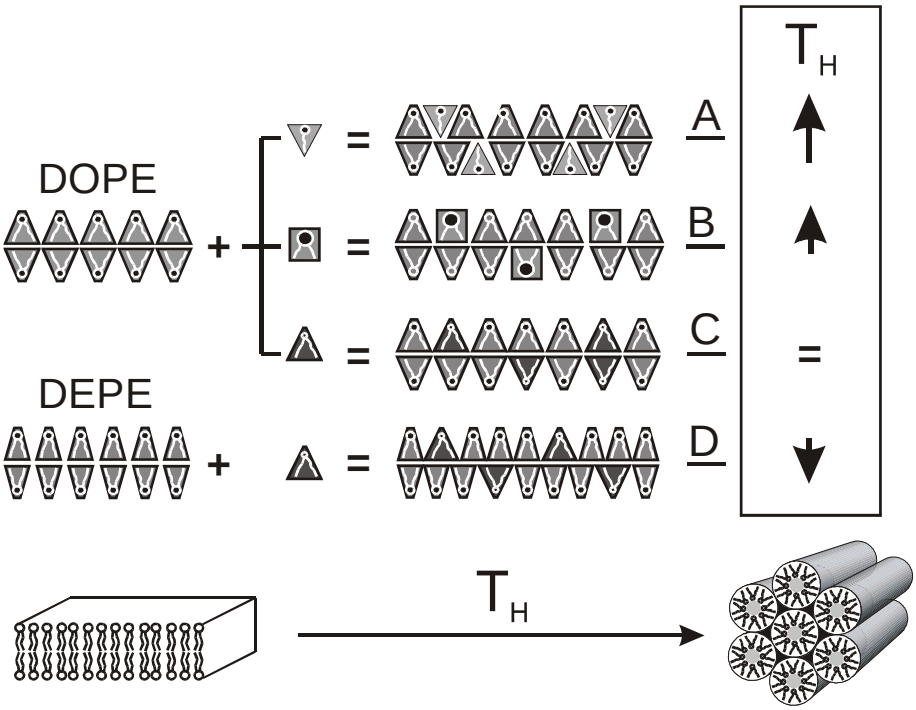

Figure 3: Determining lipid molecular shape in mixed-lipid systems containing phosphatidylethanolamine (PE). The shape of a particular lipid can be deduced from its effect on the L_α-H_{II} phase transition temperature. Type-I lipids such as lysophosphatidylcholine (A), and cylindrical lipids such as phosphatidylcholine (B) increase the L_α-H_{II} phase transition temperature. In contrast, cone-shaped (type-II) lipids, depending on how pronounced their cone-shape is relative to that of the matrix lipid, have no effect (C) or reduce the L_α-H_{II} phase transition temperature (D).

(type-II) lipids, depending on how pronounced their cone-shape is relative to that of the matrix lipid, have no effect or may even increase curvature stress and destabilize the bilayer (Figure 3C, D (23)).

DOPE has a liquid crystalline-to-hexagonal H_{II} phase transition temperature (T_H) of ~3 °C (34), in close agreement with our ^{31}P-NMR data (Figure 4A). ^{31}P-NMR data were quantified and the amount of lamellar phase determined as a function of temperature (Figure 4B). The presence of PA, 10 mol% of total lipid, resulted in a slight increase in T_H. A similar result was obtained when the PA/PE suspension was dialyzed overnight at cytosolic conditions (Figure 4B, curves 3 and 4). Note that in all these ^{31}P-NMR measurements, an isotropic signal was virtually absent. In the presence of an equimolar amount of Mg^{2+} with respect to total lipid, inclusion of PA had almost no effect on T_H (Figure 4B, compare curves 1 and 2). Overall, these data indicate very little effect of PA on T_H, suggesting a cone-shape

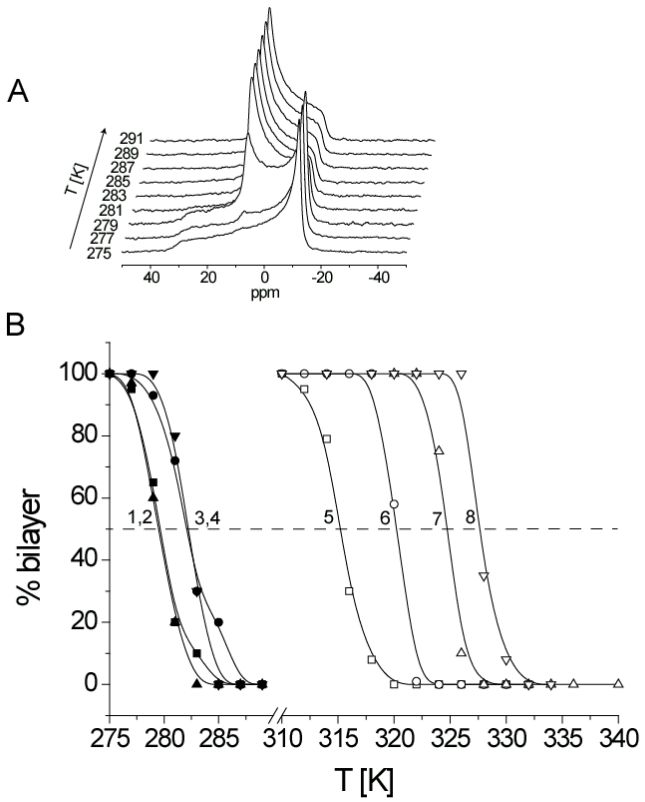

Figure 4: Phosphatidic acid (PA) destabilizes the bilayer phase of phosphatidylethanolamine (PE). Proton-decoupled ^{31}P-NMR spectra of an aqueous dispersion of DOPE (A). ^{31}P-NMR data were quantified and the amount of lamellar phase determined as a function of temperature (B). Aqueous dispersions containing DOPE (closed symbols): DOPE (pH 7.2), ■; DOPE/DOPA (10 mol%, pH 7.2), ●; DOPE/DOPA with Mg^{2+} equimolar with respect to total lipid (pH 7.2), ▲ ; DOPE/DOPA dialyzed against 0.5 mM Mg^{2+} (pH 7.2), ▼ . Aqueous dispersions containing DEPE (open symbols): DEPE dialyzed against 0.3 mM Ca^{2+} at pH 7.2, ▽; and at pH 6.0, Δ; DEPE/DOPA dialyzed against 0.3 mM Ca^{2+} at pH 7.2, ○ ; and at pH 6.0 □.

for PA under these conditions. The strong pH-dependence of the phase behavior of pure DOPA (Figure 2) urged us to examine PA/PE mixed lipid systems at intra-Golgi conditions, a mildly acidic pH and 0.3 mM free Ca^{2+}. These experiments were performed using dielaidoyl-PE (DEPE) instead of DOPE. DEPE carries 18:1 fatty acids with *trans* instead of *cis* double bonds resulting in a more extended configuration of the acyl chains and a less cone-shaped lipid. The higher T_H of DEPE allows for a more accurate determination of factors that reduce T_H. The inclusion of 10 mol% of DOPA in DEPE clearly reduced T_H as compared to pure DEPE (Figure 4B). An overnight dialysis against 0.3 mM free Ca^{2+} at neutral pH reduced T_H by 7 ^oC (Figure 4B, compare curves 6 and 8), while a parallel incubation at pH 6.0 even reduced T_H by 10 ^oC (Figure 4B, compare curves 5 and 7). The fact that DOPA hardly influences T_H in a mixture with DOPE (Figure 4B, closed symbols), while it clearly destabilizes the bilayer phase in mixtures with DEPE (Figure 4B, open symbols), indicates that the molecular shape of DOPA is similar to that of DOPE, which has a more pronounced cone-shape than DEPE (see Figure 3C, D). In summary, at physiological conditions in a mixed-lipid system, PA behaves as a cone-shaped (type-II) lipid. The strongest bilayer destabilization is observed in the presence of divalent cations at acidic pH (Figure 4B, curve 5), indicating that the type-II preference or cone-shape of DOPA will be most pronounced at intra-Golgi conditions.

Polymorphic phase behavior of lysophosphatidic acid

The polymorphic phase behavior of (1-oleoyl) LPA was determined at cytosolic conditions, i.e. at neutral pH and in the presence of Mg^{2+}. In the absence of Mg^{2+}, an isotropic ^{31}P-NMR signal was observed, suggesting the formation of lipid micelles (Figure 5A). Upon addition of divalent cations, the translucent LPA solution became turbid and the intensity of the isotropic ^{31}P-NMR signal was reduced (Figure 5A-C). X-ray and neutron diffraction measurements indicated that at low divalent cation concentrations quasi-spherical LPA micelles are transformed into long tubular micelles, which coalesce and form large cation-lipid complexes (data not shown). Analysis by freeze-fracture electron microscopy showed that these Mg-LPA complexes represented a lamellar phase composed of stacked bilayer disks (Figure 5E). Identical ^{31}P-NMR results were obtained for LPA suspensions at pH 6.0 to which Ca^{2+} was added (not shown), and freeze fracture analysis indicated the formation of a lamellar phase composed of cochleated cylinders of Ca-LPA (Figure 5F). In both cases, freeze-fracture mostly resulted in intrabilayer fracture faces, cross-fractures were rare, thus excluding acyl chain interdigitation. The anhydrous (see below) divalent cation-bilayer complexes showed a bilayer repeat distance of 4.5 ± 0.3 nm, indicating that the acyl chains are not tilted. Cross polarization ^{31}P-NMR analysis (35) of Mg-LPA revealed a powder type spectrum; the very large chemical shift anisotropy of about 80 ppm indicates a complete immobilization of the phosphate headgroup (Figure 5D), in agreement with earlier results obtained for Ca-PA (27). Together, these data show that upon

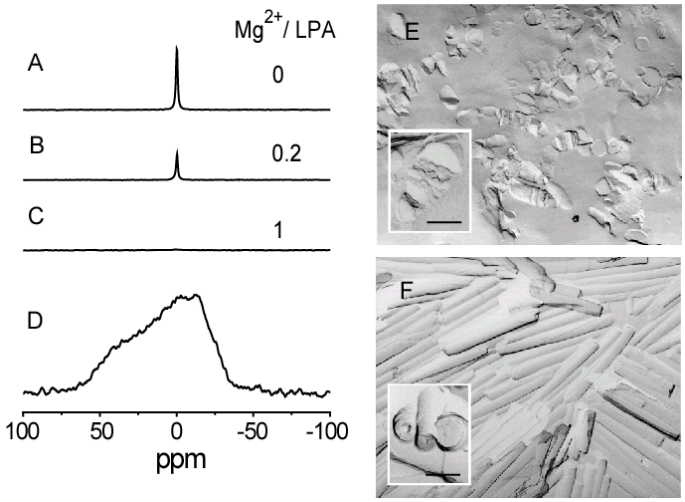

Figure 5: Polymorphic phase behavior of lysophosphatidic acid (LPA). Proton-decoupled ^{31}P-NMR spectra of aqueous dispersions of 1-oleoyl LPA recorded at 37°C and pH 7.2, at a Mg^{2+} to lipid molar ratio of 0 (no Mg^{2+} A), 0.2 (B), 1.0 (C); the intensity of these peaks can be compared as they were recorded under identical experimental conditions. Cross polarization spectrum of the Mg-LPA complex (D). Freeze fracture EM analysis of Mg-LPA complexes at pH 7.2 (E), and of Ca-LPA complexes at pH 6.0 (F); divalent cation to lipid molar ratio of 1.0. E, F at the same magnification, bars (inserts), 100 nm.

interaction with Ca^{2+} or Mg^{2+}, LPA forms anhydrous bilayer complexes in which the acyl chains are not tilted or interdigitated. Apparently, the cross sectional area of the LPA headgroup is very close to that of the oleoyl fatty acyl chain, i.e. around 21 Å^2, giving LPA an overall cylindrical shape. This is a remarkable result in view of the gel state lamellar phases described for other lyso-lipids, such as lyso-phosphatidylcholine in which bilayer formation is only possible if the relatively large cross-sectional area of the lipid headgroup is compensated by acyl chain interdigitation (36).

The molecular shape of 1-oleoyl-LPA was also studied in mixed-lipid LPA/DOPE systems. The presence of LPA, 10 mol% of total lipid, stabilized the bilayer phase shifting T_H upwards by 25 °C relative to pure DOPE (Figure 6A, quantified in 6C, curve 5). Essentially the same results were obtained in the absence and presence of Mg^{2+} (Figure 6C, curves 5 and 4), and in LPA/DEPE mixed-lipid systems (data not shown). After overnight dialysis of the LPA/PE suspension at cytosolic conditions, pH 7.2 and 0.5 mM free Mg^{2+}, T_H was also clearly shifted upwards (Figure 6B, curve 3). To obtain more information on the molecular shape of LPA, the effect of LPA on the phase behavior of DOPE was compared to that of the cylindrically shaped lipid dioleoylphosphatidylcholine (DOPC) and the strongly inverted cone-shaped lipid 1-oleoyl-LPC. The inclusion of DOPC resulted in an increase in T_H by 17 °C, 8 °C less than that caused by LPA, while LPC induced a 2 °C greater increase in T_H than LPA (Figure 6C, compare

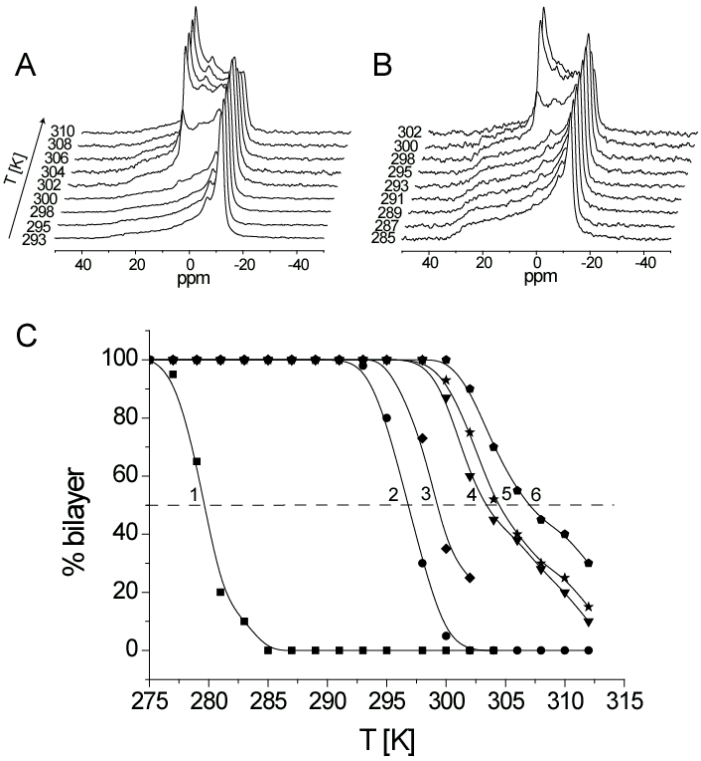

Figure 6: Lysophosphatidic acid (LPA) stabilizes the bilayer phase of phosphatidylethanolamine (PE). Proton-decoupled ^{31}P-NMR spectra recorded as a function of temperature at pH 7.2, of an aqueous dispersion of DOPE/LPA (10 mol%; A), and of DOPE/LPA dialyzed against 0.5 mM Mg^{2+} (B). The amount of lamellar phase was determined as a function of temperature at pH 7.2 (C): DOPE, ■; DOPE/DOPC (10 mol%), ●; DOPE/LPA (10 mol%), ★; DOPE/LPA dialyzed against 0.5 mM Mg^{2+}, ♦; DOPE/LPA with Mg^{2+} equimolar with respect to total lipid, ▼ ; DOPE/LPC (10 mol%), ⬟. Note that the phase behavior of DOPE and mixtures of DOPE with DOPC or LPC were not influenced by the presence of Mg^{2+} (data not shown).

curves 2, 5 and 6). Thus, in a mixed-lipid system at cytosolic conditions, LPA behaves similarly to LPC, i.e. as an inverted cone (type-I) shaped lipid. As such, the influence of LPA on the phase behavior of DOPE is opposite to that of PA, indicating that a conversion of LPA into PA by BARS or endophilin may induce negative membrane curvature.

Discussion

The local formation of polyphosphoinositides, DAG, and PA, plays a key role in the regulation of intracellular membrane traffic (5-10). Apart from an indirect role in recruiting specialized proteins involved in cargo selection and membrane tubulation, fission and fusion, these lipids may well play a direct role in membrane

bending and destabilization, by virtue of their special biophysical properties. The possibility that a change in lipid composition affects the local biophysical properties of the membrane driving membrane bending and destabilization is particularly attractive in the regulation of membrane fission (Figure 7). Fission differs from fusion in that it requires strong membrane bending and the formation of a highly constricted neck prior to local membrane contact and destabilization (2). Membrane destabilization during most biomembrane fusion events probably involves fusogenic proteins that intimately interact with and destabilize the contacting membrane leaflets (2, 3). However, although fission events such as endocytic and Golgi membrane fission appear to be regulated exclusively by cytosolic proteins, these proteins now act on the 'wrong' side of the membrane, opposite to the membrane leaflets that initially interact. Thus, a key question is how the curvature in the neck region is generated, and how the interacting membrane leaflets are destabilized. In the current study we determined the phase properties of PA and LPA carrying oleoyl fatty acids at conditions relevant to Golgi and endocytic membrane fission. The central aim was to evaluate the potential role of LPA acyltransferases in biomembrane fission, i.e. in the formation of a constricted neck and in membrane destabilization. Our data show that PA and LPA have remarkable biophysical properties and that these properties are greatly influenced by physiological concentrations of divalent cations and subtle changes in pH. These findings are summarized below and subsequently discussed in the light of current models of biomembrane fission.

The molecular shape of phosphatidic acid and lysophosphatidic acid

At physiological conditions, neutral pH and, in the presence of Mg^{2+}, both PA and LPA formed bilayers suggesting a nearly cylindrical shape for both lipids at cytosolic conditions. Despite carrying only one acyl chain, LPA formed cation-LPA bilayer complexes, which showed no sign of acyl chain tilting or interdigitation. Another unexpected observation was the extreme pH sensitivity of the phase behavior of PA under physiological conditions; a mild reduction in pH to values around pH 6.4 was sufficient to trigger H_{II} formation in the presence of divalent cations. This pH-dependence of the polymorphic behavior of PA can be explained by considering divalent cation-lipid interactions and the pH-dependent charge of the lipid headgroup. The pK_1 and pK_2 of the phosphate headgroup of PA at high ionic strength are 3.5 and 8.5 (37, 38). The H_{II} phase is only formed at (mildly) acidic pH values, at which PA has one net negative charge, and thus most likely involves the interaction of two PA molecules and one divalent cation into a neutral cation-lipid complex (15). Similar to Ca^{2+}-cardiolipin systems, H_{II} formation is driven by lipid charge neutralization and headgroup dehydration, both decreasing the effective size of the lipid headgroup (39, 40).

Although results obtained in single-lipid systems are relevant to membrane microdomains highly enriched in PA and or LPA, the molecular shape of PA and LPA deduced from these studies may not apply to physiological lipid mixtures.

Therefore, the molecular shape of DOPA and 1-oleoyl-LPA was also studied in mixed-lipid systems; a matrix of unsaturated PE to which 10 mol% LPA or PA was added. At cytosolic conditions, PA induced a shift in lipid phase behavior from bilayer towards the inverted hexagonal H_{II} phase in mixtures with DEPE but not with DOPE, indicating that DOPA behaves as a cone-shaped (type-II) lipid, with a shape similar to that of DOPE (see Figure 3C). The fact that pure DOPA at the same conditions behaves as a cylindrical bilayer-preferring lipid and forms a lamellar phase (Figures 1 and 2) can be understood by considering the higher charge density in the pure DOPA system which is likely to inhibit bilayer-to-H_{II} phase transitions (41). Qualitatively, the results obtained in the single- and mixed-lipid systems match in that the strongest bilayer destabilization in the PA/PE system was observed in the presence of divalent cations at acidic pH, indicating that the type-II preference or cone-shape of DOPA will be more pronounced at intra-Golgi than at cytosolic conditions. LPA had an opposite effect on the phase behavior of PE. At cytosolic conditions, LPA stabilized the bilayer phase of PE, and a comparison of the effects of LPA, DOPC, and 1-oleoyl-LPC, indicated a molecular shape for LPA close to that of LPC, i.e. an inverted cone (type-I) shape (see Figure 3A).

Lysophosphatidic acid acyltransferases, negative membrane curvature and membrane fission

Taken together, our data indicate that a conversion of 1-oleoyl-LPA into DOPA mediated by LPA acyltransferases such as BARS or endophilin may result in a significant shift in spontaneous monolayer curvature towards more negative values (Figure 7A). Note that although the LPA substrate requirements have not been determined in detail, available data suggest that endophilin-mediated endocytic membrane fission *in-vitro* requires conversion of oleoyl-LPA into oleoyl-arachidonoyl-PA (19). A recent study on mixed-lipid systems containing different PC species indicates that in stearoyl-arachidonoyl-PC the acyl chains have a larger cross-sectional area than in stearoyl-oleoyl-PC (42). Thus, in comparison to the dioleoyl-PA characterized in the current study, the presence of a polyunsaturated fatty acyl chain in oleoyl-arachidonoyl-PA possibly results in a more pronounced cone-shape.

Experiments on model and erythrocyte membranes have shown that a difference in spontaneous monolayer curvature between the two membrane leaflets can drive membrane bending [reviewed in (2)]. However, it is not immediately obvious how negative spontaneous monolayer curvature induced in the cytosolic leaflet would result in membrane fission. In pure lipid model systems, membrane budding and fission correlate with the induction of positive monolayer curvature (43). On the other hand, a complete biophysical and theoretical analysis of membrane fission intermediates is not yet available. The lipid requirements for the various stages of neck constriction and semi-fusion/fission may be different, and LPAAT's could regulate a particular stage of membrane constriction.

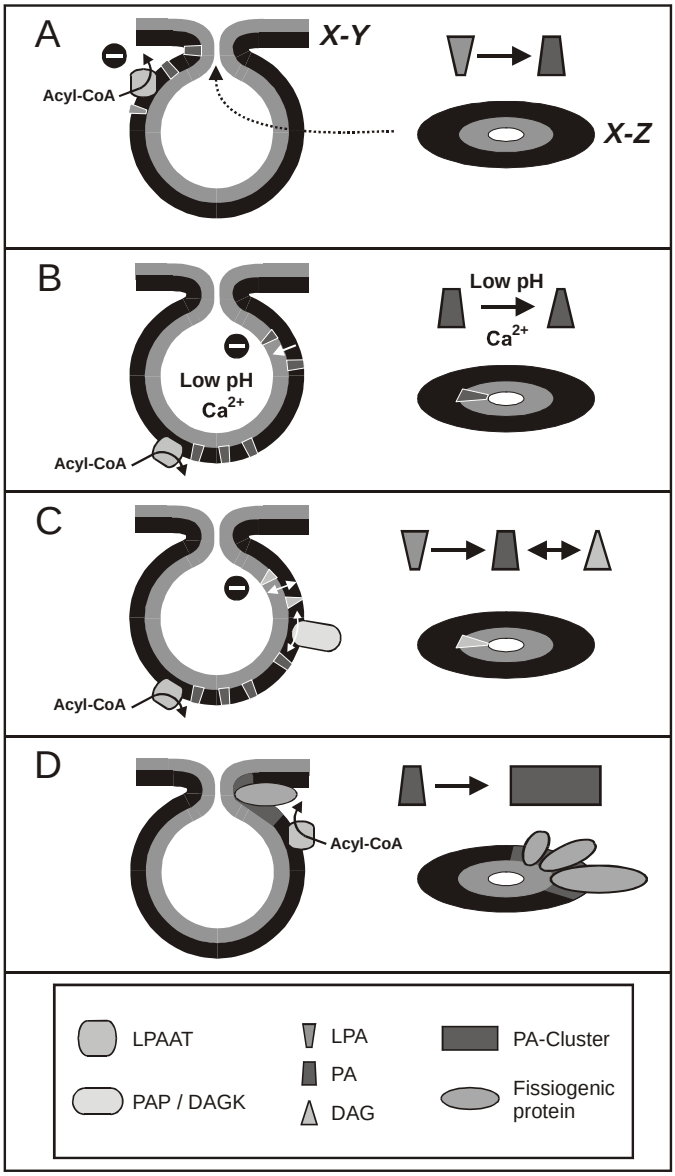

Figure 7: Speculative models for the role of lysophosphatidic acid (LPA) acyltransferases, phosphatidic acid (PA), and diacylglycerol (DAG) in biomembrane fission. LPA acyltransferases may change the spontaneous monolayer curvature towards more negative values (A). The curvature of the constricted neck is different in the x-y plane (shown on the left) as compared to the x-z plane (shown on the right). PA undergoes transbilayer movement and induces negative spontaneous monolayer curvature in the inner leaflet, and may be directly involved in closure of the neck in conjunction with Ca^{2+} and a mildly acidic pH in the Golgi lumen (B). PA is rapidly converted to DAG which is capable of very rapid transbilayer movement; DAG is a particularly potent inducer of negative spontaneous monolayer curvature (C). Intermolecular hydrogen-bonding and protein-lipid interactions result in clusters of PA molecules which may act as platforms for the membrane insertion of fissiogenic proteins destabilizing the neck region. Note that the lipid requirements for the various stages of neck constriction and semi-fusion/fission may be different, and that the models shown here are not mutually exclusive (PAP, PA-phosphatase; DAGK, DAG-kinase). For more details see text [and references (2, 44, 45)].

Moreover, membrane fission is likely to depend on a dynamic interplay between lipids and proteins. A recent theoretical analysis indicates that if a constricted neck is constrained by a rigid protein collar, a subsequent shift of the spontaneous curvature of the neck membrane towards more negative values can destabilize the neck and result in membrane fission (43). Thus, a concerted action of endophilin and dynamin may be required for endocytic membrane fission; a similar partner for BARS remains to be identified.

It should be realized that the LPAAT activity of endophilin and BARS has been found in *in-vitro* systems and that although evidence is accumulating in favor of a key role of BARS and endophilin in Golgi and endocytic membrane fission, the actual role of LPAAT activity in the induction of membrane fission *in-vivo* remains to be determined. Moreover, even if the LPAAT activity of BARS and endophilin turns out to be essential for Golgi and endocytic membrane fission, there are several alternative possibilities for the molecular mechanism involved. The most likely scenarios are discussed below [also see (2, 44, 45)].

Transbilayer movement of phosphatidic acid and membrane destabilization

A remarkable observation in the current study is the strong dependence of the molecular shape of DOPA on physiological pH values and divalent cation concentrations. PA (analogs) can easily translocate across (model) membranes (46-48), in particular in the presence of membrane spanning α-helical peptide-segments and absence of cholesterol (Kol and de Kruijff; unpublished data). In addition, Golgi membranes appear to contain a protein that stimulates transbilayer equilibration of glycerophospholipids (49). Thus, instead of changing the spontaneous curvature of the cytosolic membrane leaflet, PA may translocate to and induce negative spontaneous curvature in the exoplasmic leaflet of the membrane (Figure 7B). In the Golgi complex, the effects of PA on membrane curvature would be enhanced by the mildly acidic pH and high Ca^{2+} concentration in the Golgi lumen. Moreover, PA is a fusogenic lipid, and relatively low concentrations of PA on the surface of mixed-lipid vesicles induce efficient membrane fusion in the presence of divalent cations (48, 50). After translocating across the Golgi membrane, PA could be involved at the key stage of membrane fission, in the closure and destabilization of the membrane neck.

Conversion of phosphatidic acid to diacylglycerol: the PA-DAG cycle

Phosphatidic acid is further metabolized and converted into DAG, and vice versa DAG-kinases convert DAG into PA (6). Diacylglycerol has a very pronounced type-II shape (42, 51), and differs from PA by being uncharged and capable of extremely rapid transbilayer movement (52). Like phosphoinositides and PA, DAG is a key lipid involved in the regulation of intracellular membrane traffic (6). Diacylglycerol acts as a membrane receptor for specific proteins, such as members of the PKC family. One of these proteins, PKD, binds to DAG in the TGN, and is involved in the formation of TCs that carry cargo from the Golgi to the plasma

membrane (7). Recent data obtained in intact cells suggest that BARS is also involved in TC formation at the TGN (Alberto Luini, personal communication), suggesting that a PA-DAG cycle may play a central role in TC formation. In line with this suggestion, a recent theoretical analysis indicates that BARS-mediated conversion of LPA into PA, followed by PA-dephosphorylation and the repartitioning of the negatively curved DAG may drive the progressive constriction of Golgi membrane tubules (Figure 7C) and explain the "pearling" of Golgi tubules (8) induced by BARS (Misha Kozlov, personal communication).

Phosphatidic acid-enriched microdomains as membrane insertion sites

Finally, PA or one of its metabolites may recruit and activate downstream effectors involved in membrane bending or fission. Phosphatidic acid is unique among anionic lipids because of its small and highly charged headgroup very close to the glycerol backbone, and its high tendency to form microdomains through intermolecular hydrogen bonding (11, 12). In an earlier study we described that dynamin, a large GTPase regulating membrane constriction and fission during receptor-mediated endocytosis, is a membrane-active molecule capable of penetrating in between lipid head groups, and that lipid penetration is strongly stimulated by PA (18). A partial reduction in charge, e.g. upon divalent cation interaction reduces electrostatic repulsion between the PA headgroups and increases attractive hydrogen bonding interactions, which may result in fluid-fluid immiscibility and the formation of microdomains enriched in PA (13, 53). These still highly charged microdomains may induce conformational changes in the interacting proteins, as well as serve as membrane insertion sites (Figure 7D). Thus, instead of affecting membrane curvature, the PA generated by dynamin-bound endophilin may induce penetration of dynamin into the membrane of the neck region, followed by membrane destabilization and fission (18). Other membrane fission and fusion events may involve the generation of PA and PA-rich microdomains by enzymes such as CtBP/BARS, phospholipase D, or DAG-kinase followed by membrane insertion of a membrane-destabilizing protein.

Concluding remarks

As illustrated by the shear number of models discussed above, the current knowledge on biomembrane fission is still limited. Many of the players remain to be identified, and we are only starting to understand the biophysical principles and molecular mechanisms underlying the regulation of biomembrane fission. With respect to the role of LPA acyltransferases and biomembrane fission, it will be important to establish the role of LPA acylation in intact cells *in-vivo*. In more general terms, our understanding of the role of lipids in membrane fission, as well as in other membrane transport and cell signaling events, is hampered by the relative ignorance of both steady-state lipid compositions of organelles and of local lipid metabolism. In order to fill this gap, lipids and lipid metabolic events will have to be localized at high spatial and temporal resolution, i.e. in relation to the

actual membrane fission event in live cells. This will require both the development of cellular systems in which TC formation and membrane fission can be synchronized, as well as a new set of morphological techniques (54). Particularly promising are the use of specific lipid-binding domains in lipid localization studies (55), and combinations of live cell imaging and electron microscopy (56). Even if the protein and lipid factors and the sequence of events during membrane fission have been determined in live cells, understanding the underlying molecular mechanism will require reconstitution of (parts of) the membrane fission machineries in lipid model systems, followed by a detailed biophysical and theoretical analysis of membrane fission and the lipids and lipid-protein interactions involved.

Acknowledgments

We thank Frits Flesch, Alberto Luini, Alberto Weigert, Arie Verkleij, and Misha Kozlov for helpful discussions and critical reading of the manuscript. BdK, EEK, and KNJB are supported by NWO/FOM/ALW, "Fysische Biologie" program. KNJB is supported by the Human Frontier Science Program Organization.

References

1. Lippincott-Schwartz J. (2001) The secretory membrane system studied in real-time. Histochem. Cell Biol. *116*, 97-107.
2. Burger KNJ. (2000) Greasing membrane fusion and fission machineries. Traffic *1*, 605-613.
3. Lentz BR, Malinin V, Haque ME, and Evans K. (2000) Protein machines and lipid assemblies: current views of cell membrane fusion. Curr. Opin. Struct. Biol. *10*, 607-615.
4. Chernomordik L, Kozlov MM, and Zimmerberg J. (1995) Lipids in biological membrane fusion. J. Membr. Biol. *146*, 1-14.
5. Cremona O, and De Camilli P. (2001) Phosphoinositides in membrane traffic at the synapse. J. Cell Sci. *114*, 1041-1052.
6. Bankaitis VA. (2002) Cell biology. Slick recruitment to the Golgi. Science *295*, 290-291.
7. Baron CL, and Malhotra V. (2002) Role of diacylglycerol in PKD recruitment to the TGN and protein transport to the plasma membrane. Science *295*, 325-328.
8. Weigert R, Silletta MG, Spano S, Turacchio G, Cericola C, Colanzi A, Senatore S, Mancini R, Polishchuk EV, Salmona M, Facchiano F, Burger KNJ, Mironov A, Luini A, and Corda D. (1999) CtBP/BARS induces fission of Golgi membranes by acylating lysophosphatidic acid. Nature *402*, 429-433.
9. Roth MG, Bi K, Ktistakis NT, and Yu S. (1999) Phospholipase D as an effector for ADP-ribosylation factor in the regulation of vesicular traffic. Chem. Phys. Lipids *98*, 141-152.
10. Siddhanta A, and Shields D. (1998) Secretory vesicle budding from the trans-Golgi network is mediated by phosphatidic acid levels. J. Biol. Chem. *273*, 17995-17998.
11. Demel RA, Yin CC, Lin BZ, and Hauser H. (1992) Monolayer characteristics and thermal behaviour of phosphatidic acids. Chem. Phys. Lipids *60*, 209-223.
12. Boggs JM. (1987) Lipid intermolecular hydrogen bonding: influence on structural organization and membrane function. Biochim. Biophys. Acta *906*, 353-404.
13. Garidel P, and Blume A. (2000) Calcium induced non-ideal mixing in liquid-crystalline phosphatidylcholine-phosphatidic acid bilayer membranes. Langmuir *16*, 1662-1667.

14. Leventis R, Gagne J, Fuller N, Rand RP, and Silvius JR. (1986) Divalent cation induced fusion and lipid lateral segregation in phosphatidylcholine-phosphatidic acid vesicles. Biochemistry *25*, 6978-6987.
15. Verkleij AJ, De Maagd R, Leunissen-Bijvelt J, and de Kruijff B. (1982) Divalent cations and chlorpromazine can induce non-bilayer structures in phosphatidic acid-containing model membranes. Biochim. Biophys. Acta *684*, 255-262.
16. Farren SB, Hope MJ, and Cullis PR. (1983) Polymorphic phase preferences of phosphatidic acid: A ^{31}P and ^{2}H NMR study. Biochem. Biophys. Res. Commun. *111*, 675-682.
17. Athenstaedt K, and Daum G. (1999) Phosphatidic acid, a key intermediate in lipid metabolism. Eur. J. Biochem. *266*, 1-16.
18. Burger KNJ, Demel RA, Schmid SL, and de Kruijff B. (2000) Dynamin is membrane-active: lipid insertion is induced by phosphoinositides and phosphatidic acid. Biochemistry *39*, 12485-12493.
19. Schmidt A, Wolde M, Thiele C, Fest W, Kratzin H, Podtelejnikov AV, Witke W, Huttner WB, and Söling HD. (1999) Endophilin I mediates synaptic vesicle formation by transfer of arachidonate to lysophosphatidic acid. Nature *401*, 133-141.
20. Pfanner N, Orci L, Glick BS, Amherdt M, Arden SR, Malhotra V, and Rothman JE. (1989) Fatty acyl-coenzyme A is required for budding of transport vesicles from Golgi cisternae. Cell *59*, 95-102.
21. Israelachvili JN, Marcelja S, and Horn RG. (1980) Physical principles of membrane organization. Q. Rev. Biophys. *13*, 121-200.
22. Cullis PR, Hope MJ, and Tilcock CP. (1986) Lipid polymorphism and the roles of lipids in membranes. Chem. Phys. Lipids *40*, 127-144.
23. Janes N. (1996) Curvature stress and polymorphism in membranes. Chem. Phys. Lipids *81*, 133-150.
24. Cullis PR, and de Kruijff B. (1979) Lipid polymorphism and the functional roles of lipids in biological membranes. Biochim. Biophys. Acta *559*, 399-420.
25. Pfeiffer DR, Reed PW, and Lardy HA. (1974) Ultraviolet and fluorescent spectral properties of the divalent cation ionophore A23187 and its metal ion complexes. Biochemistry *13*, 4007-4014.
26. Smaal EB, Mandersloot JG, Demel RA, de Kruijff B, and de Gier J. (1987) Consequences of the interaction of calcium with dioleoylphosphatidate-containing model membranes: calcium-membrane and membrane-membrane interactions. Biochim. Biophys. Acta *897*, 180-190.
27. Smaal EB, Nicolay K, Mandersloot JG, de Gier J, and de Kruijff B. (1987) 2H-NMR, 31P-NMR and DSC characterization of a novel lipid organization in calcium-dioleoylphosphatidate membranes. Implications for the mechanism of the phosphatidate calcium transmembrane shuttle. Biochim. Biophys. Acta *897*, 453-466.
28. Llopis J, McCaffery JM, Miyawaki A, Farquhar MG, and Tsien RY. (1998) Measurement of cytosolic, mitochondrial, and Golgi pH in single living cells with green fluorescent proteins. Proc. Natl. Acad. Sci. USA *95*, 6803-6808.
29. Seksek O, Biwersi J, and Verkman AS. (1995) Direct measurement of trans-Golgi pH in living cells and regulation by second messengers. J. Biol. Chem. *270*, 4967-4970.
30. Demaurex N, Furuya W, D'Souza S, Bonifacino JS, and Grinstein S. (1998) Mechanism of acidification of the trans-Golgi network (TGN). In situ measurements of pH using retrieval of TGN38 and furin from the cell surface. J. Biol. Chem. *273*, 2044-2051.
31. Pinton P, Pozzan T, and Rizzuto R. (1998) The Golgi apparatus is an inositol 1,4,5-trisphosphate-sensitive Ca^{2+} store, with functional properties distinct from those of the endoplasmic reticulum. EMBO J. *17*, 5298-5308.
32. de Kruijff B, Cullis PR, Verkleij AJ, Hope MJ, Van Echteld CJA, and Taraschi TF. (1985) Lipid polymorphism and membrane function. In: Martonosi AN, editor. The Enzymes of Biological Membranes. 2 ed. New York: Plenum Press; p. 131-204.
33. Fuller N, and Rand RP. (2001) The influence of lysolipids on the spontaneous curvature and bending elasticity of phospholipid membranes. Biophys. J. *81*, 243-254.
34. Toombes GE, Finnefrock AC, Tate MW, and Gruner SM. (2002) Determination of L_{α}-H_{II} phase transition temperature for 1,2-dioleoyl-sn-glycero-3-phosphatidylethanolamine. Biophys. J. *82*, 2504-2510.
35. Griffin RG. (1981) Solid state nuclear magnetic resonance of lipid bilayers. Methods Enzymol. *72*, 108-174.

36. Slater JL, and Huang CH. (1988) Interdigitated bilayer membranes. Prog. Lipid Res. *27*, 325-359.
37. Putney JW, Jr., Weiss SJ, Van De Walle CM, and Haddas RA. (1980) Is phosphatidic acid a calcium ionophore under neurohumoral control? Nature *284*, 345-347.
38. van Dijck PW, de Kruijff B, Verkleij AJ, van Deenen LL, and de Gier J. (1978) Comparative studies on the effects of pH and Ca^{2+} on bilayers of various negatively charged phospholipids and their mixtures with phosphatidylcholine. Biochim. Biophys. Acta *512*, 84-96.
39. Rand RP, and Sengupta S. (1972) Cardiolipin forms hexagonal structures with divalent cations. Biochim. Biophys. Acta *255*, 484-92.
40. De Kruijff B, Verkleij AJ, Leunissen-Bijvelt J, Van Echteld CJ, Hille J, and Rijnbout H. (1982) Further aspects of the Ca^{2+}-dependent polymorphism of bovine heart cardiolipin. Biochim. Biophys. Acta *693*, 1-12.
41. Lewis RN, and McElhaney RN. (2000) Surface charge markedly attenuates the nonlamellar phase-forming propensities of lipid bilayer membranes: calorimetric and ^{31}P-nuclear magnetic resonance studies of mixtures of cationic, anionic, and zwitterionic lipids. Biophys. J. *79*, 1455-1464.
42. Szule JA, Fuller NL, and Rand RP. (2002) The effects of acyl chain length and saturation of diacylglycerols and phosphatidylcholines on membrane monolayer curvature. Biophys. J. *83*, 977-984.
43. Kozlov MM. (2001) Fission of biological membranes: Interplay between dynamin and lipids. Traffic *2*, 51-65.
44. Huttner WB, and Schmidt A. (2000) Lipids, lipid modification and lipid-protein interaction in membrane budding and fission - insights from the roles of endophilin A1 and synaptophysin in synaptic vesicle endocytosis. Curr Opin Neurobiol *10*, 543-551.
45. Huttner WB, and Schmidt AA. (2002) Membrane curvature: a case of "endofeelin". Tr. Cell Biol. *12*, 155-158.
46. de Kruijff B, and Baken P. (1978) Rapid transbilayer movement of phospholipids induced by an asymmetrical perturbation of the bilayer. Biochim. Biophys. Acta *507*, 38-47.
47. Eastman SJ, Hope MJ, and Cullis PR. (1991) Transbilayer transport of phosphatidic acid in response to transmembrane pH gradients. Biochemistry *30*, 1740-1745.
48. Eastman SJ, Hope MJ, Wong KF, and Cullis PR. (1992) Influence of phospholipid asymmetry on fusion between large unilamellar vesicles. Biochemistry *31*, 4262-8.
49. Buton X, Herve P, Kubelt J, Tannert A, Burger KNJ, Fellmann P, Müller P, Herrmann A, Seigneuret M, and Devaux PF. (2002) Transbilayer movement of monohexosyl sphingolipids in endoplasmic reticulum and Golgi membranes. Biochemistry *41*, 13106-13115
50. Summers SA, Guebert BA, and Shanahan MF. (1996) Polyphosphoinositide inclusion in artificial lipid bilayer vesicles promotes divalent cation-dependent membrane fusion. Biophys. J. *71*, 3199-3206.
51. Leikin S, Kozlov MM, Fuller NL, and Rand RP. (1996) Measured effects of diacylglycerol on structural and elastic properties of phospholipid membranes. Biophys. J. *71*, 2623-32.
52. Bai J, and Pagano RE. (1997) Measurement of spontaneous transfer and transbilayer movement of BODIPY-labeled lipids in lipid vesicles. Biochemistry *36*, 8840-8848.
53. Garidel P, Johann C, and Blume A. (1997) Nonideal mixing and phase separation in phosphatidylcholine-phosphatidic acid mixtures as a function of acyl chain length and pH. Biophys. J. *72*, 2196-2210.
54. Mironov AA , Beznoussenko GV , Nicoziani P, Martella O, Trucco A, Kweon HS, Di Giandomenico D, Polishchuk RS, Fusella A, Lupetti P, Berger EG, Geerts WJC, Koster AJ, Burger KNJ, and Luini A. (2001)Small cargo proteins and large aggregates can traverse the Golgi by a common mechanism without leaving the lumen of cisternae. J. Cell Biol. *155*, 1225-1238.
55. Gillooley DJ, Morrow IC, Lindsay M, Gould R, Bryant NJ, Gaullier JM, Parton RG, and Stenmark H. (2000) Localization of phosphatidylinositol 3-phosphate in yeast and mammalian cells. EMBO J. *19*, 4577-4588.
56. Polishchuk RS, Polishchuk EV, Marra P, Alberti S, Buccione R, Luini A, and Mironov AA. (2000) Correlative light-electron microscopy reveals the tubular-saccular ultrastructure of carriers operating between Golgi apparatus and plasma membrane. J. Cell Biol. *148*, 45-58.

57. Rouser G, Fleischer S, and Yamamoto A. (1970) Two-dimensional thin-layer chromatographic separation of polar lipids and determination of phospholipids by phosphorus analysis of spots. Lipids *5*, 494-496.
58. Bers DM, Patton CW, and Nuccitelli R. (1994) A practical guide to the preparation of Ca^{2+} buffers. Methods Cell Biol. *40*, 3-29.
59. Costello MJ, Fetter R, and Hochli M. (1982) Simple procedures for evaluating the cryofixation of biological samples. J. Microsc. *125*, 125-136.

CHAPTER 3

Spontaneous curvature of phosphatidic acid and lysophosphatidic acid

Taken from:
Biochemistry (2005) *44,* 2097-2102

Abstract

The formation of phosphatidic acid (PA) from lysophosphatidic acid (LPA), diacylglycerol, or phosphatidylcholine plays a key role in the regulation of intracellular membrane fission events, but the underlying molecular mechanism has not been resolved. A likely possibility is that PA affects local membrane curvature facilitating membrane bending and fission. To examine this possibility, we determined the spontaneous radius of curvature (R_{0p}) of PA and LPA, carrying oleoyl fatty acids, using well-established X-ray diffraction methods. We found that, under physiological conditions of pH and salt concentration (pH 7.0, 150 mM NaCl), the R_{0p} values of PA and LPA were -46 Å and +20 Å, respectively. Thus PA has considerable negative spontaneous curvature while LPA has the most positive spontaneous curvature of any membrane lipid measured to date. The further addition of Ca^{2+} did not significantly affect lipid spontaneous curvature; however, omitting NaCl from the hydration buffer greatly reduced the spontaneous curvature of PA, turning it into a cylindrically shaped lipid molecule (R_{0p} of -1.3×10^2 Å). Our quantitative data on the spontaneous radius of curvature of PA and LPA at a physiological pH and salt concentration will be instrumental in developing future models of biomembrane fission.

Introduction

Intracellular membrane transport occurs through the selective fission and fusion of membrane bound transport carriers (TCs), which contain specific lipid and protein cargo (*1*). Just prior to fission the TCs consist of a bud, which can be a vesicular or large saccular-tubular (pleiomorphic) structure, connected to the membrane by a narrow neck. Fission is the process that severs the neck releasing the TC from the donor membrane, and fusion is the process by which the TC merges with an acceptor membrane. The molecular rearrangements that accompany fission and fusion are related, both requiring restructuring of the equilibrium bilayer configuration into highly curved non-bilayer intermediates (*2*, *3*).

Fission and fusion are highly regulated events and do not occur spontaneously in vivo, but under strict control of specialized proteins. Recent evidence suggests that these proteins do not act alone but in concert with specific membrane lipids, such as phosphoinositides (*4-6*), diacylglycerol (DAG) (*7*, *8*), and phosphatidic acid (PA) (*7*, *9-11*). The role of these lipids maybe 2-fold: (i) to recruit specialized proteins to the sites of fission and fusion and (ii) to facilitate membrane bending and the formation of highly curved intermediates, and thus reduce the energy barriers of fission and fusion. In the current study we focus on PA and the related lipid lysophosphatidic acid (LPA).

Formation of PA is a recurring theme in signaling pathways regulating Golgi membrane transport (*10*, *11*). In the Golgi, PA is generated by ARF-activated PLD, which converts phosphatidylcholine (PC) into PA and choline (*10*), by DAG-

kinases (*7*), and by 50 kDa brefeldin A ribosylated substrate (BARS). In *in vitro* experiments on isolated Golgi membranes, BARS was shown to act as an enzyme converting LPA into PA using long chain acyl-CoA's as the acyl chain donor, and LPA acyltransferase (LPAAT) activity and Golgi membrane fission appeared to be linked (*9*). Interestingly, endophilin-A1, a protein involved in endocytic membrane fission, has been independently shown to display the same enzymatic activity (*12*), and the N-terminal lipid-modifying domain of endophilin B1 was very recently shown to be involved in the maintenance of mitochondrial morphology (*13*). Together these findings suggest that the local formation of PA from LPA, or through any of the aforementioned lipid metabolic pathways, could be part of a universal "lipid machinery" for membrane fission. If such a mechanism exists, it is likely to depend on special biophysical properties of PA. Of particular interest is the spontaneous curvature of PA and LPA because local changes in spontaneous monolayer curvature are known to affect membrane fission and fusion events (*3*, *14-16*). Lipid spontaneous (or "intrinsic") curvature is a quantitative measure of the effective lipid molecular shape, and describes the tendency of a lipid species to form non-bilayer (curved) structures (*17-20*). The aim of the current study was to directly measure the spontaneous curvature (the inverse of the spontaneous radius of curvature) of PA and LPA at a physiological pH and salt concentration. Our study extends previous more qualitative studies on the molecular shape of (L)PA (*21-24*), and now allows theoretical models of biomembrane fission to be developed (*3*, *16*). We show that, under physiological conditions of pH and ionic strength, PA has a negative spontaneous curvature that is slightly less pronounced than that of dioleoylphosphatidylethanolamine (DOPE), while LPA has a spontaneous curvature that is considerably more positive than that of lysophosphatidylcholine (LPC).

Materials and Methods

Sample Preparation

1,2-Dioleoyl-*sn*-glycero-3-phosphoethanolamine (DOPE), 1,2-dioleoyl-*sn*-glycero-3-phosphate (monosodium salt) (DOPA), and 1-oleoyl-*sn*-glycero-3-phosphate (sodium salt) (LPA) were purchased from Avanti Polar Lipids (Birmingham, AL). Lipid purity was checked by thin-layer chromatography and judged to be more than 99%. *n*-Tetradecane (td) was purchased from Sigma-Aldrich Canada Ltd. (Oakville, ON). Water used in the X-ray experiments was doubly distilled.

Lipid stocks, prepared on the basis of dry weight, were dissolved in chloroform/methanol (2/1 by volume). In the case of LPA a small (~0.6% of total solvent volume) amount of water was added to fully dissolve the lipid. From these solutions mixtures of different DOPA/DOPE and LPA/DOPE composition were prepared and then dried by rotary evaporation and vacuum desiccation. To relieve interstitial packing stresses, 16 wt % tetradecane was added to the dried lipid

stocks and equilibrated for 72 h as previously described (*25*, *26*). Aliquots from each stock were hydrated by either (1) adding weighed amounts of water; (2) adding excess amounts of buffer, 25 mM Tes, 25 mM Mes, 150 mM NaCl set to pH 7.0 using NaOH; or (3) adding excess amounts of buffer as above containing an additional 25 mM $CaCl_2$. Teflon shavings, to provide an internal X-ray calibration standard with a repeat spacing of 4.87 Å, were added just prior to sealing the samples between Mylar windows 1 mm apart.

X-ray Diffraction

The hexagonal (H_{II}) phases formed by the various DOPE/DOPA/td and DOPE/LPA/td mixtures were analyzed using X-ray diffraction, as described (*25-28*). A Rigaku rotating anode X-ray generator produced a Cu $K\alpha_1$ line (λ = 1.540 Å), isolated using a bent quartz crystal monochromator. Guinier X-ray cameras were used to capture the diffraction patterns photographically. Samples were investigated at 22.0 ± 0.5 °C and hexagonal repeat spacings determined with a measuring error of ± 0.1 Å. X-ray data analysis was performed according to refs *26-30*.

Results

Spontaneous Radius of Curvature of DOPA and LPA

In this study we focused on PA and LPA carrying oleoyl (18:1c) fatty acids, because membrane fission induced by the LPA acyltransferases, BARS and endophilin, appears to be most efficient in the presence of unsaturated fatty acyl-CoA (*9*, *12*). The spontaneous radius of curvature of DOPA and LPA can be determined from the (de)hydration behavior of mixtures containing increasing amounts of (L)PA in DOPE. A prerequisite is that hydrocarbon chain stress is relieved by the addition of 16 wt % tetradecane (*20*, *31*). Under these conditions the curvature that is expressed by the lipid monolayers in the H_{II} phase is very close to the spontaneous (intrinsic) curvature, and can be calculated from the hexagonal phase dimension d_{hex} determined by small-angle X-ray reflection.

Figure 1A and Figure 1B show hydration curves for lipid mixtures of varying composition consisting of DOPA/DOPE/td and LPA/DOPE/td, respectively. The hexagonal phase dimension d_{hex} changed with the volume fraction of added water. At low hydration, d_{hex} increased proportionally with the volume fraction of water. This proportional dependence was used to determine one of the parameters used in the calculation of the spontaneous radius of curvature, namely, the volume fraction of water inside the H_{II} phase at full hydration (i.e. in excess water (*20*, *27*)). A second parameter used in the calculation is the lattice dimension in excess water, the equilibrium lattice dimension, indicated by the horizontal lines in Figure 1A, B. These equilibrium lattice dimensions were obtained by averaging the lattice dimensions at high volume fractions of water, and are shown in Figure 2 as a func-

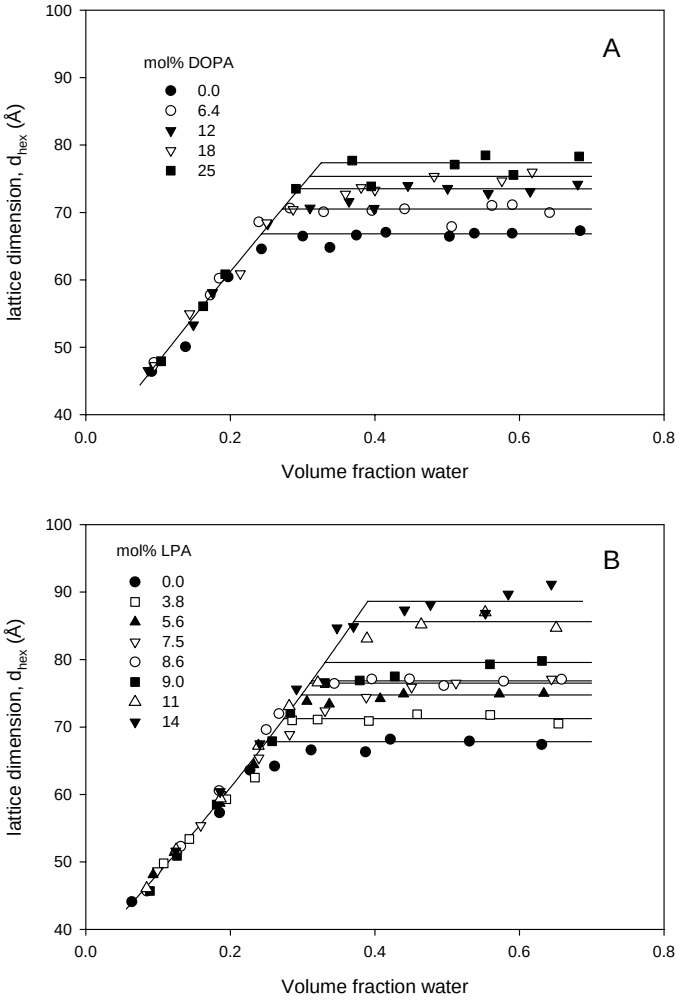

Figure 1: Hydration curves relating the hexagonal phase lattice dimension to water content for various mixtures of (A) DOPA/DOPE/td and (B) LPA/DOPE/td. Horizontal lines represent the equilibrium lattice dimension determined by the average d_{hex} measured in excess water.

tion of (L)PA content.

To calculate the spontaneous radius of curvature of (L)PA we established that a well-defined pivotal plane exists using so-called diagnostic plots (*27*). The linearity of these plots (data not shown, linear regression coefficients r^2 of 0.85 for DOPA and r^2 of 0.91 for LPA containing mixtures) indicated that for both DOPA

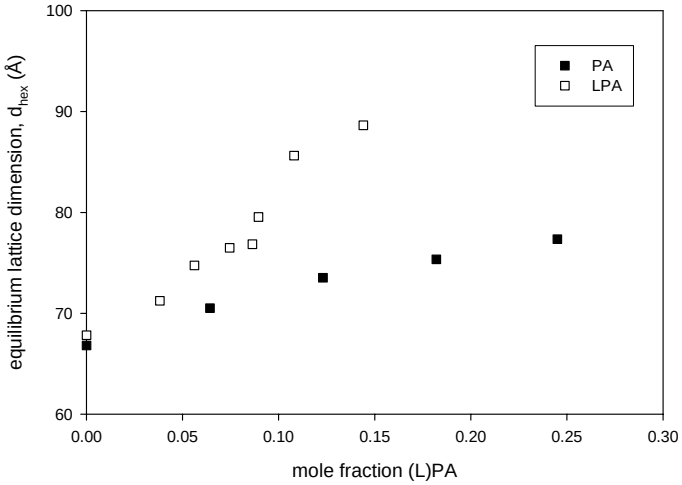

Figure 2: Plot of the average equilibrium lattice dimension for DOPA/DOPE/td and LPA/DOPE/td mixtures.

Table 1: The Spontaneous Radius of Curvature R_{0p} and Spontaneous Curvature $1/R_{0p}$ for (L)PA and DOPE in Comparison to Literature Data

	water		pH 7.0,[a] 150 mM NaCl		pH 7.0,[a] 150 mM NaCl + 25 mM Ca^{2+}		
	R_{0p} (Å)	$1/R_{0p}$ (Å^{-1})	R_{0p} (Å)	$1/R_{0p}$ (Å^{-1})	R_{0p} (Å)	$1/R_{0p}$ (Å^{-1})	refs
DOPA	–130	–0.0077	–46	–0.022	–43	–0.023	this study
LPA[c]	+20	+0.050	+20	+0.050	+23	+0.043	this study
DOPE	–27 ± 1[d]	–0.037	–23 ± 1[d]	–0.043	–22 ± 1[d]	–0.045	this study
DOPE	–28.5 ± 2	–0.035					27
DAG[c]	–11	–0.090					27
LPC	+38	+0.026					29
DOPS	+144	+0.0069					30
DOPC	–140 to –200	–0.0071 to –0.0050					26

[a]In buffer (25 mM Tes, 25 mM Mes set with NaOH) at pH 7.0 containing 150 mM NaCl. [b]In buffer (25 mM Tes, 25 mM Mes set with NaOH) at pH 7.0 containing 150 mM NaCl and 25 mM CaCl2. [c]Oleoyl fatty acid chain(s). [d]Range between data from PA and LPA datasets (n=2).

and LPA containing samples a pivotal plane could be defined and that the spontaneous curvature, $1/R_{0p}$, to this plane could be calculated. The spontaneous curvature is shown in Figure 3 as a function of (L)PA content. The linear relationship allows the spontaneous radius of curvature of the individual lipids to be calculated (see ref *27*). The results are shown in Table 1 and are compared to values previously measured for other lipids.

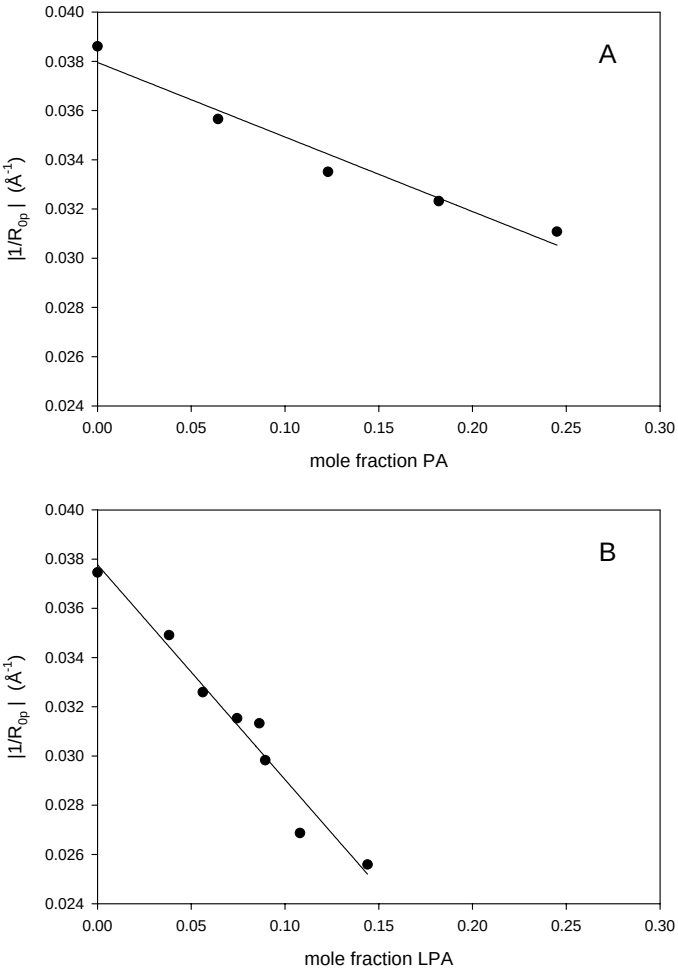

Figure 3: Plot of the absolute value of the spontaneous curvature, $|1/R_{0p}|$, calculated at the pivotal plane for (A) DOPA/DOPE/td and (B) LPA/DOPE/td mixtures as a function of DOPA and LPA content, respectively. Linear regression analysis (in panel A, r^2= 0.96; in panel B, r^2 = 0.96) gives (A) R_{0p}^{DOPA} = 1.3 × 10²Å and R_0^{DOPE} = -26 Å and (B) R_{0p}^{LPA} = +20 Å and R_{0p}^{DOPE} = -27 Å.

Effect of Salts on the Spontaneous Curvature of (L)PA

In the X-ray experiments discussed above, samples were hydrated with doubly distilled water and pH was not controlled. Because screening of lipid headgroup charge by cations is expected to affect lipid packing and spontaneous curvature, we determined the effects of physiological salt concentrations on the lipid spontaneous curvature of (L)PA. Mixtures of DOPA/DOPE/td and LPA/DOPE/td were equilibrated in an excess of buffer containing 150 mM NaCl at pH 7.0. The equilibrium lattice spacings were significantly smaller than those

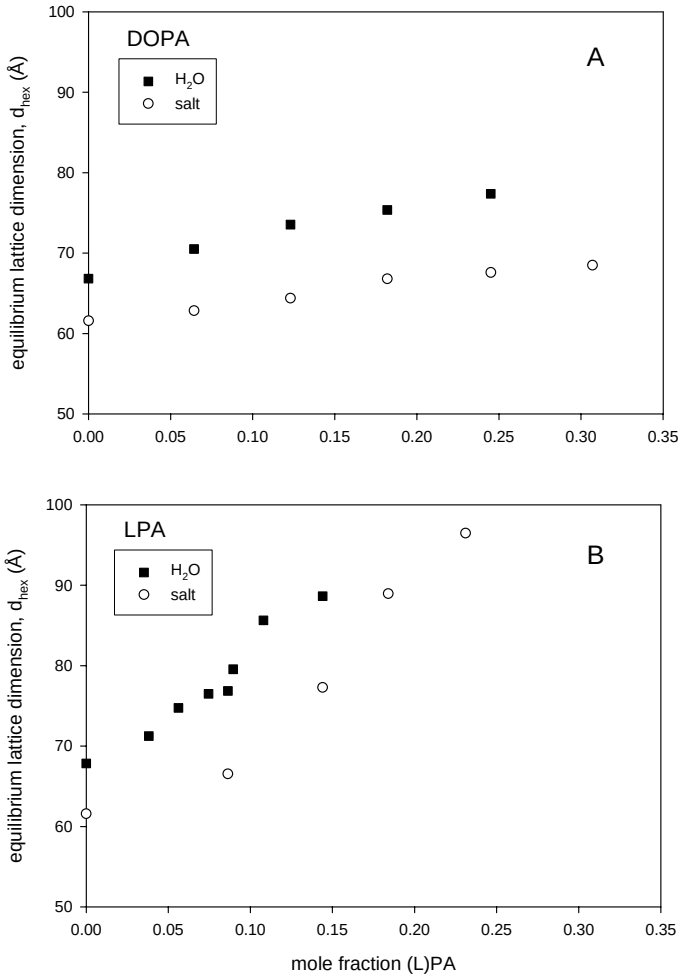

Figure 4: Plot of the equilibrium lattice dimension measured in doubly distilled water (squares) and Mes/Tes-NaOH buffer at pH 7.0 containing 150 mM salt (circles) for (A) DOPA/DOPE/td mixtures and (B) LPA/DOPE/td mixtures.

found in the samples hydrated in excess water without NaCl (Figure 4 A,B), indicating that the addition of salt results in a more negative spontaneous curvature ($1/R_{0p}$) of the mixed lipid monolayers in the H_{II} phase. Note that the addition of salt also slightly affected the spontaneous curvature of DOPE (Figure 4 and Table 1) in agreement with published calorimetric data (*32*, *33*).

To estimate R_{0p} for (L)PA from the equilibrium lattice dimension, d_{hex}, found at pH 7.0 and 150 mM NaCl, we used the proportional dependence found for the hydration behavior in water, to determine the volume fraction of water (buffer) present in the H_{II} phase. We assumed that the lipid molecular dimension, d_l (see ref *27*), is equal to that found for the corresponding lattice dimension in Figure 1 (i.e.

Table 2: Equilibrium Lattice Parameters, d_{hex} and d_l, for DOPA/DOPE/td Mixtures

mol % DOPA	water		pH 7.0,[a] 150 mM NaCl		pH 7.0,[a] 150 mM NaCl + 25 mM Ca^{2+}	
	d_{hex} (Å)	d_l (Å)	d_{hex} (Å)	d_l (Å)	d_{hex} (Å)	d_l (Å)
0.0	66.8	37.3	61.6	37.5	60.5	37.5
6.4	70.5	37.0	62.8	37.4	62.9	37.4
12	73.5	36.7	64.4	37.4	63.7	37.4
18	75.3	36.4	66.8	37.3	65.0	37.4
25	77.4	36.1	67.6	37.2	66.3	37.3
31	nd[a]	nd	68.5	37.2	67.7	37.2

[a] Not determined.

Table 3: Equilibrium Lattice Parameters, d_{hex} and d_l, for LPA/DOPE/td Mixtures

mol % DOPA	water		pH 7.0,[a] 150 mM NaCl		pH 7.0,[a] 150 mM NaCl + 25 mM Ca^{2+}	
	d_{hex} (Å)	d_l (Å)	d_{hex} (Å)	d_l (Å)	d_{hex} (Å)	d_l (Å)
0.0	67.8	37.3	61.6	37.4	60.5	37.4
3.8	71.2	37.2	nd[a]	nd	nd	nd
5.6	74.8	36.9	nd	nd	nd	nd
7.5	76.5	36.8	nd	nd	nd	nd
8.6	76.8	36.8	66.7	37.3	64.9	37.4
9.0	79.6	36.5	nd	nd	nd	nd
11	85.6	35.8	nd	nd	nd	nd
14	88.6	35.4	77.4	36.7	74.2	37.0
18	nd	nd	86.4	35.7	82.7	36.2
23	nd	nd	98.3	33.7	91.7	34.9

[a] Not determined.

in the presence of only water). This is a reasonable assumption because many previous measurements (see e.g. ref *30*) show that changes in d_l are small considering the changes observed in the equilibrium lattice dimensions in this study (Tables 2 and 3). The spontaneous curvatures for the individual mixtures were calculated as before and are shown in Figure 5. From the linearity of this plot we determined the spontaneous radius of curvature for DOPA, LPA, and DOPE. The results summarized in Table 1 indicate that the spontaneous curvature of DOPA is strongly affected by 150 mM NaCl, whereas the spontaneous curvature of LPA remains unchanged within experimental error.

Finally we investigated the effect of Ca^{2+} n the spontaneous radius of curvature in the presence of salt. Samples were equilibrated in buffer at pH 7.0 containing 150 mM NaCl and 25 mM $CaCl_2$ i.e. in large excess as compared to (L)PA (Ca^{2+}/(L)PA molar ratio of 10). The addition of calcium only slightly (see Tables 2 and 3) reduced the equilibrium lattice dimension. The spontaneous radius of curvature calculations (Table 1) indicate that the addition of Ca^{2+} does not significantly affect the spontaneous curvature of (L)PA at neutral pH in the presence of physiological salt concentrations.

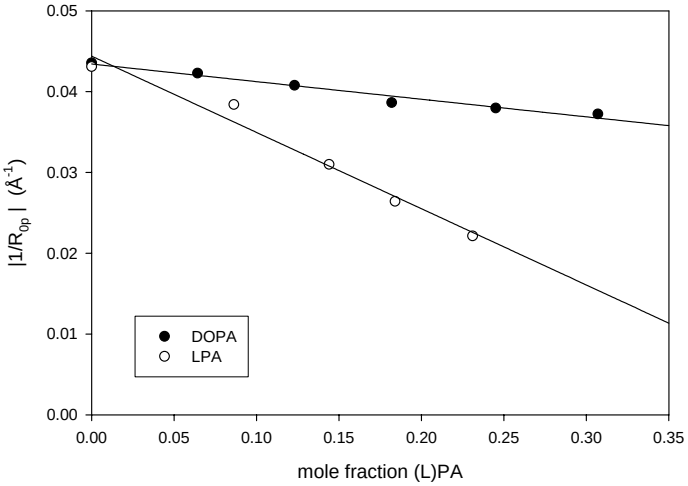

Figure 5: Plot of the absolute value of the spontaneous curvature, |1/*R*0p|, at pH 7.0 in the presence of 150 mM NaCl calculated at the pivotal plane for DOPA/DOPE/td (solid circles) and LPA/ DOPE/td (open circles) mixtures as a function of DOPA and LPA content, respectively. Linear regression analysis (r^2= 0.98 and 0.97 for PA and LPA dataset respectively) gives R_{0p}^{DOPA} = -46 Å, R_{0p}^{LPA} = +20, and R_{0p}^{DOPE} = -22 ± 1 Å.

Discussion

The local formation of PA plays a key role in the regulation of intracellular membrane fission events, possibly by affecting local membrane curvature. To examine this possibility we determined the spontaneous curvature of DOPA and LPA under physiological conditions of charge and salt concentrations. The spontaneous curvature, $1/R_{0p}$, is the inverse of the spontaneous radius of curvature R_{0p}. It is a quantitative measure of effective lipid shape, and describes the intrinsic propensity of a particular lipid to form curved, non-bilayer, structures (*19*, *20*). Table 1 summarizes the spontaneous curvature data obtained for PA and LPA (this study) in comparison to literature data on other membrane lipids. Both the spontaneous radius of curvature R_{0p} (first column) and its inverse, the spontaneous curvature $1/R_{0p}$ (second column), are shown. A small (i.e. close to zero) positive or negative spontaneous curvature (i.e. a large positive or negative spontaneous radius of curvature) describes a lipid that prefers a bilayer organization with little intrinsic curvature (e.g. DOPS and DOPC, respectively, see Table 1). Lipids with a large negative spontaneous curvature (a small and negative spontaneous radius of curvature), like DAG, form structures with a large negative monolayer curvature such as H_{II} phases, and lipids with a large positive spontaneous curvature, such as LPC, form structures with a large positive monolayer curvature, like spherical micelles or the H_I phase.

Spontaneous Curvature of DOPA

The spontaneous curvature measured for DOPA in water is close to zero and thus comparable to that of other lipids that form lamellar phases (see Table 1); i.e. under these conditions PA behaves as a cylindrically shaped lipid. Under more physiological conditions of neutral pH and in the presence of 150 mM salt, PA has a considerably more negative spontaneous curvature, in fact approaching that of DOPE. Further addition of 25 mM $CaCl_2$, at neutral pH, does not have a significant effect on the spontaneous curvature of DOPA.

These results can be understood by considering that lipid spontaneous curvature depends not only on molecular structure but also on intermolecular interactions within the lipid monolayer. Electrostatic repulsion between polar head-groups increases the effective area occupied by the headgroup and, thus, has the effect of adding positive spontaneous curvature. Electrolytes reduce electrostatic repulsion between charged lipid headgroups, decreasing their effective size, and thus shift spontaneous curvature toward more negative values. Note that the change in spontaneous curvature of DOPA induced by salt is not caused by a change in the net charge of the lipid headgroup. We directly determined this charge by solid state ^{31}P NMR methods and found that the headgroup charge on (L)PA in water falls in a relevant physiological range and is not affected by salt addition (data not shown).

The effect of Ca^{2+} on the spontaneous curvature of DOPA appears to depend critically on lipid headgroup charge. At acidic pH, the average charge of PA approaches one e^- (data not shown) and Ca^{2+} is expected to bind two PA molecules resulting in an effective lipid molecule with a more negative spontaneous curvature, similar to the effects of Ca^{2+} binding on the molecular shape of cardiolipin (34). Indeed, submillimolar concentrations of Ca^{2+} are sufficient to induce a bilayer-to-H_{II} phase transition in DOPA at 37 °C, but only at acidic and not at neutral pH (24). At neutral pH, PA carries on average more than one e^- (data not shown) and probably does not bind Ca^{2+} directly. Under these conditions, Ca^{2+} should merely have a charge screening effect, similar to that mediated by salt, and therefore does not significantly change the spontaneous curvature of PA at physiological salt concentrations. Our finding that, at neutral pH and in the presence of a physiological salt concentration, Ca^{2+} does not affect the spontaneous curvature of PA indicates that a local rise in cytosolic Ca^{2+} concentration is not likely to trigger a change in lipid shape of PA *in vivo*.

Spontaneous Curvature of LPA

The spontaneous curvature of LPA found in water is large and positive. Comparing our results to the literature data (Table 1) we find that LPA has a spontaneous curvature that is larger than that of LPC. Under more physiological conditions of neutral pH and in the presence of 150 mM salt, LPA appears to have the same spontaneous curvature as in pure water and further addition of 25 mM $CaCl_2$, at neutral pH, had no significant effect on the spontaneous curvature.

The fact that the spontaneous curvature of LPA in water is larger than that of LPC is remarkable in view of the small size of the phosphate headgroup as compared to the phosphocholine headgroup of LPC. Clearly, the spontaneous curvature of LPA is dominated by lipid headgroup repulsion, which dramatically increases the effective size of the lipid headgroup, similar to the situation described earlier for DOPA in water (see above).

In the case of DOPA, salt addition changed lipid spontaneous curvature from close to zero, i.e. essentially cylindrical, to large and negative. The reasons why salts apparently do not change the spontaneous curvature of LPA are not easily understood but may lie, to a first approximation, in a different effect of salt addition on the effective size of the lipid headgroup, and cross-sectional area of the acyl chain(s). In the case of DOPA, the cross-sectional area of the acyl chains is larger than the effective size of the phosphate headgroup, and, both in the absence and in the presence of salts, lipid packing is dominated by the acyl chains: salts reduce the effective size of the lipid headgroup without major effects on lipid packing or cross-sectional area of the acyl chains. A different situation arises for LPA which carries a single acyl chain, and where lipid packing is dominated by the effective size of the lipid headgroup: salts reduce not only the effective size of the lipid headgroup but also lipid packing. Thus a speculative explanation for the absence of an effect of salts on the spontaneous curvature of LPA assumes that salts reduce both the effective size of the lipid headgroup and the cross-sectional area of the acyl chain, and both to the same extent. However, alternative explanations can as yet not be excluded.

Biological Implications

The conversion of LPA into PA by the fission proteins BARS and endophilin has been implicated in two different membrane fission events, BARS at the level of the Golgi and endophilin in endocytosis. Our data are compatible with the initial hypothesis (12) that a conversion of LPA into PA might impose negative curvature on the membrane facilitating membrane constriction. How this putative change in curvature would facilitate the overall fission process, however, is unclear, and alternative models cannot be excluded (for a comprehensive discussion of alternative models see refs 2 and 24). For example, acylation of LPA not only changes lipid spontaneous curvature but also results in a slight increase in lipid molecular area which might, in principle, drive membrane budding by creating surface area asymmetry between the two membrane leaflets (35). However, such a mechanism requires a considerable transmembrane surface area asymmetry, and is therefore unlikely, given the relatively small amount of LPA present in biomembranes (typically below 0.6% in Golgi membranes (9)) and the fact that acylation only increases lipid molecular area by ~45%. Thus, a role of (L)PA in membrane bending and fission is more likely to be related to a change in local spontaneous curvature than to an increase in global transmembrane surface area asymmetry (also see ref 16). Indeed, a recent theoretical study shows that if the

conversion of LPA into PA is followed by a further metabolism to DAG, a membrane lipid with a more extreme negative spontaneous curvature (26, 27) (see Table 1), then the pearling of Golgi membranes upon treatment with BARS can be understood (16). Although the crucial role of BARS in Golgi membrane fission was recently confirmed in *in vivo* experiments (36), the role of PA and the putative conversion of LPA into PA have not yet been resolved. A likely possibility is that the conversion of LPA into PA is only one step in a series of steps leading up to fission in which the different lipid and protein factors work synergistically as suggested in a recent study of BARS-dependent mitotic Golgi fragmentation (36). The quantitative data on the spontaneous radius of curvature of PA and LPA at physiological pH and salt concentration presented in the current study will be instrumental in developing future models of biomembrane fission.

Acknowledgments

We thank Dave Siegel and Dena Mae Kooijman-Agra for helpful discussions and critical reading of the manuscript and Amanda Bradford-Janke for practical assistance.

References

1. Lippincott-Schwartz, J. (2001) The secretory membrane system studied in real-time. Robert Feulgen Prize Lecture, *Histochem. Cell Biol. 116*,97-107.
2. Burger, K. N. J. (2000) Greasing membrane fusion and fission machineries, *Traffic 1*, 605-13.
3. Kozlovsky, Y., and Kozlov, M. M. (2003) Membrane fission: model for intermediate structures, *Biophys. J. 85*, 85-96.
4. Cremona, O., and De Camilli, P. (2001) Phosphoinositides in membrane traffic at the synapse, *J. Cell Sci. 114*, 1041-52.
5. Siddhanta, A., Radulescu, A., Stankewich, M. C., Morrow, J. S., and Shields, D. (2003) Fragmentation of the Golgi apparatus. A role for beta III spectrin and synthesis of phosphatidylinositol 4,5-bisphosphate, *J. Biol. Chem. 278*, 1957-65.
6. Godi, A., Di Campli, A., Konstantakopoulos, A., Di Tullio, G., Alessi, D. R., Kular, G. S., Daniele, T., Marra, P., Lucocq, J. M., and De Matteis, M. A. (2004) FAPPs control Golgi-to-cell-surface membrane traffic by binding to ARF and PtdIns(4)P, *Nat. Cell Biol. 6*, 393-404.
7. Bankaitis, V. A. (2002) Cell biology. Slick recruitment to the Golgi, *Science 295*, 290-1.
8. Baron, C. L., and Malhotra, V. (2002) Role of diacylglycerol in PKD recruitment to the TGN and protein transport to the plasma membrane, *Science 295*, 325-8.
9. Weigert, R., Silletta, M. G., Spano, S., Turacchio, G., Cericola, C., Colanzi, A., Senatore, S., Mancini, R., Polishchuk, E. V., Salmona, M., Facchiano, F., Burger, K. N. J., Mironov, A., Luini, A., and Corda, D. (1999) CtBP/BARS induces fission of Golgi membranes by acylating lysophosphatidic acid, *Nature 402*, 429-33.
10. Roth, M. G., Bi, K., Ktistakis, N. T., and Yu, S. (1999) Phospholipase D as an effector for ADP-ribosylation factor in the regulation of vesicular traffic, *Chem. Phys. Lipids 98*, 141-52.
11. Siddhanta, A., and Shields, D. (1998) Secretory vesicle budding from the trans-Golgi network is mediated by phosphatidic acid levels, *J. Biol. Chem. 273*, 17995-8.
12. Schmidt, A., Wolde, M., Thiele, C., Fest, W., Kratzin, H., Podtelejnikov, A. V., Witke, W., Huttner, W. B., and So¨ling, H. D. (1999) Endophilin I mediates synaptic vesicle formation by transfer of

arachidonate to lysophosphatidic acid, *Nature 401*, 133-41.
13. Karbowski, M., Jeong, S. Y., and Youle, R. J. (2004) Endophilin B1 is required for the maintenance of mitochondrial morphology, *J. Cell Biol. 166*, 1027-39.
14. Chernomordik, L. V., and Kozlov, M. M. (2003) Protein-lipid interplay in fusion and fission of biological membranes, *Annu. Re*V. *Biochem. 72*, 175-207.
15. Kozlovsky, Y., Chernomordik, L. V., and Kozlov, M. M. (2002) Lipid intermediates in membrane fusion: formation, structure, and decay of hemifusion diaphragm, *Biophys. J. 83*, 2634-51.
16. Shemesh, T., Luini, A., Malhotra, V., Burger, K. N. J., and Kozlov, M. M. (2003) Prefission constriction of Golgi tubular carriers driven by local lipid metabolism: a theoretical model, *Biophys. J. 85*, 3813-27.
17. Helfrich, W. (1973) Elastic properties of lipid bilayers: theory and possible experiments, *Z. Naturforsch. 28C*, 693-703.
18. Israelachvili, J. N., Mitchel, D. J., and Ninham, B. W. (1976) Theory of self-assembly of hydrocarbon amphiphiles into micelles and bilayers, *J. Chem. Soc., Faraday Trans. 2 72*, 1525-68.
19. Gruner, S. M. (1985) Intrinsic curvature hypothesis for biomembrane lipid composition: a role for nonbilayer lipids, *Proc. Natl. Acad. Sci. U.S.A. 82*, 3665-9.
20. Rand, R. P., Fuller, N. L., Gruner, S. M., and Parsegian, V. A. (1990) Membrane curvature, lipid segregation, and structural transitions for phospholipids under dual-solvent stress, *Biochemistry 29*,76-87.
21. Verkleij, A. J., De Maagd, R., Leunissen-Bijvelt, J., and De Kruijff, B. (1982) Divalent cations and chlorpromazine can induce non-bilayer structures in phosphatidic acid-containing model membranes, *Biochim. Biophys. Acta 684*, 255-62.
22. Farren, S. B., Hope, M. J., and Cullis, P. R. (1983) Polymorphic phase preferences of phosphatidic acid: A 31P and 2H NMR study, *Biochem. Biophys. Res. Commun. 111*, 675-82.
23. Lee, Y. C., Taraschi, T. F., and Janes, N. (1993) Support for the shape concept of lipid structure based on a headgroup volume approach, *Biophys. J. 65*, 1429-32.
24. Kooijman, E. E., Chupin, V., de Kruijff, B., and Burger, K. N. J. (2003) Modulation of membrane curvature by phosphatidic acid and lysophosphatidic acid, *Traffic 4*, 162-74.
25. Rand, R. P., and Fuller, N. L. (1994) Structural dimensions and their changes in a reentrant hexagonal-lamellar transition of phospholipids, *Biophys. J. 66*, 2127-38.
26. Szule, J. A., Fuller, N. L., and Rand, R. P. (2002) The effects of acyl chain length and saturation of diacylglycerols and phosphatidylcholines on membrane monolayer curvature, *Biophys. J. 83*, 977-84.
27. Leikin, S., Kozlov, M. M., Fuller, N. L., and Rand, R. P. (1996) Measured effects of diacylglycerol on structural and elastic properties of phospholipid membranes, *Biophys. J. 71*, 2623-32.
28. Chen, Z., and Rand, R. P. (1997) The influence of cholesterol on phospholipid membrane curvature and bending elasticity, *Biophys. J. 73*, 267-76.
29. Fuller, N., and Rand, R. P. (2001) The influence of lysolipids on the spontaneous curvature and bending elasticity of phospholipid membranes, *Biophys. J. 81*, 243-54.
30. Fuller, N., Benatti, C. R., and Rand, R. P. (2003) Curvature and bending constants for phosphatidylserine-containing membranes, *Biophys. J. 85*, 1667-74.
31. Chen, Z., and Rand, R. P. (1998) Comparative study of the effects of several n-alkanes on phospholipid hexagonal phases, *Biophys. J. 74*, 944-52.
32. Seddon, J. M., Cevc, G., and Marsh, D. (1983) Calorimetric studies of the gel-fluid (L beta-L alpha) and lamellar-inverted hexagonal (L alpha-HII) phase transitions in dialkyl-and diacylphosphatidylethanolamines, *Biochemistry 22*, 1280-9.
33. Seddon, J. M. (1990) Structure of the inverted hexagonal (HII) phase, and non-lamellar phase transitions of lipids, *Biochim. Biophys. Acta 1031*,1-69.
34. Rand, R. P., and Sengupta, S. (1972) Cardiolipin forms hexagonal structures with divalent cations, *Biochim. Biophys. Acta 255*, 484-92.
35. Rauch C., and Farge E. (2000) Endocytosis switch controlled by transmembrane osmotic pressure and phospholipid number asymmetry, *Biophys. J. 78*, 3036-47.
36. Carcedo, C. H., Bonazzi, M., Spano, S., Turacchio, G., Colanzi, A., Luini, A., and Corda, D. (2004) Mitotic Golgi partitioning is driven by the membrane-fissioning protein CtBP3/BARS, *Science 305*,93-6.

CHAPTER 4

What makes the bioactive lipids phosphatidic acid and lysophosphatidic acid so special?

Taken from:
Biochemistry (2005) ***44,*** 17007-17015

Abstract

Phosphatidic acid and lysophosphatidic acid are minor but important anionic bioactive lipids involved in a number of key cellular processes, yet these molecules have a simple phosphate headgroup. To find out what is so special about these lipids, we determined the ionization behavior of phosphatidic acid (PA) and lysophosphatidic acid (LPA) in extended (flat) mixed lipid bilayers using magic angle spinning ^{31}P-NMR. Our data show two surprising results. First, despite identical phosphomonoester headgroups, LPA carries more negative charge than PA when present in a phosphatidylcholine bilayer. Dehydroxy-LPA [1-oleoyl-3-(phosphoryl)propanediol] behaves in a manner identical to that of PA, indicating that the difference in negative charge between LPA and PA is caused by the hydroxyl on the glycerol backbone of LPA and its interaction with the phosphomonoester headgroup. Second, deprotonation of phosphatidic acid and lysophosphatidic acid was found to be strongly stimulated by the inclusion of phosphatidylethanolamine in the bilayer, indicating that lipid headgroup charge depends on local lipid composition and will vary between the different subcellular locations of (L)PA. Our findings can be understood in terms of a hydrogen bond formed within the phosphomonoester headgroup of (L)PA and its destabilization by competing intra- or intermolecular hydrogen bonds. We propose that this hydrogen bonding property of (L)PA is involved in the various cellular functions of these lipids.

Introduction

Phosphatidic acid (PA) and the related lipid lysophosphatidic acid (LPA) are important minor lipid species in the cell. They are involved in many intracellular processes, and are important intermediates in lipid biosynthesis (*1*). For example, binding of LPA to its receptors evokes various cellular responses, and the local formation of (L)PA is part of signaling cascades, in particular in the regulation of membrane dynamics such as fusion and fission events, either indirectly through the recruitment of downstream effectors or directly by mediating (local) changes in the biophysical properties of the membrane (*2-12*).

PA and LPA have a relatively simple chemical structure consisting of only a glycerol, one (LPA) or two (PA) acyl chains, and a phosphate, and it is interesting to note that these simple phospholipids are involved in such diverse processes, and are able to bind specifically to so many different types of proteins (*3*, *13*). The question then is what is so special about these lipids. An obvious suggestion relates to the phosphate headgroup, which is attached to the glycerol backbone as a phosphomonoester, a unique feature of these lipids. Phosphomonoesters have two pK_a's, one of which is expected to be in the physiological pH range. As a consequence, small changes in (physiological) pH will affect the charge and influence the molecular shape and lipid phase behavior of these lipids (*14*, *15*).

Under physiological con65ditions at neutral pH, phosphatidic acid is a cone (type II)-shaped lipid with a negative spontaneous curvature close to that of unsaturated phosphatidylethanolamine (PE), whereas LPA is an inverted cone (type I)-shaped lipid with the most positive spontaneous curvature of any membrane lipid measured to date (*11*, *12*). Lipid headgroup charge not only is a key determinant of the molecular shape of (L)PA but also is expected to greatly influence interactions with neighboring lipids and (L)PA-binding proteins. Clearly, insight into the charge of (L)PA and the way this charge is influenced by physiological factors such as pH and membrane lipid composition is essential to our understanding of the biological roles of PA and LPA.

We therefore set out to determine the charge on (L)PA in model membrane systems that are relevant to biological membranes. Lipid headgroup charge cannot easily be determined by pH-dependent phase transition studies, surface potential measurements, or traditional acid-base titration methods since these methods are indirect or hampered by difficulties and uncertainties in data analysis (*16*, *17*). However, because the hydroxyls on (L)PA are close to the phosphorus nucleus (protons separated from the phosphor by only an oxygen), their ionization will influence the magnetic properties of this nucleus, which can be measured by ^{31}P NMR as a pH-dependent chemical shift in high-resolution ^{31}P NMR spectra. However, ^{31}P NMR spectra of extended bilayers are characterized by broad lines due to the large chemical shift anisotropy, which masks pH-dependent changes in chemical shift. To circumvent this problem, earlier studies made use of small unilamellar vesicles (SUVs) and micelles in which the phospholipids undergo rapid isotropic motion, thereby giving rise to high-resolution ^{31}P NMR spectra (*18-20*). A disadvantage of these systems is their high curvature, which is not typical for biological membranes. With the advance of magic angle spinning (MAS) NMR, it is now possible to directly measure the chemical shift of phospholipids in biologically more relevant extended bilayer systems (*21*). We used this technique to determine the ionization of PA and LPA in extended bilayers composed of the abundant membrane phospholipids PC (phosphatidylcholine), PE, and their mixtures.

We show that titration curves can be measured using MAS ^{31}P NMR and that pK_{a1} and pK_{a2} (and thus charge) can be determined with high accuracy. We find that, despite identical phosphate headgroups, LPA has a significantly lower pK_{a2} value than PA in pure PC, indicating that LPA carries more negative charge than PA at physiological pH. In mixed lipid bilayers of PC and PE, the pK_{a2} of LPA and PA decreases with an increase in PE content, and therefore depends critically on the composition of the surrounding zwitterionic lipids, i.e., the PC:PE ratio. A unifying mechanism will be proposed to explain these findings based on unique hydrogen bonding possibilities of the phosphomonoester headgroup.

Materials and Methods

Sample Preparation

1,2-Dioleoyl-*sn*-glycero-3-phosphoethanolamine (DOPE), 1,2-dioleoyl-*sn*-glycero-3-phosphocholine (DOPC), 1,2-dioleoyl-*sn*-glycero-3-phosphate (monosodium salt; DOPA), 1,2-dioleoyl-*sn*-glycero-3-phosphoserine (sodium salt; DOPS), 1-oleoyl-*sn*-glycero-3-phosphate (sodium salt; LPA), and 1-oleoyl-*sn*-glycero-3-phosphocholine (LPC) were purchased from Avanti Polar Lipids (Birmingham, AL). 1-Oleoyl-3-(phosphoryl)propanediol (dehydroxy-LPA) was synthesized as reported previously (*22*). Lipid purity was checked by thin-layer chromatography and judged to be >99%. Water used in the experiments came from a Milli-Q system (Millipore, Bedford, MA) and had a resistivity of 18.2 MΩ cm.

NMR samples, for pH titration purposes, were prepared by mixing appropriate amounts of lipid stock [concentration determined by a Pi determination (*23*)] from chloroform and methanol, subsequently dried under a stream of N_2, and placed under high vacuum overnight. Samples were hydrated using an appropriate buffer. The following buffers were used: 100 mM KCl-HCl for pH 1.5-2.5, 10 mM Hepes, 20 mM Mes, 30 mM citric acid-NaOH, and 100 mM NaCl for pH 2.5-7.5, 50 mM Tris-HCl and 100 mM NaCl for pH 7.5-9.0, or 50 mM glycine-NaOH and 100 mM NaCl for pH 9.0-10.5. Each contained 2 mM EDTA to complex any traces of divalent cations. The samples were then subjected to a minimum of two freeze-thaw-vortex cycles, after which the pH of the samples was measured. This pH, measured after lipid hydration, was used to construct the pH titration curves. NMR samples for measurement at constant pH were prepared as described above and hydrated with a buffer containing 100 mM Hepes, 5 mM acetic acid-NaOH, 100 mM NaCl, and 2 mM EDTA (pH 7.2). After hydration, the pH of these lipid dispersions was found to be generally within 0.05 pH unit of pH 7.2; in some cases, the pH was adjusted by the addition of NaOH or HCl to come within this range. The lipid dispersions were concentrated in a tabletop centrifuge (70 000 rpm for 45 min at room temperature), and the (wet) lipid pellet was transferred to 4 mm TiO2 MAS NMR sample tubes.

NMR

^{31}P NMR spectra were recorded on a Bruker Avance (Karlsruhe, Germany) 500 widebore spectrometer at 202.48 MHz, using a 4 mm cross-polarization (CP) MAS NMR probe. Samples were spun at the magic angle (54.7°) at 5 kHz to average the chemical shift anisotropy, and the chemical shift position of (L)PA was recorded relative to 85% H_3PO_4. Under stable spinning conditions, typically 100-1000 scans were recorded depending on the amount of lipid recovered in the pellet. Static spectra were recorded by the spin-echo technique with proton decoupling in a 4 mm CP MAS NMR probe to check the lipid phase of the samples, where appropriate. Experiments were carried out at 20.0 ± 0.5 °C.

Determination of pK_a Values.

The pK_a values for (L)PA were determined by using a relation derived from the Henderson-Hasselbach equation (*24*) and a nonlinear least-squares fit.

$$\delta = \frac{\delta_{AB} + \delta_{AA} \times 10^{pK_{a1} - pH} + \delta_{BB} \times 10^{pH - pK_{a2}}}{1 + 10^{pK_{a1} - pH} + 10^{pH - pK_{a2}}} \quad (1)$$

δ_{AA}, δ_{AB}, and δ_{BB} are the chemical shifts of the associated, singly dissociated, and doubly dissociated state, respectively. δ is the measured chemical shift. pH is the log of the measured hydrogen concentration, and pK_{a1} and pK_{a2} are the dissociation constants.

In cases where only the top part of the titration curve was measured (pH 4-10), the data were fitted with a modified equation now containing only one dissociation constant (*24*):

$$\delta = \frac{\delta_A \times 10^{pK_a - pH} + \delta_B}{1 + 10^{pK_a - pH}} \quad (2)$$

Note that this barely influences the determination of the second pK_a of (L)PA. Fitting the data for a full titration curve [e.g., (L)PA in DOPC] over this pH range (4-10), using eq 2 instead of eq 1, did not change the value of pK_{a2} by more than 0.2% (data not shown).

Results

MAS ^{31}P NMR was used to measure the dissociation constants of PA and LPA present at low concentrations in dispersions of PC and PE. The phospholipids used in this study contained unsaturated (oleoyl, 18:1) chains since these give rise to fluid bilayers representative of biological membranes. All experiments were carried out in 100 mM salt to mimic physiological conditions, and all measurements were recorded at 20 °C to eliminate temperature effects on ionization and ^{31}P chemical shift.

Dissociation Constants of (L)PA in PC Bilayers

We first determined the dissociation constants of LPA and PA in PC bilayers. Figure 1 shows representative MAS ^{31}P NMR spectra for 10 mol % LPA in DOPC as a function of pH. The individual peaks of LPA and PC are well resolved as the minor low-field peak and the large high-field peak, respectively. The pH-dependent protonation of the phosphate headgroup resulted in a large downfield shift of the LPA peak. The titration behavior indicated the presence of two pK_a's, as anticipated for this phosphomonoester headgroup. The nearly constant position of

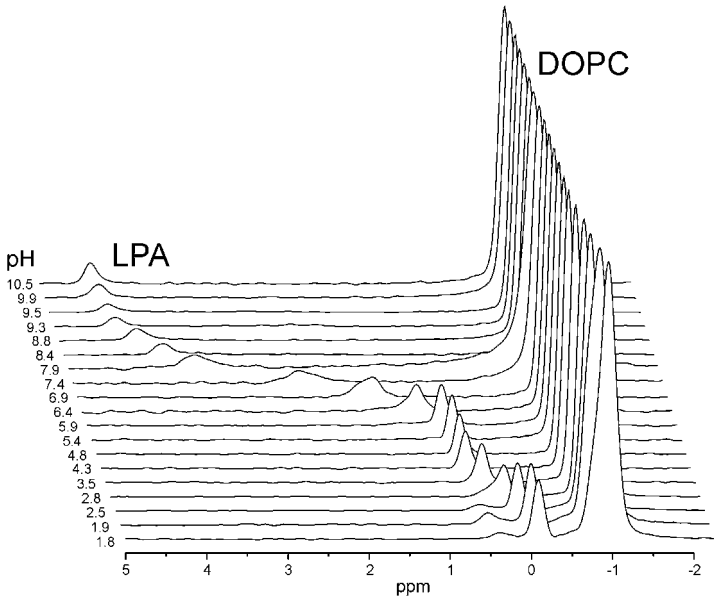

Figure 1: Solid-state MAS ^{31}P NMR spectra for 10 mol % LPA in DOPC as a function of pH.

the PC peak demonstrates that the charge on the phosphate group of PC did not change, according to the expectation for this zwitterionic headgroup (*17*). A similar behavior was found for the position of the LPC and PE peak in the PE/LPC bilayer (see below), except that the PE peak moved slightly to downfield values at high pH (pH >9.0), reflecting the onset of deprotonation of the primary amine of the PE headgroup (data not shown). At very low pH values, a third minor (<1-2%) peak downfield of LPA was present due to a small amount of lipid hydrolysis at this very low pH. Similar spectra as a function of pH were recorded for 10 mol % PA in DOPC (spectra not shown).

The chemical shifts of LPA and PA were plotted as a function of pH to yield the titration curves shown in Figure 2. The double-sigmoidal shape of the titration curves reflects the sequential dissociation of two protons from the phosphate headgroup. The first dissociation occurs at very low pH ($2 < pH < 4$), whereas the second dissociation occurs in a more physiological pH range ($6 < pH < 9$). The actual pK_a's were determined as described in Materials and Methods, and the results are given in Table 1. These data show that pK_a's and in particular the more physiologically relevant pK_{a2} can be determined with high accuracy in extended bilayers using MAS ^{31}P NMR. Interestingly, despite identical phosphomonoester headgroups, the pK_{a2} of PA is 0.45 pH unit higher than that of LPA in a PC bilayer. This charge difference between LPA and PA was maintained in the presence of physiological concentrations of Mg^{2+} (free Mg^{2+} concentration of ~1 mM; data not shown). Although Mg^{2+} increased the charge of both LPA and PA, most likely by

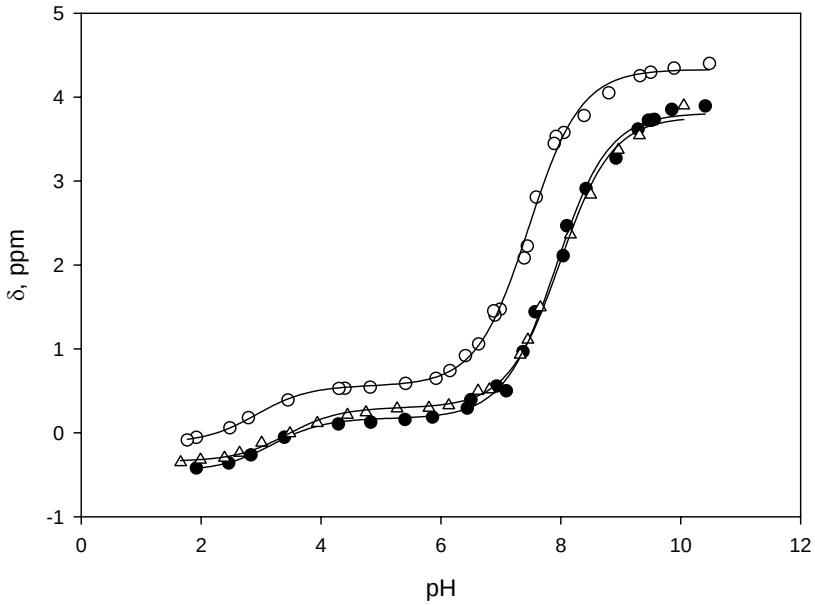

Figure 2: Titration curves for 10 mol % LPA (○), DOPA (●), and dehydroxy-LPA (Δ) in DOPC, relating bulk pH to chemical shift. Lines represent the nonlinear least-squares fits of the data to eq 1 (see Materials and Methods).

Table 1: Dissociation Constants for LPA, PA, and Dehydroxy-LPA in Extended Bilayers and Hexagonal H_{II} Phase[a]

	LPA	PA	dehydroxy-LPA
PC bilayer			
pK_{a1}	2.9 ± 0.3	3.2 ± 0.3	3.4 ± 0.15
pK_{a2}	7.47 ± 0.03	7.92 ± 0.03	7.99 ± 0.03
PE bilayer			
pK_{a1}	nd[b]	nd[b]	
pK_{a2}	6.88 ± 0.04	6.89 ± 0.05	
PE hexagonal phase			
pK_{a1}	3.1 ± 0.6	3.2 ± 0.4	
pK_{a2}	6.60 ± 0.04	7.02 ± 0.04	

[a]The PE bilayer system contained 25 mol % LPC to force PE into a bilayer organization (for details, see the text). The LPA, PA, and dehydroxy-LPA content was 10 mol % in all systems except for the PE hexagonal phase, where LPA content was 5 mol %. [b] Not determined.

decreasing the proton concentration at the membrane interface, both lipids were affected to the same extent, and a substantial difference in charge between PA and LPA remained. The striking difference in ionization between PA and LPA must be related to the chemical structure of the backbone, all other conditions being the

same [i.e., lipid background, (L)PA concentration, and ionic strength]. Therefore, we determined the titration behavior of a LPA compound lacking the free hydroxyl group at the *sn*-2 position of the glycerol backbone (dehydroxy-LPA). The dissociation behavior of dehydroxy-LPA was essentially identical to that of PA (see Figure 2 and Table 1), demonstrating that the hydroxyl group of the LPA backbone is responsible for the difference in ionization behavior between LPA and PA. The difference in ionization behavior between LPA, on one hand, and dehydroxy-LPA and PA, on the other hand, could potentially be related to a difference in the orientation of the headgroup. To examine this possibility, we determined the residual chemical shift anisotropy of LPA and dehydroxy-LPA (10 mol % in DOPC at pH 7.2) and found it to be very similar (data not shown). This result indicated that the conformation of dehydroxy-LPA is close to that of LPA, and strongly suggested that the difference in ionization behavior was not related to a difference in the orientation of the headgroup but to a property of the hydroxyl group at the *sn*-2 position of LPA.

Dissociation Constants of (L)PA in Bilayers and the Hexagonal H_{II} Phase of PE

Another major cellular membrane phospholipid is phosphatidylethanolamine (PE). PE is zwitterionic, like PC, but its headgroup is much smaller and carries a protonatable primary instead of a nonprotonatable quaternary amine. To test whether PE affects the protonation behavior of (L)PA, we first designed an experimental system rich in unsaturated PE, but organized in a bilayer. Aqueous dispersions of dioleoyl-PE do not form bilayers at room temperature but prefer organization in an inverted H_{II} phase due to the cone shape of this PE [bilayer to inverted hexagonal, L_α-H_{II}, phase transition temperature of ~3 °C (*25*, *26*)]. However, bilayers are formed if an appropriate amount of lysoPC (LPC) is added to complement the cone shape of PE (*11*, *27-29*).

A low-field shoulder and a high-field peak characterize static ^{31}P NMR spectra of lipid mixtures organized in a fluid bilayer (*30*). Mixtures of 65 mol % PE, 25 mol % LPC, and 10 mol % LPA or PA were analyzed over a range of pH values (4.0 < pH < 10.5), and the ^{31}P NMR spectra confirmed an organization in fluid lipid bilayers over the complete pH range (Figure 3B,D). Occasionally a minor peak was present at the isotropic position (around 0 ppm), most likely originating from small vesicles. These PE/LPC bilayer systems were used for MAS NMR analysis, and will be termed “PE bilayer” throughout the rest of this paper. Results are shown in panels A and C of Figure 3 for LPA and PA, respectively (black lines); for comparison, the titration curves of (L)PA in a PC bilayer are also shown (gray lines). When the PE bilayer system is compared to the PC bilayer system, the titration curves for both LPA and PA are clearly shifted to lower pH values. This is reflected in the pK_{a2} for (L)PA that is significantly lower in the PE bilayer than in the PC bilayer (Table 1). Interestingly, the dissociation constants (pK_{a2}) of LPA and PA in this PE bilayer are now identical within experimental error (Table 1). These data clearly demonstrate that the charge on PA and LPA in extended bilayers is

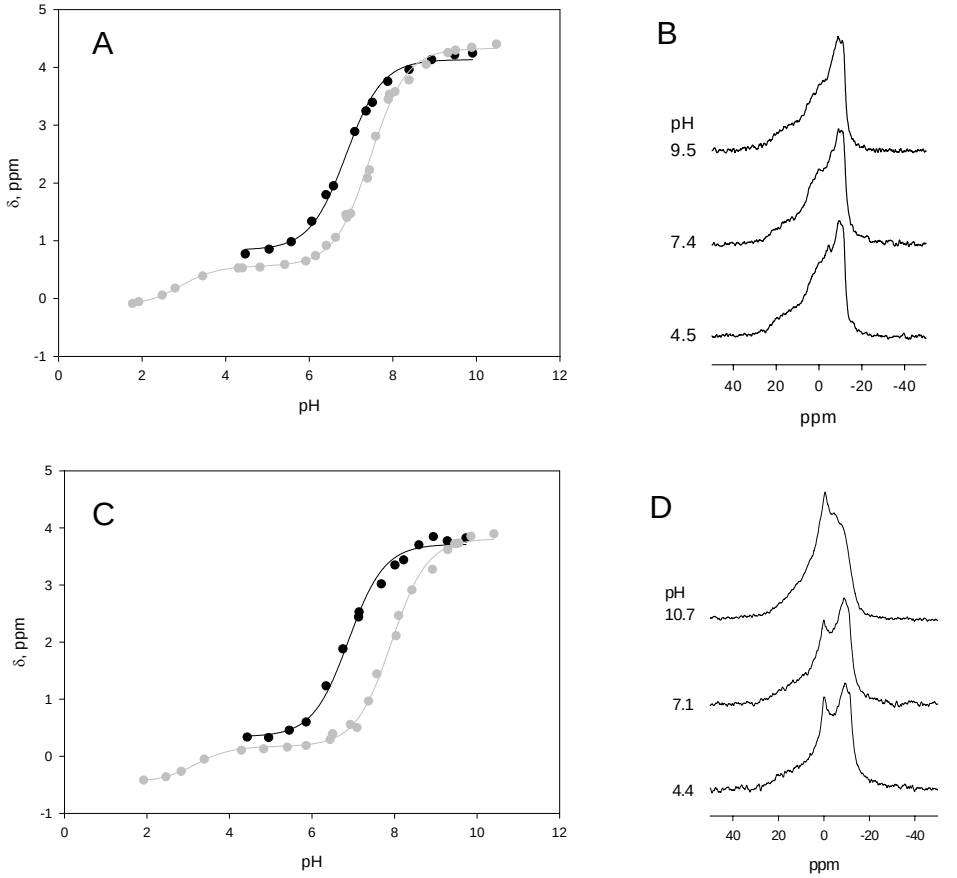

Figure 3: Titration curves for 10 mol % LPA (A) and 10 mol % DOPA (C) in PE/LPC (65:25) bilayers (black circles) and PC bilayers (gray circles; data from Figure 1). Lines represent the nonlinear least-squares fits to eq 1 (gray line) or 2 (black line). Representative static spectra at three representative pH values for 10 mol % LPA (B) and 10 mol % DOPA (D) in PE/LPC (65:25) bilayers.

sensitive to the lipid composition. The observed effect of lipid composition on the ionization of (L)PA may be due either to a difference in lipid packing or, more likely, to a difference in the chemical properties of PC and PE.

To gain further insight into these possibilities, we determined the dissociation constants of (L)PA in a pure DOPE matrix which is organized in a hexagonal H_{II} phase at 20 °C. Also, in the presence of 5 mol % LPA [a type I lipid (*12*)], a hexagonal phase was formed as determined by broad line ^{31}P NMR (data not shown). Titration curves for 5 mol % LPA and 10 mol % PA in a PE hexagonal phase were recorded by MAS ^{31}P NMR. The chemical shift position of the PE peak was virtually constant except at high pH, where it moved slightly to downfield values similar to what was observed in the PE bilayer system (data not shown).

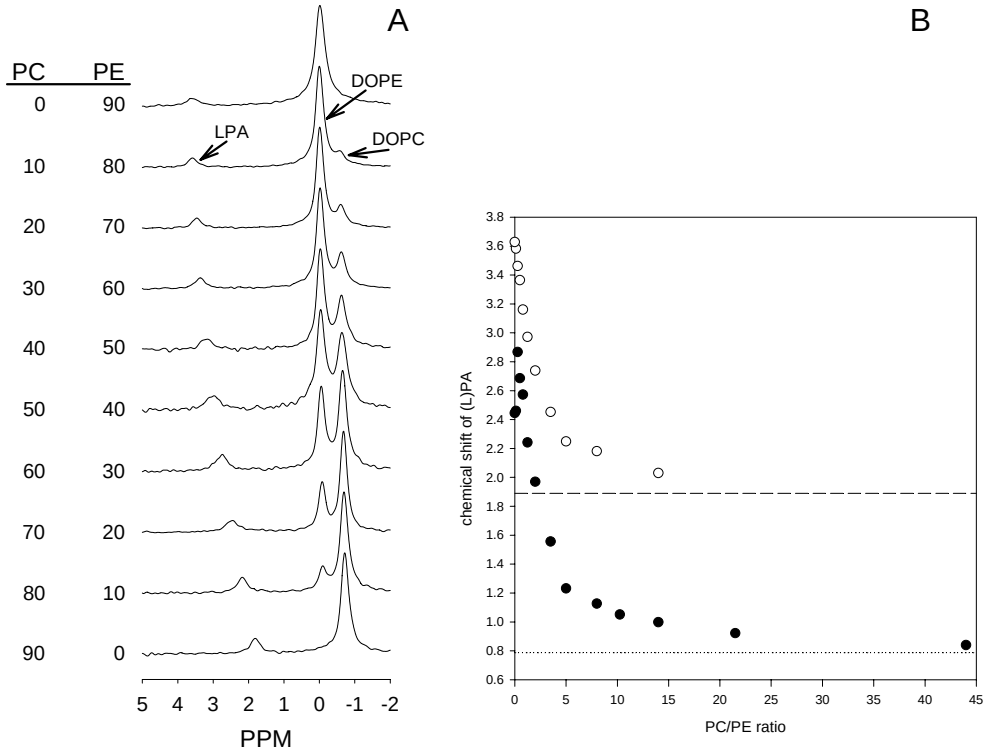

Figure 4: (A) Solid-state MAS ^{31}P NMR spectra for 10 mol % LPA as a function of PC:PE ratio at pH 7.20 ± 0.05. In panel B, the chemical shift of LPA (○) and PA (●) at pH 7.20 ± 0.05 is plotted as a function of the PC:PE molar ratio. The dotted and dashed lines represent the values of the chemical shift in pure PC, for 10 mol % PA and LPA, respectively (infinite PC:PE ratio).

From the titration behavior of (L)PA, the dissociation constants were determined, and the results are given in Table 1. The pK_{a2} of PA is higher than that of LPA in the PE hexagonal phase, similar to the situation observed in the PC bilayer. Importantly, the pK_{a2} for (L)PA in the PE hexagonal phase is close to that found for (L)PA in the PE bilayer, but clearly deviates from that in PC bilayers, suggesting that indeed a difference in chemical properties between PE and PC is responsible for the different titration behavior of (L)PA in PE compared to PC. Since lipid packing is very different in a bilayer and H_{II} phase (*31*), lipid packing apparently does not have a major effect on the ionization of (L)PA. The difference in the behavior of the PC and PE bilayer must thus be due to differences in their headgroup.

Headgroup Charge of (L)PA as a Function of PC:PE Ratio

To gain further insight into this headgroup specificity, we measured the ^{31}P chemical shift of 10 mol % (L)PA in extended bilayers containing PC and PE at physiological pH (pH 7.2), while varying the PC:PE ratio. Figure 4A shows representative MAS ^{31}P NMR spectra for LPA-containing samples, and the chemical shift positions of LPA, PE, and PC were clearly resolved (as indicated in Figure 4A). Indeed, an increase in PE concentration (decrease in PC concentration) resulted in a large downfield shift of the LPA peak corresponding to an increase in the charge for the LPA headgroup. These results are quantified in Figure 4B, which also includes a similar titration curve for PA. The ^{31}P chemical shift of (L)PA is plotted as a function of the PC:PE ratio, and the value of the chemical shift for LPA and PA in the pure PC bilayer is indicated by the dashed and dotted asymptotes, respectively (infinite PC:PE ratio). The large downfield change in the chemical shift of both LPA and PA shows that the ionization of (L)PA is indeed strongly enhanced with an increase in PE content (decrease in the PC:PE ratio).

It is well-known that intracellular membranes vary greatly in lipid composition with a large difference in the PC:PE ratio, in particular between the cytoplasmic and luminal leaflet of the Golgi membrane, and between the ER and cytoplasmic leaflet of the plasma membrane (*32*). To examine whether the charge on (L)PA varies between physiologically relevant phospholipid compositions, we measured the chemical shift of PA at physiological cytosolic pH (pH 7.2) for phospholipid mixtures mimicking the ER and cytoplasmic leaflet of the PM. At these locations, (L)PA is involved in lipid synthesis and signaling. Lipid compositions are based on those of rat liver ER and plasma membrane (*33*), assuming a symmetric transbilayer lipid distribution for the ER, and an asymmetric transbilayer distribution in the plasma membrane identical to that of human erythrocytes (*34*). Minor lipids at these locations such as sphingomyelin and phosphoinositides were not included in these mixtures. The lipid mixtures mimicking the cytoplasmic leaflet of the PM and the ER membrane had PC:PE:PS:PA molar ratios of 1:2:2:0.26 and 3:1:0.7:0.25, respectively. Figure 5A shows representative MAS ^{31}P NMR spectra, with PC, PE/PS, and PA peaks indicated. The chemical shift position of PA in the PM lipid mixture is shifted downfield by ~0.7 ppm as compared to its position in the ER lipid mixture, supporting the hypothesis that the PC:PE ratio is a major determinant of PA charge.

The relation between the chemical shift difference and the PE content of the two samples was somewhat masked by the differences in PS content. PS as an anionic lipid will increase the proton concentration at the membrane interface, which in turn will affect the ionization of PA. Figure 5B indeed shows the expected PS dependence of the chemical shift of PA but also demonstrates that at a constant PS concentration, ionization of PA is strongly PE dependent.

In a similar experiment, the effects of cholesterol were examined (data not shown). At a high PE content (PC:PE molar ratio of 0.5), 20 mol % cholesterol had

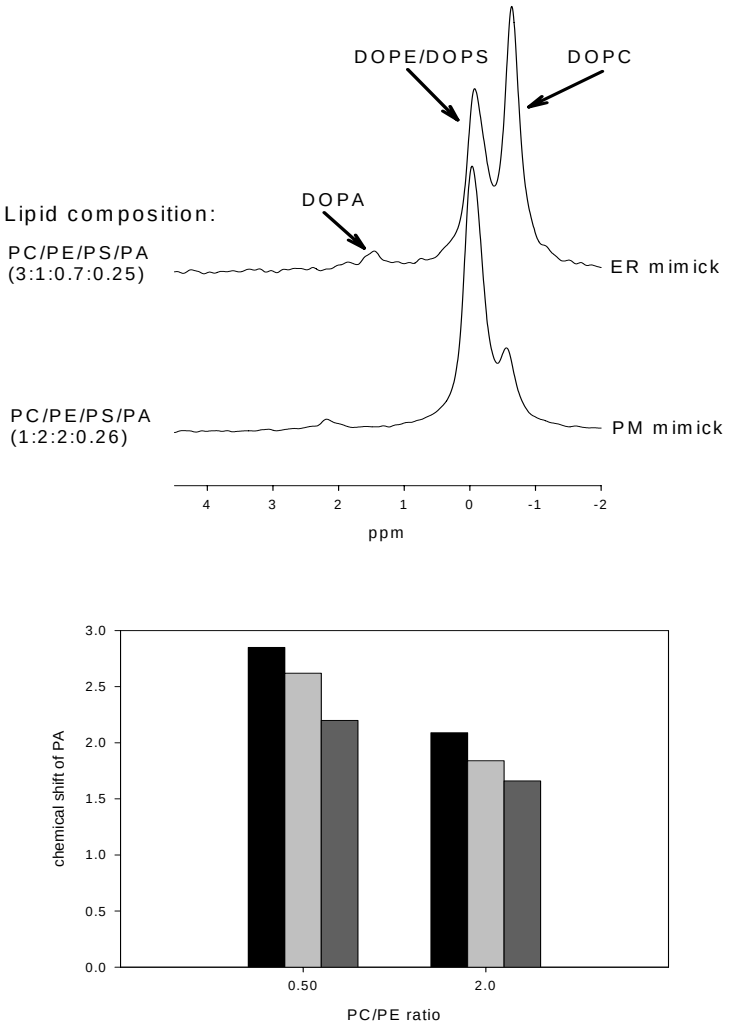

Figure 5: (A) Solid-state MAS ^{31}P NMR spectra for 5 mol % PA in lipid mixtures mimicking the cytoplasmic leaflet of the plasma membrane (bottom curve) and ER membrane (top curve). (B) Chemical shift for 5 mol % PA in bilayers with a PC:PE molar ratio of 0.5 and 2.0 at a PS concentration of 0 (black), 10 (light gray), and 20 mol % (dark gray).

virtually no effect on the ionization of PA. At low PE concentrations (PC:PE molar ratio of 2), cholesterol induced a larger increase in the negative charge of PA, but the effect was small compared to that induced by PE (<50% of the chemical shift induced by adding 20 mol % PE to the same PC/PE mixture). Thus, the PC:PE ratio is a major determinant of PA charge, while cholesterol has only a weak effect on the ionization of PA.

Discussion

In this study, we have determined by MAS ^{31}P NMR the dissociation constants of LPA and PA in bilayers of the zwitterionic phospholipids PC and PE. The second p*K*a of LPA, which falls in the physiological range, was found to be lower than that of PA, and we showed that it is the free hydroxyl on the LPA backbone that is responsible for this difference in ionization behavior. Furthermore, the degree of ionization of both LPA and PA was found to depend strongly on bilayer lipid composition, i.e., the PC:PE ratio, of the membrane. These data will be discussed in terms of the unique hydrogen bonding possibilities of the phosphomonoester headgroup of (L)PA.

First, we will briefly discuss the factors influencing phospholipid ionization (for more comprehensive reviews, see refs *16*, *17*, and *35*). Phospholipid protonation in a bilayer membrane deviates from that of the free molecule in solution. The main reason for this difference is the membrane-water interface. Protonation depends on the local pH at this interface, and this (intrinsic) pH can be dramatically different from that found in solution. Introducing an overall negative charge in the membrane, for instance, by incorporating PS, increases the proton concentration at the lipid-water interface by attracting protons from the bulk solution, thereby lowering the intrinsic pH and increasing the apparent pK_a of a protonatable group. Similarly, the presence of a positive charge, as, for instance, found in the zwitterionic lipid PC, increases the local pH at the lipid headgroup and decreases the apparent pK_a of the phosphate of the same molecule. Indeed, PS decreases the charge of PA as shown in Figure 5B, and the pK_a of the phosphate of PC is well below that of the first pK_a of (L)PA as shown in Figure 1.

The pK_a of a protonatable group can also be affected by the formation of hydrogen bonds. A proton that is participating in a hydrogen bond will dissociate less easily, resulting in a higher pK_a for the protonatable group (*36*-*38*).

Ionization Behavior of LPA and PA in Extended Phospholipid Bilayers

The dissociation constants of 10 mol % PA and LPA were measured in a PC bilayer. Interestingly, we find that the second pK_a differs significantly between the two lipids, despite identical headgroups. The pK_{a2} of LPA is 0.45 ± 0.06 pH unit lower than that of PA.

This difference in dissociation constant must be due to an intrinsic difference between PA and LPA, and we provided direct evidence that the hydroxyl group at the *sn*-2 position of the backbone of LPA is responsible for this difference (see Figure 2). How is this hydroxyl group able to lower the second pK_a of LPA with respect to PA? This is most likely not due to a difference in headgroup orientation. The residual CSAs, a measure of lipid order and dynamics, of LPA and dehydroxy-LPA are similar, suggesting that the conformation of the headgroup in dehydroxy-LPA is close to that in LPA. In support of this, the orientation of the glycerol backbone in LPA and a dehydroxy-LPA-related compound (acyl chain

attached via an ether instead of an ester linkage) was found to be nearly identical [but very different from that of PA (*39-41*)]. Instead, we propose that the difference in ionization of LPA and PA is the result of an intramolecular hydrogen bond between the 2-hydroxyl and the deprotonated headgroup in LPA. Such a hydrogen bond is indeed observed in the LPA crystal structure (*40*). Apparently, this intramolecular hydrogen bond is a special feature of LPA that is preserved in excess water. Intramolecular hydrogen bonds are known to influence the (de)protonation behavior of phospholipids. Haines and co-workers showed for cardiolipin (CL; see Figure 6A) that the pK_a's for the two hydroxyls in the headgroup of CL are not identical (*37*, *42*). The authors also showed that this is due to the hydroxyl on the glycerol connecting the two phosphates of CL, and proposed that as soon as one of the two hydroxyls has dissociated its proton it is able to form a hydrogen bond network (see Figure 6A), which stabilizes the proton on the other hydroxyl. In analogy to CL, we propose that at near-physiological pH both PA and LPA are able to form an intramolecular hydrogen bond between the deprotonated and protonated hydroxyl of their phosphomonoester headgroup (Figure 6B), a feature unique to the phosphomonoester. This intramolecular hydrogen bond stabilizes the second proton of the phosphomonoester and would therefore increase pK_{a2}. However, LPA also has the possibility to form an intramolecular hydrogen bond between the hydroxyl at the *sn*-2 position of its glycerol backbone and the deprotonated hydroxyl of the phosphomonoester headgroup (Figure 6B), destabilizing the second proton and resulting in a lower pK_{a2} (and a charge more negative than that of PA at the same pH). Indeed, the LPA compound lacking the hydroxyl at the *sn*-2 position, and thus unable to form this intramolecular hydrogen bond, behaves in a manner identical to that of PA. An important implication of this interpretation is that the phosphate of LPA is localized within hydrogen bonding distance of the hydroxyl at the *sn*-2 position of the glycerol backbone.

This hydrogen bond model also provides an explanation for the other major observation in our study, namely, that PE facilitates deprotonation of (L)PA in a bilayer. As opposed to the quaternary amine of PC, PE carries a primary amine group that is able to efficiently donate protons to form hydrogen bonds (see Figure 6B). Moreover, the headgroup of PE lies more or less parallel to the membrane surface (*43*), and the positively charged amine is therefore uniquely positioned to interact electrostatically with the phosphate (when it is negatively charged) of the (L)PA headgroup bringing both sufficiently close in space to allow hydrogen bond formation. This intermolecular hydrogen bond will destabilize the intramolecular hydrogen bond within the phosphomonoester headgroup, and thus lower the second dissociation constant.

Our model also explains the observation that LPA and PA have essentially the same pK_{a2} in a bilayer rich in PE. The large amount of hydrogen bond donors provided by the amine group of PE will overrule the hydrogen bonding ability of the hydroxyl at the *sn*-2 position of LPA.

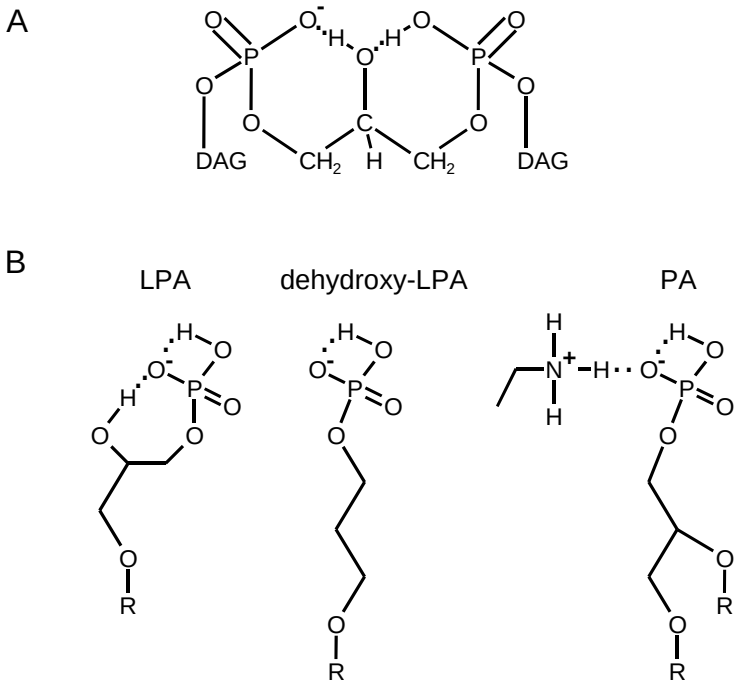

Figure 6: (A) Chemical structure of the headgroup of cardiolipin (DAG, diacylglycerol) when one (left) of the two phosphodiesters has dissociated its proton; hydrogen bonds are represented by two dots (adapted from refs *37* and *42*). (B) Chemical structure of LPA (left), dehydroxy-LPA (middle), and PA (right) when carrying one negative charge. R stands for an oleoyl (18:1) acyl chain, and the primary amine group to the left of PA represents part of a PE headgroup.

We also noticed a small contribution of lipid packing on the ionization of PA upon a change from the PE bilayer to the PE hexagonal phase, as indicated by a slight increase in pK_{a2} (see Table 1). We interpret this result in terms of curvature. Lipid headgroups in the hexagonal phase are more tightly packed than in a flat lipid bilayer due to the concave (negative) curvature of this lipid organization. This tighter headgroup packing is only possible at a lower PA charge, reducing the effective headgroup area. These results agree well with previous observations describing the effects of lipid packing on PA charge (*20*, *21*), and also explain the effects of cholesterol on the ionization of PA. Cholesterol has a negative spontaneous curvature close to that of DOPE (*44*), and the small increase in the negative charge of PA that we observed in the presence of cholesterol can be explained by its effects on lipid packing. An alternative explanation, the formation of a hydrogen bond between the OH group of cholesterol and PA, is unlikely given the position of the OH group within the lipid bilayer. Instead, cholesterol appears to form a hydrogen bond with the carbonyl oxygen of the ester-bound acyl chains (*45*); similar hydrogen bonds have been suggested for the OH group of sphingomyelin (*36*).

Biological Implications

The phosphomonoester headgroup of (L)PA with its unique intra- and intermolecular hydrogen bond capabilities is what makes these simple but key phospholipids so special. For example, our observation that LPA carries more charge than PA in a PC bilayer at the same (physiological) pH implies that the metabolic interconversion of these lipids by, for example, PLA1 and PLA2 (PA → LPA) or LPA acyltransferases (LPAATs) such as $CtBP_3$/BARS and endophilin (LPA → PA) will affect local membrane charge if the membrane has a sufficiently high PC:PE ratio. This charge difference between LPA and PA is maintained in the presence of physiological (cytosolic) concentrations of Mg^{2+}, and may well have important consequences for lipid and lipid-protein interactions. The intramolecular hydrogen bond between the headgroup of LPA and the hydroxyl on the glycerol backbone is also likely to contribute to specific recognition of LPA by LPA-binding proteins such as the LPA receptors.

In addition, our observation that the deprotonation of (L)PA depends on the local PC:PE ratio and should thus be different in the different organelles of a eukaryotic cell may have important implications for (L)PA-protein interactions at these subcellular locations. The specific recruitment of downstream effectors to PA at a particular intracellular site might, in part, rely on the deprotonation behavior of PA at this site. In yeast, for example, the protein Opi1 is retained by PA at the ER and not elsewhere in the cell (*46*), whereas Raf-1 kinase is specifically recruited by PA to the plasma membrane (*47*, *48*). Our data also imply that hydrogen bonds between PA and basic residues such as lysines and arginines in proteins probably play an important role in protein-lipid interactions. Indeed, we have strong indications for such hydrogen bonds in model membrane experiments (manuscript in preparation).

Finally, modulation of headgroup charge may be part of the mechanism by which (L)PA regulates biomembrane fusion and fission events. For example, PA formed in a budding transport carrier at the Golgi by $CtBP_3$/BARS or diacylglycerol kinase will carry more charge in the cytoplasmic leaflet than in the luminal leaflet of the Golgi due to the large difference in the PC:PE ratio (~8-fold lower in the cytoplasmic leaflet) and pH (~7.2 at the cytoplasmic leaflet and ~6.0 in the Golgi lumen). This would result in PA with more negative curvature in the Golgi luminal leaflet than in the cytoplasmic leaflet. If PA formed in the cytoplasmic leaflet would be able to translocate (*49*) to the luminal site, it might facilitate the fission of the budding transport carrier by $CtBP_3$/BARS (*11*, *50*, *51*). Thus, a defined charge of (L)PA at a particular (intra)cellular location, determined largely by the local PC:PE ratio, may be a key element of the action of (L)PA at that specific location, and regulate protein recruitment, activation, etc. Our observations on the unique ionization properties of LPA and PA may well be the basis of their special functions in the cell.

Acknowledgments

We thank Antoinette Killian, Eefjan Breukink, and Mandy Lutters for helpful discussions and practical assistance.

References

1. Athenstaedt, K., and Daum, G. (1999) Phosphatidic acid, a key intermediate in lipid metabolism, *Eur. J. Biochem. 266*,1-16.
2. Contos, J. J., Ishii, I., and Chun, J. (2000) Lysophosphatidic acid receptors, *Mol. Pharmacol. 58*, 1188-96.
3. Tigyi, G., and Parrill, A. L. (2003) Molecular mechanisms of lysophosphatidic acid action, *Prog. Lipid Res. 42*, 498-526.
4. Ishii, I., Fukushima, N., Ye, X., and Chun, J. (2004) Lysophospholipid receptors: Signaling and biology, *Annu. Rev. Biochem. 73*, 321-54.
5. Siddhanta, A., and Shields, D. (1998) Secretory vesicle budding from the trans-Golgi network is mediated by phosphatidic acid levels, *J. Biol. Chem. 273*, 17995-8.
6. Roth, M. G., Bi, K., Ktistakis, N. T., and Yu, S. (1999) Phospholipase D as an effector for ADP-ribosylation factor in the regulation of vesicular traffic, *Chem. Phys. Lipids 98*, 141-52.
7. Schmidt, A., Wolde, M., Thiele, C., Fest, W., Kratzin, H., Podtelejnikov, A. V., Witke, W., Huttner, W. B., and So¨ling, H. D. (1999) Endophilin I mediates synaptic vesicle formation by transfer of arachidonate to lysophosphatidic acid, *Nature 401*, 133-41.
8. Weigert, R., Silletta, M. G., Spano, S., Turacchio, G., Cericola, C., Colanzi, A., Senatore, S., Mancini, R., Polishchuk, E. V., Salmona, M., Facchiano, F., Burger, K. N. J., Mironov, A., Luini, A., and Corda, D. (1999) CtBP/BARS induces fission of Golgi membranes by acylating lysophosphatidic acid, *Nature 402*, 429-33.
9. Bankaitis, V. A. (2002) Cell biology. Slick recruitment to the Golgi, *Science 295*, 290-1.
10. Karbowski, M., Jeong, S. Y., and Youle, R. J. (2004) Endophilin B1 is required for the maintenance of mitochondrial morphology, *J. Cell Biol. 166*, 1027-39.
11. Kooijman, E. E., Chupin, V., de Kruijff, B., and Burger, K. N. J. (2003) Modulation of membrane curvature by phosphatidic acid and lysophosphatidic acid, *Traffic 4*, 162-74.
12. Kooijman, E. E., Chupin, V., Fuller, N. L., Kozlov, M. M., de Kruijff, B., Burger, K. N. J., and Rand, P. R. (2005) Spontaneous curvature of phosphatidic acid and lysophosphatidic acid, *Biochemistry 44*, 2097-102.
13. Testerink, C., and Munnik, T. (2005) Phosphatidic acid: A multifunctional stress signaling lipid in plants, *Trends Plant Sci. 10*, 368-75.
14. Verkleij, A. J., De Maagd, R., Leunissen-Bijvelt, J., and De Kruijff, B. (1982) Divalent cations and chlorpromazine can induce non-bilayer structures in phosphatidic acid-containing model membranes, *Biochim. Biophys. Acta 684*, 255-62.
15. Farren, S. B., Hope, M. J., and Cullis, P. R. (1983) Polymorphic phase preferences of phosphatidic acid: A ^{31}P and ^{2}H NMR study, *Biochem. Biophys. Res. Commun. 111*, 675-82.
16. Cevc, G. (1990) Membrane electrostatics, *Biochim. Biophys. Acta 1031*, 311-82.
17. Tocanne, J. F., and Teissie, J. (1990) Ionization of phospholipids and phospholipid-supported interfacial lateral diffusion of protons in membrane model systems, *Biochim. Biophys. Acta 1031*, 111-42.
18. Koter, M., de Kruijff, B., and van Deenen, L. L. (1978) Calcium-induced aggregation and fusion of mixed phosphatidylcholine-phosphatidic acid vesicles as studied by ^{31}P NMR, *Biochim. Biophys. Acta 514*, 255-63.
19. Hauser, H. (1989) Mechanism of spontaneous vesiculation, *Proc. Natl. Acad. Sci. U.S.A. 86*, 5351-5.
20. Swairjo, M. A., Seaton, B. A., and Roberts, M. F. (1994) Effect of vesicle composition and curvature on the dissociation of phosphatidic acid in small unilamellar vesicles: A ^{31}P NMR study, *Biochim. Biophys. Acta 1191*, 354-61.

21. Traikia, M., Warschawski, D. E., Lambert, O., Rigaud, J. L., and Devaux, P. F. (2002) Asymmetrical membranes and surface tension, *Biophys. J. 83*, 1443-54.
22. Lynch, K. R., Hopper, D. W., Carlisle, S. J., Catalano, J. G., Zhang, M., and MacDonald, T. L. (1997) Structure/activity relationships in lysophosphatidic acid: The 2-hydroxyl moiety, *Mol. Pharmacol. 52*,75-81.
23. Rouser, G., Fleischer, S., and Yamamoto, A. (1970) Two-dimensional thin layer chromatographic separation of polar lipids and determination of phospholipids by phosphorus analysis of spots, *Lipids 5*, 494-6.
24. Appleton, T. G., Hall, J. R., Ralph, S. F., and Thompson, C. S. M. (1989) NMR Study of Acid-Base Equilibria and Other Reactions of Ammineplatinum Complexes with Aqua and Hydroxo Ligands, *Inorg. Chem. 28*, 1989-93.
25. Tate, M. W., and Gruner, S. M. (1987) Lipid polymorphism of mixtures of dioleoylphosphatidylethanolamine and saturated and monounsaturated phosphatidylcholines of various chain lengths, *Biochemistry 26*, 231-6.
26. Toombes, G. E., Finnefrock, A. C., Tate, M. W., and Gruner, S. M. (2002) Determination of L(α)-H(II) phase transition temperature for 1,2-dioleoyl-*sn*-glycero-3-phosphatidylethanolamine, *Biophys. J. 82*, 2504-10.
27. Gruner, S. M., Cullis, P. R., Hope, M. J., and Tilcock, C. P. (1985) Lipid polymorphism: The molecular basis of nonbilayer phases, *Annu. Re*V. *Biophys. Biophys. Chem. 14*, 211-38.
28. Janes, N. (1996) Curvature stress and polymorphism in membranes, *Chem. Phys. Lipids 81*, 133-50.
29. Fuller, N., and Rand, R. P. (2001) The influence of lysolipids on the spontaneous curvature and bending elasticity of phospholipid membranes, *Biophys. J. 81*, 243-54.
30. Cullis, P. R., and de Kruijff, B. (1979) Lipid polymorphism and the functional roles of lipids in biological membranes, *Biochim. Biophys. Acta 559*, 399-420.
31. Lafleur, M., Bloom, M., and Cullis, P. R. (1990) Lipid polymorphism and hydrocarbon order, *Biochem. Cell Biol. 68*,1-8.
32. van Meer, G., and Sprong, H. (2004) Membrane lipids and vesicular traffic, *Curr. Opin. Cell Biol. 16*, 373-8.
33. Fleischer, B., Zambrano, F., and Fleischer, S. (1974) Biochemical characterization of the golgi complex of mammalian cells, *J. Supramol. Struct. 2*, 737-50.
34. Verkleij, A. J., Zwaal, R. F., Roelofsen, B., Comfurius, P., Kastelijn, D., and van Deenen, L. L. (1973) The asymmetric distribution of phospholipids in the human red cell membrane. A combined study using phospholipases and freeze-etch electron microscopy, *Biochim. Biophys. Acta 323*, 178-93.
35. McLaughlin, S. (1989) The electrostatic properties of membranes, *Annu. Re*V. *Biophys. Biophys. Chem. 18*, 113-36.
36. Boggs, J. M. (1987) Lipid intermolecular hydrogen bonding: Influence on structural organization and membrane function, *Biochim. Biophys. Acta 906*, 353-404.
37. Kates, M., Syz, J. Y., Gosser, D., and Haines, T. H. (1993) pH-dissociation characteristics of cardiolipin and its 2'-deoxy analogue, *Lipids 28*, 877-82.
38. Moncelli, M. R., Becucci, L., and Guidelli, R. (1994) The intrinsic pK_a values for phosphatidylcholine, phosphatidylethanolamine, and phosphatidylserine in monolayers deposited on mercury electrodes, *Biophys. J. 66*, 1969-80.
39. Harlos, K., Eibl, H., Pascher, I., and Sundell, S. (1984) Conformation and packing properties of phosphatidic acid: The crystal structure of monosodium dimyristoylphosphatidate, *Chem. Phys. Lipids 34*, 115-26.
40. Pascher, I., and Sundell, S. (1985) Interactions and space requirements of the phosphate head group in membrane lipids. The crystal structure of disodium lysophosphatidate dihydrate, *Chem. Phys. Lipids 37*, 241-50.
41. Pascher, I., Sundell, S., Eibl, H., and Harlos, K. (1984) Interactions and space requirement of the phosphate head group of membrane lipids: The single-crystal structures of a triclinic and a monoclinic form of hexadecyl-2-deoxy-glycerophosphoric acid monohydrate, *Chem. Phys. Lipids 35*, 103-15.
42. Haines, T. H., and Dencher, N. A. (2002) Cardiolipin: A proton trap for oxidative phosphorylation, *FEBS Lett. 528*,35-9.
43. Langner, M., and Kubica, K. (1999) The electrostatics of lipid surfaces, *Chem. Phys. Lipids 101*,3-35.

44. Chen, Z., and Rand, R. P. (1997) The influence of cholesterol on phospholipid membrane curvature and bending elasticity, *Biophys. J. 73*, 267-76.
45. Ramsammy, L. S., Volwerk, H., Lipton, L. C., and Brockerhoff, H. (1983) Association of cholesterol with lysophosphatidylcholine, *Chem. Phys. Lipids 32*,83-9.
46. Loewen, C. J., Gaspar, M. L., Jesch, S. A., Delon, C., Ktistakis, N. T., Henry, S. A., and Levine, T. P. (2004) Phospholipid metabolism regulated by a transcription factor sensing phosphatidic acid, *Science 304*, 1644-7.
47. Ghosh, S., Strum, J. C., Sciorra, V. A., Daniel, L., and Bell, R. M. (1996) Raf-1 kinase possesses distinct binding domains for phosphatidylserine and phosphatidic acid. Phosphatidic acid regulates the translocation of Raf-1 in 12-O-tetradecanoylphorbol-13-acetate-stimulated Madin Darby canine kidney cells, *J. Biol. Chem. 271*, 8472-80.
48. Rizzo, M. A., Shome, K., Watkins, S. C., and Romero, G. (2000) The recruitment of Raf-1 to membranes is mediated by direct interaction with phosphatidic acid and is independent of association with Ras, *J. Biol. Chem. 275*, 23911-8.
49. Kol, M. A., van Laak, A. N., Rijkers, D. T., Killian, J. A., de Kroon, A. I., and de Kruijff, B. (2003) Phospholipid flop induced by transmembrane peptides in model membranes is modulated by lipid composition, *Biochemistry 42*, 231-7.
50. Bonazzi, M., Spano, S., Turacchio, G., Cericola, C., Valente, C., Colanzi, A., Kweon, H. S., Hsu, V. W., Polishchuck, E. V., Polishchuck, R. S., Sallese, M., Pulvirenti, T., Corda, D., and Luini, A. (2005) CtBP3/BARS drives membrane fission in dynamin-independent transport pathways, *Nat. Cell Biol. 7*, 570-80.
51. Kozlovsky, Y., and Kozlov, M. M. (2003) Membrane fission: Model for intermediate structures, *Biophys. J. 85*,85-96.

CHAPTER 5

A molecular basis for the specific interaction between phosphatidic acid and proteins

Abstract

Despite its simple chemical structure, phosphatidic acid (PA) is an important bioactive phospholipid involved in a number of key cellular processes. The regulatory role of PA in these cellular processes often involves its specific interaction with PA-binding proteins. It is clear that positively charged amino acid residues such as lysine and arginine are essential in the interaction with PA, however, the exact nature of the interaction between PA and PA-binding proteins is unknown. In order to gain insight into the molecular mechanism by which PA interacts with these proteins we studied the effect of lysine and arginine residues in membrane interacting polypeptides on the negative charge of PA. In lipid model systems we show, using solid state magic angle spinning ^{31}P-NMR that, surprisingly, lysine and arginine residues in membrane interacting peptides are able to increase the charge of PA. We provide evidence that this increase in charge is predominantly caused by hydrogen bond interactions between lysine or arginine residues and the phosphate headgroup of PA. We propose that the phosphomonoester headgroup of PA is an effective docking site for lysine and arginine residues and that its capacity to act as a hydrogen bond acceptor forms the basis of the specific interaction between PA and it's protein effectors.

Introduction

Phosphatidic acid (PA) is a minor but important bioactive lipid involved in at least three essential and likely interrelated processes in a typical eukaryotic cell. PA is a key intermediate in the biosynthetic route of the main membrane phospholipids and triglycerides (*1*), it is involved in membrane dynamics (*2-4*), and has important signaling functions (*5-7*). PA formed as part of a signaling cascade is usually produced either by phospholipase D (PLD) enzymes, which cleave the headgroup of abundant lipids such as PC and PE, or by the sequential action of phospholipase C (PLC), which produces diacylglycerol (DAG), and diacylglycerol kinase (DGK) that can rapidly convert DAG into PA. The role of PA in membrane dynamics and signaling maybe two-fold, either via an effect on the packing properties of the membrane lipids, or via the specific binding of effector proteins. Changes in lipid packing by local lipid metabolism is an attractive hypothesis for PA, which is a cone shaped lipid that may potentially facilitate membrane bending (*2-4, 8*). Alternatively, the local production of PA by PLD or PLC-DGK enzymes can result in the recruitment, inhibition or activation of downstream proteins. Most of these functions are mediated via PA's ability to specifically bind to the protein in question.

This raises the important question; "What is the underlying mechanism of PA binding to its effector domains?" Remarkably, the genuine PA binding domains thus far identified (*7, 9, 10*) are diverse and share no apparent sequence homology, in contrast to other lipid binding domains, such as e.g. the PH, PX, FYVE, and C2

domains (*11-15*). One general feature that these domains do have in common is the presence of basic amino acids (*7*). Where examined in detail these basic amino acids were shown to be essential for the interaction with PA, which underscores the importance of electrostatic interactions. Indeed, the negatively charged phosphomonoester headgroup of PA would be expected to interact electrostatically with basic amino acids in a lipid binding domain, however, such a simple electrostatic interaction cannot explain the strong preference of PA-binding proteins for PA as compared to other negatively charged phospholipids.

In a recent study, we showed that the phosphomonoester headgroup of PA has remarkable properties (*16*). The phosphomonoester headgroup is able to form an intramolecular hydrogen bond upon initial deprotonation (when its charge is –1) which stabilizes the second proton against dissociation. We provided evidence that competing hydrogen bonds, e.g. from the primary amine of the headgroup of phosphatidylethanolamine (PE), can destabilize this intramolecular hydrogen bond and thus favor the further deprotonation, i.e. increase the negative charge, of PA (*16*). These data raised the intriguing hypothesis that a combination of electrostatic and hydrogen bond interactions, and not just electrostatic interactions, of PA with basic amino acids, i.e. lysine and arginine, may contribute to the (specific) binding of PA to PA binding proteins.

We set out to test this hypothesis by determining the ability of lysine and arginine residues in various membrane interacting polypeptides to form a hydrogen bond with the phosphomonoester headgroup of PA in a lipid bilayer. Consistent with our hypothesis, we find using magic angle spinning ^{31}P-NMR, that the positively charged amino acids lysine and arginine, in these peptides, are able to increase the charge of PA. We conclude that this increase in charge is due to the formation of hydrogen bonds between PA and the basic amino acids and speculate that hydrogen bonds form the basis of the specific interaction between PA and its protein partners.

Materials and Methods

Sample Preparation

1,2-dioleoyl-*sn*-glycero-3-phosphate (monosodium salt; DOPA), 1,2-dioleoyl-*sn*-glycero-3-phosphocholine (DOPC), 1,2-dioleoyl-*sn*-glycero-3-phosphoethanolamine (DOPE), and 1,2-dioleoyl-3-trimethylammonium-propanediol (chloride salt; DOTAP) were purchased from Avanti Polar lipids (Birmingham, AL). Dimethyldioctadecylammonium (chloride salt) was a kind gift from dr. M. Scarzello, University of Groningen, The Netherlands. The detergents, dodecylamine and dodecyltrimethylammonium chloride, were purchased from Sigma chemical company (St. Louis, MO). Lipid purity was checked by thin layer chromatography and judged to be more than 99%. Polyleucine-alanine based peptides: KALP, RALP and WALP (Table 1) were synthesized as described

previously and were more than 98% pure as determined by quantitative HPLC (*17*), poly-L-lysines (hydrobromide) with polymerization degree n of 20 and 100, were purchased from Sigma chemical company (St. Louis, MO) and used without further purification.

Dry lipid films and lipid suspensions were prepared as described previously (*16*). Lipid/poly-L-lysine samples were prepared by hydrating the lipid film with Hepes buffer (100 mM Hepes, 5 mM acetic acid-NaOH, 100 mM NaCl, and 2 mM EDTA pH 7.20) containing poly-L-lysine. The resulting lipid/poly-L-lysine dispersions were freeze thawed at least once after which the pH of the dispersions was generally found to be within 0.05 pH units of pH 7.20 (if not, the pH was adjusted to fall within this range). The dispersions were centrifuged at 70 krpm for 30 min at RT in a Beckman TL-100 ultracentrifuge and the pellet was transferred to 4 mm TiO_2 MAS-NMR sample tubes for ^{31}P-NMR measurement. Lipid/polyleucine-alanine peptide films were prepared as described previously (*17*). These films were hydrated with Hepes buffer and the dispersions were centrifuged as described above. The clear supernatant was removed and the pellet was resuspended in Hepes buffer and centrifuged again. This procedure was repeated until the pH of the supernatant was within 0.05 pH units of pH 7.20, after which the samples were freeze thawed at least once. When the pH of this dispersion was still within 0.05 pH units of pH 7.20 it was centrifuged and the pellet was transferred to 4 mm TiO_2 MAS-NMR sample tubes, otherwise the above procedure was repeated until the pH was in the desired range (pH 7.20 ± 0.05).

NMR spectroscopy

^{31}P-NMR spectra were recorded on a Bruker Avance 500 widebore spectrometer (Karlsruhe, Germany) at 202.48 MHz, using a 4 mm cross polarization (CP) MAS-NMR probe. Samples were spun at the magic angle (54.7°) at 5 kHz to average the chemical shift anisotropy, and the chemical shift position of PA was recorded relative to 85% H_3PO_4. Under stable spinning conditions typically, 500-3000 scans were recorded. Experiments were carried out at a temperature of 20.0 ± 0.5 ^{o}C.

Results

The effect of basic amino acids in membrane interacting polypeptides on the ionization behavior of PA was investigated using MAS-^{31}P-NMR. MAS-^{31}P-NMR allows for the measurement of high-resolution spectra of phospholipids in extended, i.e. physiologically most relevant, bilayers (*20, 21*). Experiments were performed in 100 mM salt to mimic physiological conditions and were conducted at neutral pH (pH 7.2) and temperature in order to eliminate pH and temperature effects on ionization and ^{31}P chemical shift. The phospholipid bilayer consisted of the phospholipids PC and PA in a 9:1 molar ratio (unless noted otherwise).

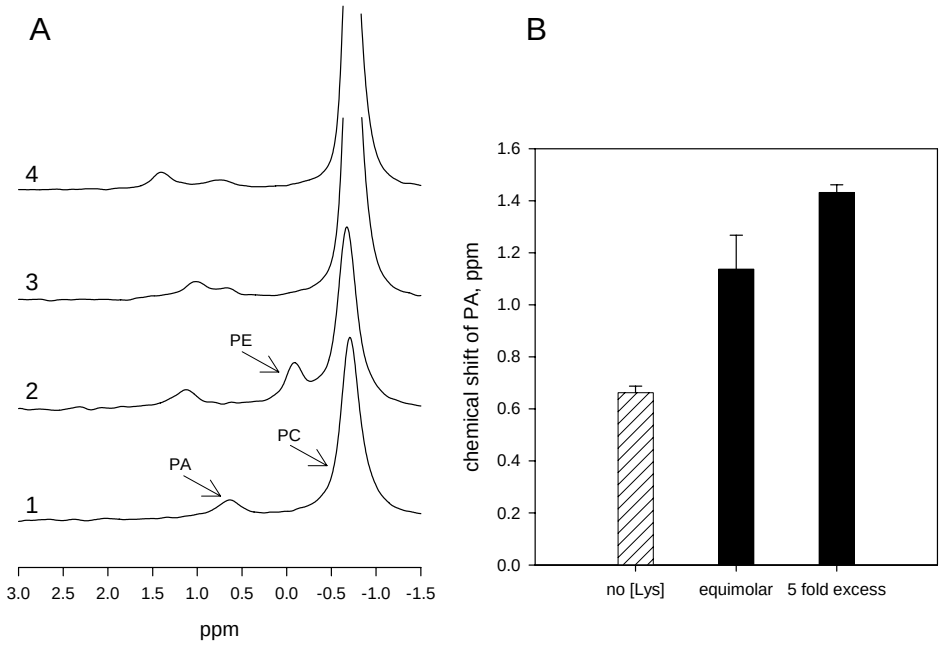

Figure 1: (A) MAS-^{31}P-NMR spectra at pH 7.20 for 10 mol % PA, in PC (curve 1), in PC containing 10 mol % PE (curve 2), in PC hydrated in the presence of poly-L-lysine ($[Lys]_{20}$) either equimolar (lysine residues) with respect to PA (curve 3), or at a 5 fold molar excess (curve 4). The y-axis for curves 3 and 4 was amplified (x2) compared to that for curves 1 and 2. (B) Quantitation of the effect of poly-L-lysine on the chemical shift of PA in PC/PA (9:1). In this and subsequent figures the error bar associated with the control, i.e. PC/PA vesicles, corresponds to the standard deviation of 8 separate experiments, whereas the error bars for peptide and amphiphile containing samples corresponds to the range of at least two individual experiments

The ^{31}P chemical shift of PA was previously found to be very sensitive to the ionization (charge) state of the phosphate headgroup, and a change in chemical shift to downfield values, e.g. induced by an increase in pH, corresponds to an increase in negative charge (*16, 22, 23*). In an earlier study, we observed that inclusion of PE in a PA containing PC bilayer resulted in a profound downfield shift of the ^{31}P-NMR peak of PA (*16*). This is exemplified in Figure 1A (compare curves 1 and 2). Curve 1 shows the MAS-^{31}P-NMR spectrum of a PC/PA bilayer with the minor downfield peak (to the left) corresponding to PA and the major upfield peak (to the right) to PC. Inclusion of 10 mol % PE (PC/PE/PA 8:1:1, curve 2), results in a large shift of the PA peak to downfield values resulting from an increase in the charge of PA. This increase in negative charge of PA induced by PE is caused by hydrogen bonding between the primary amine in the headgroup of PE and the phosphomonoester headgroup of PA (see (*16*)).

In order to determine whether the basic amino acid lysine, which contains a primary amine, is also able to form a hydrogen bond with PA we first determined the effect of polylysine$_{20}$ on the chemical shift of PA at neutral pH. Polylysine$_{20}$ was chosen because it binds with high affinity to membranes containing negatively

charged phospholipid (*24, 25*). Figure 1 A (curve 3) shows data obtained for a PC/PA lipid film hydrated with buffer containing an equimolar amount of lysine residues with respect to PA. The majority of the PA peak has moved to downfield values. A minor part of the PA peak does not shift upon polylysine addition under the experimental conditions employed, and most likely represents a small pool of PA in the multilamellar vesicles that is not reached by polylysine. In the presence of an excess of lysine residues with respect to PA (Figure 1 A, curve 4), maximizing the PA-polylysine interaction, the PA peak shifts even further (see Figure 1B for quantitation). These results were confirmed using another, longer, polylysine (n=100) (data not shown). Thus, at constant pH, the addition of polylysine results in an increase in the negative charge of PA.

The binding of polylysine to negatively charged lipid membranes is cooperative and requires a polymerization degree of at least 5 lysine residues (*24*). In contrast, the PA binding domains that have been identified to date contain a smaller cluster of only 2-4 basic amino acids in their PA binding site (*7, 26*). In order to more closely mimic the natural situation, we chose a well-characterized experimental system of synthetic polyleucine-alanine α-helical transmembrane peptides flanked on either side by two basic amino acids to study the interaction of small clusters of the basic amino acids, Lys and Arg, with PA (see Table 1 and (*17, 27*)). The hydrophobic core of these peptides matches the hydrophobic core of the lipid bilayer (*27*), and thereby positions the amino acid side chains of the flanking residues in the acyl-chain/headgroup interface where the phosphate group of PA is located. We first determined the effect of the lysine-flanked peptide, KALP23. Figure 2 A shows that at a lipid-to-peptide ratio of 25, KALP23 causes a large shift of the PA peak (curve 4; control, curve 1, quantified in Figure 2 B). This demonstrates that KALP23 is indeed able to increase the charge of PA, similar to the effects of PE and polylysine. The effect of KALP23 on the charge of PA depends on the lipid-to-peptide ratio, as is shown in Figure 2 B (black bars). Identical results were obtained with a KALP31 peptide (data not shown), which has a considerably longer transmembrane segment than the KALP23 peptide (*27*). We next investigated the effect of arginine by incorporating RALP23 in the PC/PA bilayer. Figures 2 A (curve 3) and B (light gray bars) clearly show that this peptide is also able to increase the negative charge of PA in the PC/PA bilayer, although slightly less efficient than KALP23. As a control we investigated the effect of the tryptophan-flanked peptide WALP23. WALP23 incorporated at different concentrations did not appreciably affect the chemical shift of PA (Figure 2 A, curve 2; and Figure 2 B), and the considerably longer WALP31 peptide displayed a similar behavior (data not shown). WALP peptides are thus unable to increase the charge of PA even at high peptide to lipid ratios. Clearly, the positively charged residues in KALP and RALP are responsible for the observed charge increase of PA and not just the presence of a transmembrane peptide.

What is the cause behind the increase in the negative charge of PA induced by the positively charged residues lysine and arginine? Apart from the possibility to form a hydrogen bond with the phosphomonoester headgroup of PA, lysine and

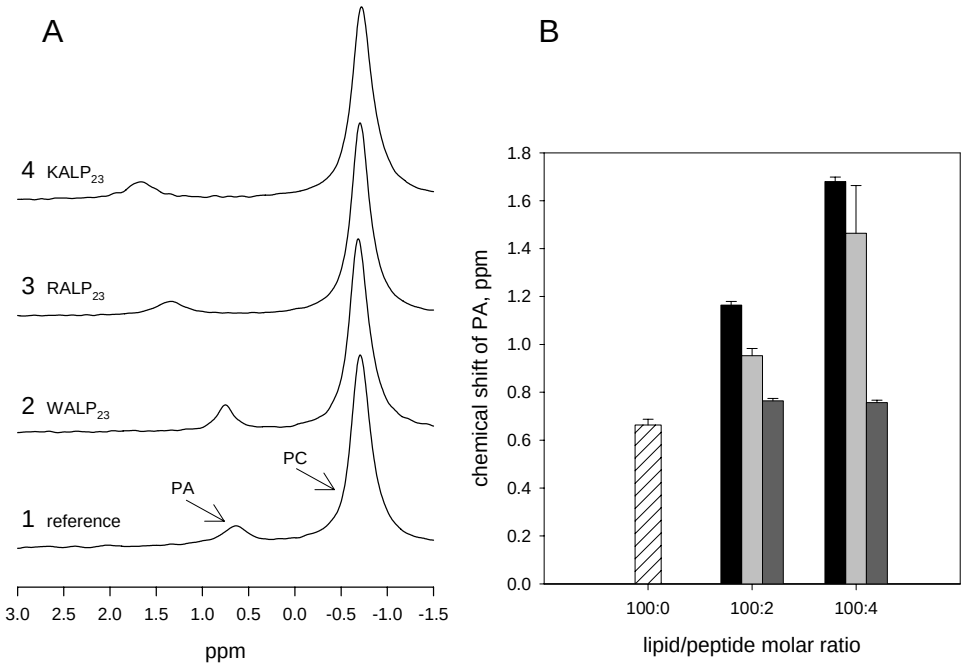

Figure 2: (A) MAS-^{31}P-NMR spectra at pH 7.20 for PC/PA (9:1, curve 1, same as in Figure 1.) and for PC/PA (9:1) bilayers containing either WALP23 (curve 2), RALP23 (curve 3) or KALP23 (curve 4) peptides at a lipid to protein molar ratio of 25:1. (B) Quantification of the chemical shift effects; PC/PA bilayer without peptide (dashed bar), PC/PA bilayer containing KALP23 (black), RALP23 (light gray), and WALP23 (dark gray), at two different lipid to protein ratios.

Table 1 Amino acid sequences of peptides used; flanked by lysine, arginine and tryptophan residues (Ac, acetyl).

KALP23	Ac-GKKLALALALALALALALKKA-amide
KALP31	Ac-GKKLALALALALALALALALALALALKKA-amide
RALP23	Ac-GRRLALALALALALALALRRA-amide
WALP23	Ac-GWWLALALALALALALALWWA-amide
WALP31	Ac-GWWLALALALALALALALALALALALWWA-amide

arginine also introduce a net positive charge at the membrane surface. This will decrease the local proton concentration (due to charge repulsion) and thus increase the local (interfacial) pH. An increase in the interfacial pH will result in an increase in the negative charge of PA, and is accompanied by a downfield shift of the PA peak. In order to distinguish between positive charge and hydrogen bond effects we sought a simpler system in which to address this issue. We chose the positively

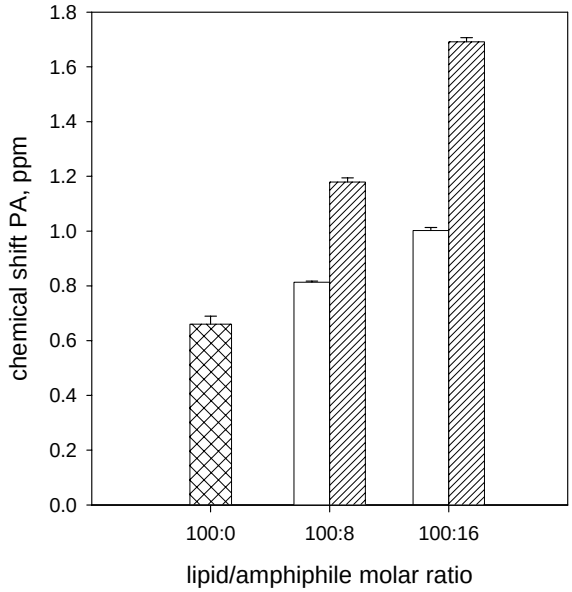

Figure 3: Effects of the amphiphiles dodecyltrimethylammonium (white bars) and dodecylamine (dashed bars) on the chemical shift of PA at two lipid to amphiphile molar ratios; control without amphiphiles (checkered bar, identical to that shown in Figures 1B and 2B).

charged amphiphiles dodecyltrimethylammonium chloride and dodecylamine, since these amphiphiles carry the same positive charge but differ in the ability to form hydrogen bonds, in that the quaternary amine cannot act as a hydrogen bond donor. Dodecyltrimethylammonium chloride and dodecylamine were included in the PC/PA bilayer at a lipid-to-amphiphile molar ratio of 12.5 and 6.25 to be able to compare the positive charge effects induced by these amphiphiles with those induced by the transmembrane peptides (each KALP and RALP peptide contains 4 positive charges); the results are shown in Figure 3. As expected, the positively charged dodecyltrimethylammonium chloride, increased the charge of PA due to the interaction of a positive charge (Figure 3, white bars; control, checkered bar). Similar results were obtained for the structurally very different, quaternary amine containing, diacyl amphiphiles, 1,2-dioleoyl-3-trimethylammonium-propanediol (DOTAP) and dimethyldioctadecylammonium, which also only caused a small increase in the chemical shift and thus the negative charge of PA (data not shown). However, the dodecylamine amphiphile, which in addition to being positively charged can also form a hydrogen bond, induced a substantially larger increase in the negative charge of PA (Figure 3, dashed bars). Quantitation of the change in charge induced by primary and quaternary amines required full titration curves, which are shown in the Appendix. They revealed that, at pH 7.2, primary amines caused a ~60 % larger increase in the negative charge when compared to quaternary amines. These results clearly demonstrate that hydrogen bond forming

primary amines are able to further increase the negative charge of PA beyond the increase induced by quaternary amines, and indicate that the extra increase in negative charge induced by the primary amine is due to the formation of a hydrogen bond with the phosphomonoester headgroup of PA.

Importantly, the effects induced by the quarternary amines are substantially less than those induced by KALP and RALP peptides, while the effect of the primary amine dodecylamine is essentially identical to that of KALP (compare Figures 2B and 3). Therefore, we conclude that the interaction of KALP and RALP peptides with PA involves the formation of hydrogen bonds between the basic amino acid residues and the phosphomonoester headgroup of PA.

Discussion

The aim of the current study was to gain insight into the mechanism of the interaction between PA and basic amino acids known to be present in the lipid-binding domain of its protein effectors. Using magic angle spinning ^{31}P-NMR we studied the interaction between the basic amino acids, lysine and arginine in membrane interacting peptides with PA and show that both lysine and arginine residues directly interact, via hydrogen bonds, with PA and thereby significantly increase the charge of PA.

Basic amino acids in membrane interacting peptides increase the charge of PA

We observed that the positively charged amino acids lysine and arginine in the membrane interacting peptides, polylysine, KALP and RALP, caused a downfield shift in the ^{31}P-NMR peak of PA at constant pH. We and others have shown that such a downfield shift of the ^{31}P-NMR peak of PA is due to deprotonation of the phosphomonoester headgroup of PA which results in a deshielding of the phosphorus nucleus (*16, 22, 23, 28*). A downfield shift of the ^{31}P-NMR peak of PA is therefore indicative of an increase in the negative charge. A similar effect on PA charge is observed irrespective of whether the lysine residues are added from the outside as polylysine, or are already stably anchored in the membrane water interface as is the case in the KALP experiments (compare Figures 1 and 2). Interestingly, the lysine residues in KALP23 and KALP31 induced an identical shift of the PA peak, indicating an equal effect on the negative charge of PA. This is despite the fact that KALP31 is considerably longer than KALP23, with a hydrophobic segment that is ~10Å longer than the hydrophobic thickness of a DOPC bilayer (*27*). Earlier studies on KALP peptides in PC bilayers indicate that the lysine residues in KALP are flexibly anchored in the headgroup region of the lipid bilayer and effectively modulate the hydrophobic length of the peptide to "match" that of the PC bilayer (snorkeling effect, see (*17*)). Apparently, in the presence of PA the lysines localize to the PA phosphate instead of throughout the headgroup region suggesting that the phosphomonoester headgroup of PA acts as an effective docking site for the lysine residues.

PA as a docking site for basic amino acids through H-bond formation

What then is the molecular mechanism behind the increase in negative charge of PA caused by basic amino acids present in membrane interacting peptides? One possibility is that the attraction of the positively charged side chain of basic amino acids towards the negatively charged phosphate of PA leads to a local decrease in the interfacial proton concentration. It is well known that positive charges introduced in the headgroup/water interface of the lipid bilayer repel protons away from the interface and result in a decrease of the local proton concentration and increase in local pH (*29-31*). Indeed, incorporation of the quaternary amine containing amphiphiles dodecyltrimethylammonium, DOTAP and dimethyldioctadecylammonium, which carry a positive charge but are not able to interact with PA via a hydrogen bond, causes an increase in the negative charge of PA (Figure 3). However, this increase is considerably less than that induced by the basic amino acids lysine and arginine in membrane interacting peptides. Most of the increase in negative charge caused by these basic amino acids must thus be caused by a different mechanism. We previously showed that the phosphomonoester headgroup of PA is special in that it forms an intramolecular hydrogen bond upon loosing its first proton. Competing intermolecular hydrogen bonds may destabilize this intramolecular hydrogen bond, facilitating further deprotonation of the phosphomonoester headgroup of PA (*16*). Indeed, we show that the dodecylamine amphiphile, which aside from being positively charged is able to form a hydrogen bond with PA, had a three fold larger effect (as judged by changes in the ^{31}P-NMR peak of PA) on the negative charge of PA than dodecyltrimethylammonium. The shift in the PA peak caused by dodecylamine is essentially identical to that induced by KALP and thus provides strong support for a prominent role for hydrogen bonds in the increase in the negative charge of PA by lysine residues (also see appendix). Importantly, the formation of hydrogen bonds between lysine residues and PA implies direct docking of the membrane interacting peptide on the phosphomonoester headgroup of PA, and not merely an electrostatic attraction into the electric layer over the lipid headgroups.

Lysines and arginines both increase PA charge

The increase in PA charge induced by arginine residues in RALP23 is less than that induced by the lysine residues in KALP23. The exact nature of this difference is unclear but may be related to the substantial delocalization of charge in the guanidinium group of arginine when compared to the primary amine of lysine, potentially reducing its hydrogen bond donating capacity. This suggestion is supported by a search of the Cambridge Structural database for the hydrogen bond length of lysine (primary amine) and arginine (guanidinium group) like geometries to a phosphate oxygen, which shows that the mean hydrogen bond length for the lysine like compounds is ~0.1 Å shorter than that of the arginine like compounds (see Appendix), indicating that indeed the guanidinium group of arginine is a weaker hydrogen bond donor than the primary amine of lysine.

Nonetheless, RALP23 had a ~2 fold larger effect on the negative charge of PA than dodecyltrimethylammonium, indicating that hydrogen bonds also play a prominent role in the increase in PA charge caused by arginine residues. The WALP23 peptide did not increase the charge of PA, even at high peptide to lipid ratios, indicating that the tryptophans do not form a hydrogen bond with the phosphomonoester headgroup of PA. The absence of such a hydrogen bond with PA despite the presence of the NH group in the indole side chain of tryptophan, may be due to a preferential localization of the indole side chain in the hydrophobic interior of the lipid bilayer as compared to the phosphate region of the lipid headgroup/water interface (32). Even the WALP31 peptide, which has a considerably longer hydrophobic segment and might potentially position its tryptophan side chains higher in the acyl chain/headgroup interface, is not able to form a hydrogen bond with PA. Positive charges in the membrane interacting peptides thus appear to be essential for the formation of a hydrogen bond with PA and effective docking of the membrane interacting peptide on the phosphomonoester headgroup of PA.

Molecular model and biological implications

Collectively our data point to the following mechanism for the interaction of lysine and arginine residues in membrane interacting peptides with PA (Figure 4). The positive charge of lysine and arginine side chains first results in electrostatic attraction to the negatively charged phosphomonoester headgroup of PA. Next, as soon as the side chain hydrogen bond donor and phosphate headgroup come into close proximity (<3Å) a hydrogen bond is formed, leading to a further deprotonation of the headgroup of PA, thereby enhancing the electrostatic attraction, and docking of the lysine and arginine side chain. We propose that the hydrogen bond forming properties of PA are a key element of the specific recognition of PA by PA binding proteins.

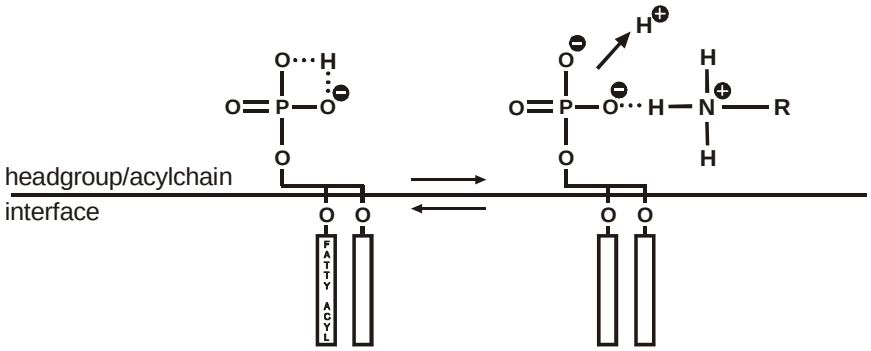

Figure 4: Schematic representation of the proposed electrostatic and hydrogen bond model for the increase in negative charge of PA induced by positively charged amino acid residues. Positive charge and hydrogen bond formation is shown for the primary amine of a lysine residue, but can, in principle, be any combination of positively charged ion and hydrogen bond donor. Intra- and intermolecular hydrogen bond interactions are indicated by a dotted line.

Our proposal that the phosphomonoester headgroup of PA acts as a docking site for lysine and arginine residues may also have important biological implications. First, many transmembrane proteins are flanked on the cytosolic side of the membrane by basic amino acids, which are thought to stabilize the transmembrane orientation of the protein and/or regulate its activity (*33-36*). Clusters of these basic amino acids may specifically bind to PA. Indeed, recent evidence suggests that this is the case for the mechanosensitive channel of large conductance MscL. MscL carries a cluster of three basic amino acids (R98, K99, and K100) on its cytosolic face, and has a special, high affinity, interaction with PA (*37*). Second, the docking of basic protein domains on PA may be followed by insertion of hydrophobic protein domains into the hydrophobic interior of the lipid bilayer. Such a favorable hydrophobic interaction has indeed been observed *in vitro* for the GTPase dynamin. Dynamin, which binds to negatively charged membranes, shows considerably more insertion in mixed-lipid monolayers containing PA instead of other negatively charged phospholipids (*38*). How can we understand these hydrophobic interactions? On top of its high charge and capacity to form hydrogen bonds, (unsaturated) PA also has a special molecular shape (*3, 8*). PA is the only anionic phospholipid with a pronounced cone shape under physiological conditions (*36*). Cone shaped lipids facilitate protein penetration into the membrane by forming favorable insertion sites in the headgroup region of lipids (*39*). Our observation that PA may act as a docking site for membrane interacting peptides very close to the hydrophobic interior of the lipid bilayer, together with the cone shape of PA, turns PA into a very effective insertion site for membrane-active proteins. We propose that the hydrogen bonding capacity of PA coupled to the location of the phosphate headgroup close to the hydrophobic interior of the lipid bilayer sets PA apart from all the other anionic membrane lipids.

Acknowledgments

We would like to thank Antoinette Killian for helpful discussions and suggestions on the use and properties of the polyleucine-alanine peptides, and Huub Kooijman for his expert advice on the Cambridge structural database.

Appendix

Quantitation of changes in PA charge: positive charge and H-bond interactions

The interaction of positive charge and hydrogen bonds with the phosphomonoester headgroup of PA increases its negative charge. Both effects could be discriminated by the use of simple quaternary- (positive charge only) and primary- (identical positive charge and H-bond donor) amine containing amphiphiles. From changes in the chemical shift of PA induced by these amphiphiles it was clear that hydrogen bond formation increases the negative charge of PA over that induced by the interaction of a positive charge only. However, these results did not quantify this effect in terms of actual changes in negative charge (i.e. changes in pK_{a2}).

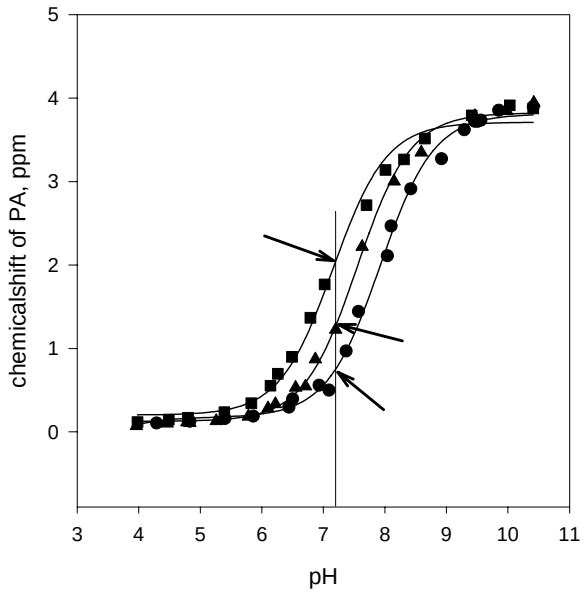

Figure A1: pH titration curves for PA in PC/PA (9:1, molar ratio) bilayers containing KALP23 (squares) at a lipid to KALP23 molar ratio of 25, DOTAP (triangles) at a lipid to DOTAP molar ratio of 6.25. The control (circles) is also shown, taken from (*16*). The arrows emphasize the differences in charge at pH 7.2.

Therefore, pH titration curves, shown in Figure A1, were constructed according to previously established procedures (see chapter 4, (*16*)). KALP23, containing 4 lysine residues, was chosen as the primary amine containing compound, whereas DOTAP was chosen as the quaternary amine containing

compound. The control, 10 mol% PA in 90 mol% PC was taken from (*16*), see chapter 4 Figure 2. The pK_{a2} of PA changed from 7.92 ± 0.03 for the PC/PA (9:1) bilayer, to 7.55 ± 0.03 for the PC/PA (9:1) bilayer containing DOTAP at a lipid to DOTAP molar ratio of 6.25, to 7.16 ± 0.05 for the PC/PA (9:1) bilayer containing KALP23 at a lipid to KALP23 molar ratio of 25 (i.e. a lysine to lipid ratio of 6.25). At pH 7.2, indicated in the figure by the vertical line, this corresponds to the following changes in the negative charge of PA: 1.16 e (negative charge unit), to 1.32 e to 1.54 e for the control, DOTAP and KALP23 containing bilayers respectively. These results indicate that primary amines increase the negative charge of PA by ~60% over that induced by quaternary amines and subsequently confirm the important role of hydrogen bonds in the increase in negative charge of PA by membrane interacting peptides containing the basic amino acids lysine and arginine.

Mean H-bond length of lysine-to-phosphate- and arginine-to-phosphate-like geometries

Lysine and arginine, in KALP23 and RALP23, respectively increase the negative charge of PA in a PC/PA (9:1) bilayer. However, the increase induced by RALP23 is less than that induced by KALP23. This is despite their identical positive charge and ability to form a hydrogen bond with the phosphomonoester headgroup of PA.

One suggestion that would explain the smaller effect of RALP23 on the negative charge of PA is that arginine is a weaker side chain hydrogen bond donor than lysine. In order to investigate this hypothesis we searched the Cambridge Structural database for the mean hydrogen bond length, which is a measure of hydrogen bond strength, of lysine-to-phosphate- and arginine-to-phosphate-like geometries. These geometries are shown in Figure A2 A and B respectively.

Hydrogen bond length determination

In the Cambridge Structural Database (version November 2004, with updates of February and May 2005, total number of entries 347767) 395 crystal structure determinations were found containing 1716 fragments that fit the lysine geometry, i.e. primary amine-to-phosphate hydrogen bond length as shown in Figure A2 A. For the arginine geometry, i.e. guanidinium-to-phosphate hydrogen bond length as shown in Figure A2 B, 30 crystal structure determinations were found containing 158 fragments. Searches were performed with the program ConQuest (*18*), for data analysis the program Vista (*19*) was used.

The resulting histograms are shown in Figure A2, A and B for the lysine and arginine geometry respecitvely. From these data the mean hydrogen bond length found for “lysine” was 2.813 Å and for “arginine” 2.919 Å, clearly indicating that

lysine residues are likely to be stronger side chain hydrogen bond donors than arginine residues.

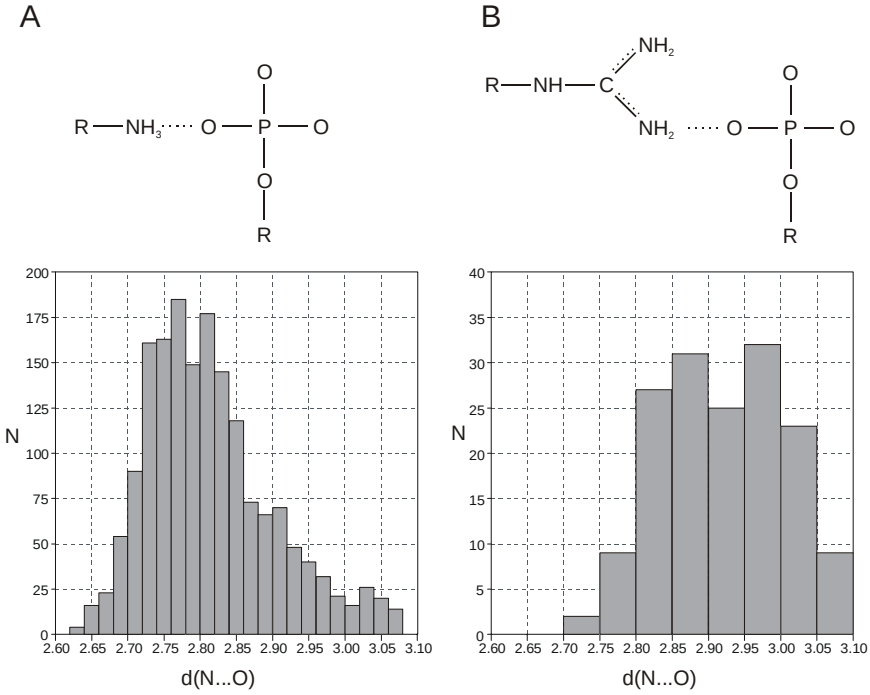

Figure A2: Histograms of the N…O hydrogen bond length for *A*, lysine-to-phosphate-like geometries, and *B*, arginine-to-phosphate-like geometries. The hydrogen bond is indicated by the dotted line between the nitrogen and oxygen atom. Data were compiled using the Cambridge Structural database as described in this Appendix.

References

1. Athenstaedt, K., and Daum, G. (1999) Phosphatidic acid, a key intermediate in lipid metabolism. *Eur. J. Biochem. 266*, 1-16.
2. Chen, Y. G., Siddhanta, A., Austin, C. D., Hammond, S. M., Sung, T. C., Frohman, M. A., Morris, A. J., and Shields, D. (1997) Phospholipase D stimulates release of nascent secretory vesicles from the trans-Golgi network. *J. Cell Biol. 138*, 495-504.
3. Kooijman, E. E., Chupin, V., de Kruijff, B., and Burger, K. N. J. (2003) Modulation of membrane curvature by phosphatidic acid and lysophosphatidic acid. *Traffic 4*, 162-74.
4. Ktistakis, N. T., Brown, H. A., Waters, M. G., Sternweis, P. C., and Roth, M. G. (1996) Evidence that phospholipase D mediates ADP ribosylation factor-dependent formation of Golgi coated vesicles. *J. Cell Biol. 134*, 295-306.
5. English, D., Cui, Y., and Siddiqui, R. A. (1996) Messenger functions of phosphatidic acid. *Chem. Phys. Lipids 80*, 117-32.
6. Freyberg, Z., Siddhanta, A., and Shields, D. (2003) "Slip, sliding away": phospholipase D and the Golgi apparatus. *Trends Cell. Biol. 13*, 540-6.
7. Testerink, C., and Munnik, T. (2005) Phosphatidic acid: a multifunctional stress signaling lipid in plants. *Trends Plant Sci. 10*, 368-75.

8. Kooijman, E. E., Chupin, V., Fuller, N. L., Kozlov, M. M., de Kruijff, B., Burger, K. N. J., and Rand, P. R. (2005) Spontaneous curvature of phosphatidic acid and lysophosphatidic acid. *Biochemistry 44*, 2097-102.
9. Ktistakis, N. T., Delon, C., Manifava, M., Wood, E., Ganley, I., and Sugars, J. M. (2003) Phospholipase D1 and potential targets of its hydrolysis product, phosphatidic acid. *Biochem. Soc. Trans. 31*, 94-7.
10. Testerink, C., Dekker, H. L., Lim, Z. Y., Johns, M. K., Holmes, A. B., Koster, C. G., Ktistakis, N. T., and Munnik, T. (2004) Isolation and identification of phosphatidic acid targets from plants. *Plant J. 39*, 527-36.
11. Ellson, C. D., Andrews, S., Stephens, L. R., and Hawkins, P. T. (2002) The PX domain: a new phosphoinositide-binding module. *J. Cell Sci. 115*, 1099-105.
12. Lemmon, M. A. (2003) Phosphoinositide recognition domains. *Traffic 4*, 201-13.
13. Maffucci, T., and Falasca, M. (2001) Specificity in pleckstrin homology (PH) domain membrane targeting: a role for a phosphoinositide-protein co-operative mechanism. *FEBS Lett. 506*, 173-9.
14. Rizo, J., and Sudhof, T. C. (1998) C2-domains, structure and function of a universal Ca2+-binding domain. *J. Biol. Chem. 273*, 15879-82.
15. Stenmark, H., Aasland, R., and Driscoll, P. C. (2002) The phosphatidylinositol 3-phosphate-binding FYVE finger. *FEBS Lett. 513*, 77-84.
16. Kooijman, E. E., Carter, K. M., van Laar, E. G., Chupin, V., Burger, K. N. J., and de Kruijff, B. (2005) What Makes the Bioactive Lipids Phosphatidic Acid and Lysophosphatidic Acid So Special? *Biochemistry 44*, 17007-17015.
17. de Planque, M. R., Boots, J. W., Rijkers, D. T., Liskamp, R. M., Greathouse, D. V., and Killian, J. A. (2002) The effects of hydrophobic mismatch between phosphatidylcholine bilayers and transmembrane alpha-helical peptides depend on the nature of interfacially exposed aromatic and charged residues. *Biochemistry 41*, 8396-404.
18. Bruno, I. J., Cole, J. C., Edgington, P. R., Kessler, M., Macrae, C. F., McCabe, P., Pearson, J., and Taylor, R. (2002) New software for searching the Cambridge Structural Database and visualizing crystal structures. *Acta Crystallogr. B 58*, 389-97.
19. CCDC (1994) *Vista - A Program for the Analysis and Display of Data Retrieved from the CSD.*, Cambridge Crystallographic Data Center, 12 Union Road, Cambridge, England.
20. Watts, A. (1998) Solid-state NMR approaches for studying the interaction of peptides and proteins with membranes. *Biochim. Biophys. Acta 1376*, 297-318.
21. Traikia, M., Warschawski, D. E., Lambert, O., Rigaud, J. L., and Devaux, P. F. (2002) Asymmetrical membranes and surface tension. *Biophys. J. 83*, 1443-54.
22. Koter, M., de Kruijff, B., and van Deenen, L. L. (1978) Calcium-induced aggregation and fusion of mixed phosphatidylcholine-phosphatidic acid vesicles as studied by 31P NMR. *Biochim. Biophys. Acta 514*, 255-63.
23. Hauser, H. (1989) Mechanism of spontaneous vesiculation. *Proc. Natl. Acad. Sci. U S A 86*, 5351-5.
24. de Kruijff, B., Rietveld, A., Telders, N., and Vaandrager, B. (1985) Molecular aspects of the bilayer stabilization induced by poly(L-lysines) of varying size in cardiolipin liposomes. *Biochim. Biophys. Acta 820*, 295-304.
25. Kim, J., Mosior, M., Chung, L. A., Wu, H., and McLaughlin, S. (1991) Binding of peptides with basic residues to membranes containing acidic phospholipids. *Biophys. J. 60*, 135-48.
26. Andresen, B. T., Rizzo, M. A., Shome, K., and Romero, G. (2002) The role of phosphatidic acid in the regulation of the Ras/MEK/Erk signaling cascade. *FEBS Lett. 531*, 65-8.
27. de Planque, M. R., Goormaghtigh, E., Greathouse, D. V., Koeppe, R. E., 2nd, Kruijtzer, J. A., Liskamp, R. M., de Kruijff, B., and Killian, J. A. (2001) Sensitivity of single membrane-spanning alpha-helical peptides to hydrophobic mismatch with a lipid bilayer: effects on backbone structure, orientation, and extent of membrane incorporation. *Biochemistry 40*, 5000-10.
28. Swairjo, M. A., Seaton, B. A., and Roberts, M. F. (1994) Effect of vesicle composition and curvature on the dissociation of phosphatidic acid in small unilamellar vesicles--a 31P-NMR study. *Biochim. Biophys. Acta 1191*, 354-61.
29. McLaughlin, S. (1989) The electrostatic properties of membranes. *Annu. Rev. Biophys. Biophys. Chem. 18*, 113-36.
30. Cevc, G. (1990) Membrane electrostatics. *Biochim. Biophys. Acta 1031*, 311-82.

31. Tocanne, J. F., and Teissie, J. (1990) Ionization of phospholipids and phospholipid-supported interfacial lateral diffusion of protons in membrane model systems. *Biochim. Biophys. Acta 1031*, 111-42.
32. Persson, S., Killian, J. A., and Lindblom, G. (1998) Molecular ordering of interfacially localized tryptophan analogs in ester- and ether-lipid bilayers studied by 2H-NMR. *Biophys. J. 75*, 1365-71.
33. van Klompenburg, W., Nilsson, I., von Heijne, G., and de Kruijff, B. (1997) Anionic phospholipids are determinants of membrane protein topology. *Embo J. 16*, 4261-6.
34. Killian, J. A., and von Heijne, G. (2000) How proteins adapt to a membrane-water interface. *Trends Biochem. Sci. 25*, 429-34.
35. Lee, A. G. (2004) How lipids affect the activities of integral membrane proteins. *Biochim. Biophys. Acta 1666*, 62-87.
36. Zimmerberg, J., and Kozlov, M. M. (2005) How proteins produce cellular membrane curvature. *Nat. Rev. Mol. Cell Biol.*.
37. Powl, A. M., East, J. M., and Lee, A. G. (2005) Heterogeneity in the binding of lipid molecules to the surface of a membrane protein: hot spots for anionic lipids on the mechanosensitive channel of large conductance MscL and effects on conformation. *Biochemistry 44*, 5873-83.
38. Burger, K. N. J., Demel, R. A., Schmid, S. L., and de Kruijff, B. (2000) Dynamin is membrane-active: lipid insertion is induced by phosphoinositides and phosphatidic acid. *Biochemistry 39*, 12485-93.
39. van den Brink-van der Laan, E., Killian, J. A., and de Kruijff, B. (2004) Nonbilayer lipids affect peripheral and integral membrane proteins via changes in the lateral pressure profile. *Biochim. Biophys. Acta 1666*, 275-88.

CHAPTER 6

Summary and Discussion

Summarizing discussion

This thesis describes the molecular shape and charge of the phospholipids lysophosphatidic acid (LPA) and phosphatidic acid (PA), which is of key importance to understand the diverse biological roles ascribed to these simple phospholipids. Our studies were inspired by the role these lipids play in membrane dynamics, in particular membrane fission. In this discussion I will highlight our main results and give my personal view on the role of PA in membrane fission and of (L)PA/protein interactions.

Summary and further insights

Phosphatidic acid, and the conversion of LPA into PA, has been implicated in membrane traffic, in particular along the secretory pathway (*1-6*), and the molecular shape of PA was proposed to facilitate membrane bending during or prior to fission (*4*). In chapter 2 we determined the molecular shape of PA and LPA when present as a single lipid species, so-called single lipid system, and in a mixture with PE, so-called mixed lipid system, under relevant physiological conditions of temperature, pH, and ionic conditions (including divalent cations Mg^{2+} and Ca^{2+}). In the single lipid system, we find that at cytosolic conditions (neutral pH and a 0.5 mM free Mg^{2+}) both PA and LPA appear to be cylindrically shaped, i.e. they are bilayer preferring lipids. Interestingly, we find that the effective molecular shape of PA is very sensitive to pH, and that at typical intra-Golgi conditions (pH 6.6-5.9, and 0.3 mM Ca^{2+}) PA is a type II lipid, i.e. has a cone shape. Contrary to the single lipid systems, the molecular shape of PA and LPA was found to be not the same in mixed lipid systems. In these mixed lipid systems, which more closely mimic biomembranes, LPA behaves as a typical type I (inverted cone shaped) lipid, strongly stabilizing the bilayer phase of unsaturated PE, whereas PA destabilizes the bilayer phase of PE indicating that PA is a type II (cone shaped) lipid. In mixed lipid systems the effective molecular shape of PA is also extremely pH sensitive, exhibiting a more pronounced type II shape at slightly acidic pH. In chapter 3 these results were further quantified by determining the spontaneous curvature of PA and LPA using x-ray methods. We find that at neutral pH, in the presence of 150 mM NaCl, dioleoyl-PA has a negative spontaneous curvature close to that of dioleoyl-PE, whereas LPA has the most positive spontaneous curvature of any membrane lipid measured to date (see (*7*), for a comprehensive overview of lipid spontaneous curvatures). Again, we find that the molecular shape of PA is sensitive to environmental factors, omitting salt from the hydration buffer strongly reduces the spontaneous curvature of PA, turning it into a cylindrically shaped lipid. This effect of salt on the effective molecular shape of PA was confirmed in mixed lipid systems using ^{31}P-NMR, according to the procedures discussed in chapter 2. Omission of salt (150 mM NaCl) from the hydration buffer resulted in a stabilization of the bilayer phase of PE by 10 mol% PA (E.E. Kooijman, unpublished results), similar to the behavior of 10 mol% PC in PE (see Figure 6, curve 2 in chapter 2). Aside from affecting the

biophysical properties of the membrane due to its molecular shape, PA may also exert it's effect via binding to specific proteins (*8-10*). Interaction with proteins is likely to depend on the charge properties of PA. Interestingly, charge is also likely to play an important role in the sensitivity of the molecular shape of PA to pH and ionic conditions.

In chapter 4 we find that LPA carries more charge than PA and that inclusion of PE in the bilayer facilitates the deprotonation of both PA and LPA. These seemingly unrelated results could be rationalized by the proposal that upon the loss of the first proton, the second proton of the phosphomonoester headgroup forms an intramolecular hydrogen bond, which stabilizes the second proton against dissociation (for model see Figure 6 of chapter 4). This hydrogen bond can be destabilized by competing hydrogen bonds that facilitate the deprotonation of PA and LPA. Examples of such competing hydrogen bonds are those formed by the sn-2 hydroxyl moiety of LPA, and the primary amine of PE, as discussed in chapter 4.

In addition, we observed that the charge of PA is sensitive to changes in lipid packing in agreement with Swairjo et al. (*11*), and Traikia et al. (*12*). In the hexagonal H_{II} phase, PA carries less charge than in the PE bilayer most likely due to a tighter packing of lipid headgroups in the H_{II} phase (*13*). Similarly, inclusion of cholesterol, a type II lipid (*14*), expected to reduce lipid headgroup packing (*15*), led to an increase in the charge of PA. This effect of lipid packing could be confirmed in experiments identical to those described in Figure 4 of chapter 4, if at high PE content PC was replaced by LPC. LPC has a shape complementary to that of PE and as a result reduces the curvature stress of the PE bilayer (*16-18*). The "tighter" packing in the headgroup region due to the replacement of PC by LPC indeed results in a decrease in the negative charge of PA (E.E. Kooijman, unpublished results).

Basic amino acids are known to be present in PA binding proteins. In chapter 5 we find that these basic amino acids when present in membrane interacting peptides increase the negative charge of PA. Comparison of the increase in negative charge induced by lysine and arginine residues with those induced by simple amphiphiles revealed that the increase in negative charge is mainly caused by hydrogen bonds between lysine and/or arginine residues and the phosphomonoester headgroup of PA, in agreement with the mechanism proposed in chapter 4 for the interaction between (L)PA and PE. Based on these and additional results reported in chapter 5 we propose that the phosphomonoester headgroup of PA is an effective docking site for lysine and arginine residues present in PA binding proteins.

In chapter 4 we showed that PE is able to interact with PA via the formation of a hydrogen bond and in chapter 5 we demonstrate that the phosphomonoester headgroup of PA is able to form a hydrogen bond with lysine and arginine residues present in membrane interacting peptides. An interesting question that now arises is whether or not PE might hamper the binding of a PA binding protein to PA, since the primary amine of PE may compete with the primary amine of

lysine or the guanidinium group of arginine in the formation of hydrogen bonds. Electrostatic arguments and recent PA binding data argue against this possibility. The headgroup of PE, containing a primary amine, is not a "point" charge, like the side chain of a lysine residue, but a dipole due to the presence of the negatively charged phosphate. The electrostatic potential of a dipole drops off as the inverse square of the distance from the dipole ($V \sim 1/r^2$), whereas that of a point charge allows for much longer-range interactions ($V \sim 1/r$, see (*19*)). Although this is an oversimplification, e.g. we ignored the presence of the bilayer interface, the argument above suggests that at least the initial affinity of a lysine residue for the phosphate of PA is likely higher than that of PE, which argues against a competition between lysine residues (or any other point charges) and PE.

Lipid-binding experiments with a PA-binding protein support this notion. The plant protein Constitutive response 1 (CTR1), a key regulator of ethylene signaling (*20-22*) and a close homologue of the mammalian PA binding protein Raf-1 kinase (*23-25*), specifically binds vesicles containing PA *in vitro* (C. Testerink, personal communication). Replacing half of the PC with PE does not prevent binding of the PA-binding domain of CTR1 but increases binding indicating that there is no competition between PE and this PA-binding domain (C. Testerink, personal communication).

Role of PA and LPA-acyltransferases in biomembrane fission

One of the models put forward in the discussion of chapter 2 of this thesis poses that a conversion of LPA into PA, an activity ascribed to the unrelated fission proteins $CtBP_3$/BARS (*6*) and endophilin (*4*), leads to a change in the spontaneous curvature of the membrane and thereby facilitates fission. The results as described in chapter 2 and 3 indeed indicate that such a conversion might lead to a change in the spontaneous curvature of the cytosolic membrane leaflet. Subsequent biophysical modeling of BARS-mediated Golgi fragmentation (Golgi pearling, (*6*)), showed that a conversion of LPA to PA was not enough to explain the observed pearling behavior from a lipid point of view, but rather that further metabolism of PA to DAG would be required (*26*). The important role of BARS in membrane fission has recently been confirmed in *in vivo* experiments (*27, 28*). *In vivo*, BARS plays a critical role in mitosis, inhibition of endogenous BARS activity by an antibody against BARS or by BARS dominant negative mutants inhibited Golgi fragmentation and mitosis (*28*). Furthermore, BARS appears to be an essential protein for membrane fission in several dynamin-independent transport pathways (*27*). Clearly, BARS is an important fission protein involved in multiple transport pathways in the cell. Importantly however, the proposed LPAAT activity of BARS was not found to be an absolute requirement for fission, but rather appears to have a facilitating role at best (*27, 28*). In the case of endophilin-mediated fission, the role of endophilin's LPAAT activity has also not been resolved/clarified. The role of LPA-to-PA conversion in BARS- and endophilin-mediated fission is thus

unclear. Indeed, the LPAAT activities measured for BARS and endophilin (*in vitro*) are very low. Moreover, recent work by McMahon, et al. suggests that the LPAAT activity of BARS and endophilin may even be a co-purification artifact (*29*). This thus raises the important question of the potential role of PA in these membrane fission events. A remarkable observation is that BARS, which *in vitro* has LPAAT activity, facilitates membrane fission *in vivo* compared to BARS mutants that have no *in vitro* LPAAT activity (*27, 28*), suggesting PA is involved in BARS mediated membrane fission. The important role of PA in fission along the secretory pathway is not debated and numerous recent studies have shown that formation of PA by PLD activity is required for numerous fission and membrane dynamics events (*30-35*). One hypothesis that may explain the facilitating role of (*in vitro*) LPAAT activity in BARS mediated fission *in vivo* is that PA may be formed via additional routes, notably PLD activity. Due to redundancy in the formation of PA during (or prior) to fission PA formed by BARS is non-essential.

In the scheme of lipid facilitated membrane traffic, PA may take a unique place. We have shown that PA is a very versatile lipid in that its molecular shape and negative charge are very sensitive to such factors as pH, ionic conditions, and local lipid composition, and will thus be different depending of PA's intracellular location. At these different locations PA may affect membrane fission by directly facilitating membrane bending (chapters 2 and 3) or alternatively, as discussed in chapter 5, bind to proteins that are then uniquely positioned to insert hydrophobic residues into the bilayer and destabilize it (*7, 36, 37*).

Clearly, in future studies it will be important to localize lipids and lipid metabolic events in relation to the actual membrane fission event in live cells, at high spatial and temporal resolution. Of particular interest is the use of specific lipid binding domains in the localization of different lipid species (*38-40*), and the use of a combination of live cell imaging and electron microscopy (*41, 42*). Another, novel technique that might have the potential to localize proteins (and perhaps lipids) at high spatial resolution is matrix enhanced secondary ion mass spectrometry (ME-SIMS, (*43*)).

Implications for (L)PA binding domains

The PA binding domains that have been identified to date, although sharing no apparent sequence homology, do share several common features that are likely essential for the interaction with PA. One of these common features is the presence of lysine and arginine residues that are expected to form a positively charged binding pocket/site for PA. The electrostatic attraction and hydrogen bonding between these basic residues and the phosphate of PA is not likely to be sufficient for an efficient interaction (*44*), especially if we keep in mind that PA is usually present in an excess pool of other anionic phospholipids, such as PS and PI. A second feature shared by PA binding domains is the presence of hydrophobic

residues such as tryptophans and phenylalanines, which may engage in hydrophobic interactions with the membrane.

(L)PA binding proteins bind a di-anionic phosphomonoester moiety

The charge properties of PA, which we investigated in this thesis, are markedly different from the abundant anionic phospholipids PS and PI. For example, PA is able to carry two negative charges and its pK_{a2} falls in the physiological range and lipid charge is thus sensitive to pH, ionic conditions and hydrogen bond formation, as we have shown in chapters 4 and 5. The fact that PA has the ability to carry two net negative charges instead of one may facilitate the recognition of PA by PA binding proteins. The results described in chapters 4 and 5 indicate that the positive charge and potential hydrogen bond interactions of PA binding proteins with PA lead to an increase in the negative charge of PA, making it likely that PA binding domains bind to a di-anionic PA molecule. Modeling of the structure of the PA binding domain, TAPAS, in the presence of PA, indeed suggests that PA binds this domain in a di-anionic form (*45*). Furthermore, the hypothesis is supported by a careful inspection of the crystal structures of other protein domains that selectively bind phosphomonoester-containing compounds, such as glucose-6-phosphate, glucose-1-phosphate and the numerous polyphosphoinositide-binding domains. The phosphomonoester binding sites as determined from the crystal/solution structures of proteins such as the PX domain of the $P40^{phox}$ subunit of NADPH oxidase (*46*), the FYVE domain of EEA1 (*47-49*), the PI-3,4,5-P_3 specific PH domains (*50-53*), phosphoglucose isomerase (*54, 55*), glucose-1-phosphatase (*56*), glucosamine 6-phosphate deaminase (*57*), and hexokinase (*58*), all contain a positively charged binding pocket, which makes numerous hydrogen bond contacts with the phosphoryl moiety, which inevitably carries two negative charges. The lysine and arginine residues in these binding sites, aside from forming the positive pocket itself, often form the hydrogen bond donors but other residues donating side chain hydrogen bonds also regularly occur. The most common of these residues (after inspection of the crystal structures discussed above) are serine, threonine and tyrosine, whereas histidine, glutamine and asparagine are somewhat less common hydrogen bond donors, but all can donate a side chain hydrogen bond to coordinate the phosphomonoester. Interestingly, the recently identified PA binding domain of protein phosphatase 1 contains a serine residue (in the proximity of a positively charged region) that is essential for binding to PA (*59*), indicating that not only lysine and arginine residues but a combination of positive charge and hydrogen bond donor are sufficient to fulfill the electrostatic requirements for the binding of PA by PA binding proteins.

LPA like PA has a phosphomonoester headgroup and binding of LPA to its G protein-coupled receptors is likely to depend on similar principles as those discussed above for PA. Indeed, the binding of LPA (and coincidentally also its sphingolipid counterpart sphingosine-1-phosphate (S1P)) to its receptors critically depends on the phosphomonoester headgroup (*60, 61*), and the phosphate binding

region of the LPA receptors all contain two conserved basic residues (one arginine and one lysine residue, (*61*)). Our experimental results and the discussion above would suggest that LPA thus binds to its receptors in a di-anionic form, contrary to a previous suggestion (*62*). Interestingly, recent calculation of the pKa2 of S1P, which like LPA has a phosphomonoester headgroup, in the binding pocket of the S1P1 receptor shows that S1P likely binds in a di-anionic form (A.L. Parrill, personal communication).

Model of the interaction of PA binding proteins with the membrane

The electrostatic and hydrogen bond interaction of PA binding proteins with a di-anionic PA will create some specificity for the interaction, over that with lipids such as PS and PI(Px). Based on studies with polyphosphoinositide bindings domains, reviewed in (*44*), we can conclude that this interaction is not enough for a high affinity interaction. For example, the PI-3P binding domain FYVE, which makes more hydrogen bond interactions with PI-3P than would be possible for a PA binding domain with PA, only has a low affinity (micromolar range), and high affinity (nanomolar range) is achieved by dimerization of the FYVE domain (*47*). The headgroup of the polyphosphoinositides is likely extended away from the glycerol/acylchain interface, and specificity of the PI(Px) binding domains is achieved by a defined binding pocket, that makes numerous hydrogen bond contacts with the phosphates and inositol moiety (*46, 50-53*). In the case of PA the situation is radically different, since its headgroup is located close to the glycerol/acyl-chain interface of the bilayer, which stericly hinders PI(Px) specific domains from binding to PA in a lipid bilayer. Docking of a PA binding domain to PA uniquely positions the domain for hydrophobic interactions with the bilayer, which is further facilitated by the cone shape of PA (chapters 2 and 3). This PA specific hydrophobic interaction likely increases the affinity of the PA binding domains for PA. This is illustrated by the interaction of raf-1 kinase, which binds specifically to PA in membranes. Interestingly, high ionic strength, expected to diminish electrostatic interactions due to screening of charge, does not affect the interaction of raf-1 kinase with PA (*24*), suggesting the presence of additional, hydrophobic, interactions.

We can now also understand the results obtained with CTR1 (see above), which showed that incorporation of PE in the PC bilayer facilitated the interaction of CTR1 with PA. Incorporation of PE in the bilayer reduces the lateral tension in the headgroup region (*15*) and reduces the energy barrier for insertion of hydrophobic protein domains.

Our results lead to the following model for PA/protein interaction. Initially the PA binding domain is guided to the membrane via non-specific electrostatic interactions. Recognition of PA is facilitated by charge/charge and hydrogen bond interactions that both increase the negative charge of PA and lead to a docking of the domain onto a di-anionic PA molecule. This docking is then accompanied or

followed by the insertion of hydrophobic residues in the hydrophobic interior of the lipid bilayer. This sequence of events is schematically shown in Figure 1.

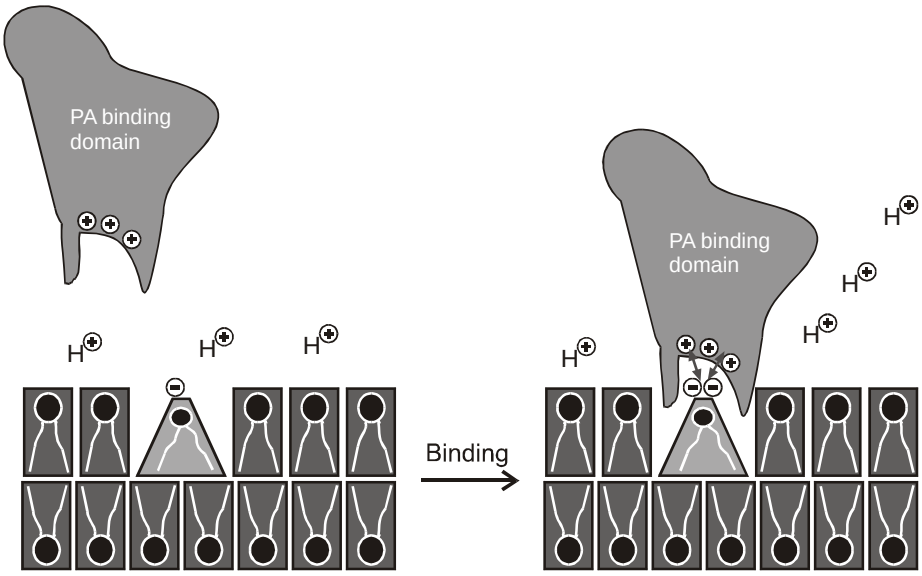

Figure 1: Model for the binding of a PA binding domain to PA. The positively charged PA binding domain is attracted to the negatively charged membrane via non-specific electrostatic interactions (left). Binding of the domain (right) to PA (cone shaped lipid) leads to a di-anionic PA molecule due to the formation of hydrogen bonds and results in docking of the domain onto the membrane. The red arrows schematically indicate the proposed hydrogen bond interactions.

References

1. Chen, Y. G., Siddhanta, A., Austin, C. D., Hammond, S. M., Sung, T. C., Frohman, M. A., Morris, A. J., and Shields, D. (1997) Phospholipase D stimulates release of nascent secretory vesicles from the trans-Golgi network. *J. Cell Biol. 138*, 495-504.
2. Ktistakis, N. T., Brown, H. A., Waters, M. G., Sternweis, P. C., and Roth, M. G. (1996) Evidence that phospholipase D mediates ADP ribosylation factor-dependent formation of Golgi coated vesicles. *J. Cell Biol. 134*, 295-306.
3. Roth, M. G., Bi, K., Ktistakis, N. T., and Yu, S. (1999) Phospholipase D as an effector for ADP-ribosylation factor in the regulation of vesicular traffic. *Chem. Phys. Lipids 98*, 141-52.
4. Schmidt, A., Wolde, M., Thiele, C., Fest, W., Kratzin, H., Podtelejnikov, A. V., Witke, W., Huttner, W. B., and Soling, H. D. (1999) Endophilin I mediates synaptic vesicle formation by transfer of arachidonate to lysophosphatidic acid. *Nature 401*, 133-41.
5. Siddhanta, A., and Shields, D. (1998) Secretory vesicle budding from the trans-Golgi network is mediated by phosphatidic acid levels. *J. Biol. Chem. 273*, 17995-8.
6. Weigert, R., Silletta, M. G., Spano, S., Turacchio, G., Cericola, C., Colanzi, A., Senatore, S., Mancini, R., Polishchuk, E. V., Salmona, M., Facchiano, F., Burger, K. N. J., Mironov, A., Luini, A., and Corda, D. (1999) CtBP/BARS induces fission of Golgi membranes by acylating lysophosphatidic acid. *Nature 402*, 429-33.

7. Zimmerberg, J., and Kozlov, M. M. (2005) How proteins produce cellular membrane curvature. *Nat. Rev. Mol. Cell Biol. 7*, 9-19.
8. Ktistakis, N. T., Delon, C., Manifava, M., Wood, E., Ganley, I., and Sugars, J. M. (2003) Phospholipase D1 and potential targets of its hydrolysis product, phosphatidic acid. *Biochem. Soc. Trans. 31*, 94-7.
9. Testerink, C., Dekker, H. L., Lim, Z. Y., Johns, M. K., Holmes, A. B., Koster, C. G., Ktistakis, N. T., and Munnik, T. (2004) Isolation and identification of phosphatidic acid targets from plants. *Plant J. 39*, 527-36.
10. Testerink, C., and Munnik, T. (2005) Phosphatidic acid: a multifunctional stress signaling lipid in plants. *Trends Plant. Sci. 10*, 368-75.
11. Swairjo, M. A., Seaton, B. A., and Roberts, M. F. (1994) Effect of vesicle composition and curvature on the dissociation of phosphatidic acid in small unilamellar vesicles--a 31P-NMR study. *Biochim. Biophys. Acta 1191*, 354-61.
12. Traikia, M., Warschawski, D. E., Lambert, O., Rigaud, J. L., and Devaux, P. F. (2002) Asymmetrical membranes and surface tension. *Biophys. J. 83*, 1443-54.
13. Lafleur, M., Bloom, M., and Cullis, P. R. (1990) Lipid polymorphism and hydrocarbon order. *Biochem. Cell Biol. 68*, 1-8.
14. Chen, Z., and Rand, R. P. (1997) The influence of cholesterol on phospholipid membrane curvature and bending elasticity. *Biophys. J. 73*, 267-76.
15. van den Brink-van der Laan, E., Killian, J. A., and de Kruijff, B. (2004) Nonbilayer lipids affect peripheral and integral membrane proteins via changes in the lateral pressure profile. *Biochim. Biophys. Acta 1666*, 275-88.
16. Fuller, N., and Rand, R. P. (2001) The influence of lysolipids on the spontaneous curvature and bending elasticity of phospholipid membranes. *Biophys. J. 81*, 243-54.
17. Janes, N. (1996) Curvature stress and polymorphism in membranes. *Chem. Phys. Lipids 81*, 133-150.
18. Madden, T. D., and Cullis, P. R. (1982) Stabilization of bilayer structure for unsaturated phosphatidylethanolamines by detergents. *Biochim. Biophys. Acta 684*, 149-53.
19. Griffiths, D. J. (1989) *Introduction to electrodynamics*, 2nd edition ed., Prentice Hall, New Jersey.
20. Kieber, J. J., Rothenberg, M., Roman, G., Feldmann, K. A., and Ecker, J. R. (1993) CTR1, a negative regulator of the ethylene response pathway in Arabidopsis, encodes a member of the raf family of protein kinases. *Cell 72*, 427-41.
21. Chen, Y. F., Etheridge, N., and Schaller, G. E. (2005) Ethylene signal transduction. *Ann. Bot. (Lond.) 95*, 901-15.
22. Guo, H., and Ecker, J. R. (2004) The ethylene signaling pathway: new insights. *Curr. Opin. Plant Biol. 7*, 40-9.
23. Ghosh, S., Moore, S., Bell, R. M., and Dush, M. (2003) Functional analysis of a phosphatidic acid binding domain in human Raf-1 kinase: mutations in the phosphatidate binding domain lead to tail and trunk abnormalities in developing zebrafish embryos. *J. Biol. Chem. 278*, 45690-6.
24. Ghosh, S., Strum, J. C., Sciorra, V. A., Daniel, L., and Bell, R. M. (1996) Raf-1 kinase possesses distinct binding domains for phosphatidylserine and phosphatidic acid. Phosphatidic acid regulates the translocation of Raf-1 in 12-O-tetradecanoylphorbol-13-acetate-stimulated Madin-Darby canine kidney cells. *J. Biol. Chem. 271*, 8472-80.
25. Rizzo, M. A., Shome, K., Watkins, S. C., and Romero, G. (2000) The recruitment of Raf-1 to membranes is mediated by direct interaction with phosphatidic acid and is independent of association with Ras. *J. Biol. Chem. 275*, 23911-8.
26. Shemesh, T., Luini, A., Malhotra, V., Burger, K. N., and Kozlov, M. M. (2003) Prefission constriction of Golgi tubular carriers driven by local lipid metabolism: a theoretical model. *Biophys. J. 85*, 3813-27.
27. Bonazzi, M., Spano, S., Turacchio, G., Cericola, C., Valente, C., Colanzi, A., Kweon, H. S., Hsu, V. W., Polishchuck, E. V., Polishchuck, R. S., Sallese, M., Pulvirenti, T., Corda, D., and Luini, A. (2005) CtBP3/BARS drives membrane fission in dynamin-independent transport pathways. *Nat. Cell Biol. 7*, 570-80.
28. Hidalgo Carcedo, C., Bonazzi, M., Spano, S., Turacchio, G., Colanzi, A., Luini, A., and Corda, D. (2004) Mitotic Golgi partitioning is driven by the membrane-fissioning protein CtBP3/BARS. *Science 305*, 93-6.

29. Gallop, J. L., Butler, P. J., and McMahon, H. T. (2005) Endophilin and CtBP/BARS are not acyl transferases in endocytosis or Golgi fission. *Nature 438*, 675-8.
30. Pathre, P., Shome, K., Blumental-Perry, A., Bielli, A., Haney, C. J., Alber, S., Watkins, S. C., Romero, G., and Aridor, M. (2003) Activation of phospholipase D by the small GTPase Sar1p is required to support COPII assembly and ER export. *Embo J. 22*, 4059-69.
31. Potocky, M., Elias, M., Profotova, B., Novotna, Z., Valentova, O., and Zarsky, V. (2003) Phosphatidic acid produced by phospholipase D is required for tobacco pollen tube growth. *Planta 217*, 122-30.
32. Monteiro, D., Liu, Q., Lisboa, S., Scherer, G. E., Quader, H., and Malho, R. (2005) Phosphoinositides and phosphatidic acid regulate pollen tube growth and reorientation through modulation of [Ca2+]c and membrane secretion. *J. Exp. Bot. 56*, 1665-74.
33. Zouwail, S., Pettitt, T. R., Dove, S. K., Chibalina, M. V., Powner, D. J., Haynes, L., Wakelam, M. J., and Insall, R. H. (2005) Phospholipase D activity is essential for actin localization and actin-based motility in Dictyostelium. *Biochem. J. 389*, 207-14.
34. Connolly, J. E., and Engebrecht, J. (2006) The Arf-GTPase-Activating Protein Gcs1p Is Essential for Sporulation and Regulates the Phospholipase D Spo14p. *Eukaryot. Cell 5*, 112-24.
35. Nakanishi, H., Morishita, M., Schwartz, C. L., Coluccio, A., Engebrecht, J., and Neiman, A. M. (2006) Phospholipase D and the SNARE Sso1p are necessary for vesicle fusion during sporulation in yeast. *J. Cell Sci. 119*, 1406-15.
36. Burger, K. N. J., Demel, R. A., Schmid, S. L., and de Kruijff, B. (2000) Dynamin is membrane-active: lipid insertion is induced by phosphoinositides and phosphatidic acid. *Biochemistry 39*, 12485-93.
37. McMahon, H. T., and Gallop, J. L. (2005) Membrane curvature and mechanisms of dynamic cell membrane remodelling. *Nature 438*, 590-6.
38. DiNitto, J. P., Cronin, T. C., and Lambright, D. G. (2003) Membrane recognition and targeting by lipid-binding domains. *Sci. STKE 213*, re16.
39. Gillooly, D. J., Morrow, I. C., Lindsay, M., Gould, R., Bryant, N. J., Gaullier, J. M., Parton, R. G., and Stenmark, H. (2000) Localization of phosphatidylinositol 3-phosphate in yeast and mammalian cells. *Embo J.. 19*, 4577-88.
40. Hurley, J. H., and Misra, S. (2000) Signaling and subcellular targeting by membrane-binding domains. *Annu. Rev. Biophys. Biomol. Struct. 29*, 49-79.
41. Mironov, A. A., Beznoussenko, G. V., Luini, A., and Polishchuk, R. S. (2005) Visualizing intracellular events in vivo by combined video fluorescence and 3-D electron microscopy. *Methods Enzymol. 404*, 43-57.
42. Polishchuk, R. S., Polishchuk, E. V., Marra, P., Alberti, S., Buccione, R., Luini, A., and Mironov, A. A. (2000) Correlative light-electron microscopy reveals the tubular-saccular ultrastructure of carriers operating between Golgi apparatus and plasma membrane. *J. Cell Biol. 148*, 45-58.
43. Altelaar, A. F., van Minnen, J., Jimenez, C. R., Heeren, R. M., and Piersma, S. R. (2005) Direct molecular imaging of Lymnaea stagnalis nervous tissue at subcellular spatial resolution by mass spectrometry. *Anal. Chem. 77*, 735-41.
44. Lemmon, M. A. (2003) Phosphoinositide recognition domains. *Traffic 4*, 201-13.
45. Baillie, G. S., Huston, E., Scotland, G., Hodgkin, M., Gall, I., Peden, A. H., MacKenzie, C., Houslay, E. S., Currie, R., Pettitt, T. R., Walmsley, A. R., Wakelam, M. J., Warwicker, J., and Houslay, M. D. (2002) TAPAS-1, a novel microdomain within the unique N-terminal region of the PDE4A1 cAMP-specific phosphodiesterase that allows rapid, Ca2+-triggered membrane association with selectivity for interaction with phosphatidic acid. *J. Biol. Chem. 277*, 28298-309.
46. Bravo, J., Karathanassis, D., Pacold, C. M., Pacold, M. E., Ellson, C. D., Anderson, K. E., Butler, P. J., Lavenir, I., Perisic, O., Hawkins, P. T., Stephens, L., and Williams, R. L. (2001) The crystal structure of the PX domain from p40(phox) bound to phosphatidylinositol 3-phosphate. *Mol. Cell 8*, 829-39.
47. Dumas, J. J., Merithew, E., Sudharshan, E., Rajamani, D., Hayes, S., Lawe, D., Corvera, S., and Lambright, D. G. (2001) Multivalent endosome targeting by homodimeric EEA1. *Mol. Cell 8*, 947-58.
48. Kutateladze, T., and Overduin, M. (2001) Structural mechanism of endosome docking by the FYVE domain. *Science 291*, 1793-6.

49. Lee, S. A., Eyeson, R., Cheever, M. L., Geng, J., Verkhusha, V. V., Burd, C., Overduin, M., and Kutateladze, T. G. (2005) Targeting of the FYVE domain to endosomal membranes is regulated by a histidine switch. *Proc. Natl. Acad. Sci. U S A 102*, 13052-7.
50. Baraldi, E., Carugo, K. D., Hyvonen, M., Surdo, P. L., Riley, A. M., Potter, B. V., O'Brien, R., Ladbury, J. E., and Saraste, M. (1999) Structure of the PH domain from Bruton's tyrosine kinase in complex with inositol 1,3,4,5-tetrakisphosphate. *Structure 7*, 449-60.
51. Ferguson, K. M., Kavran, J. M., Sankaran, V. G., Fournier, E., Isakoff, S. J., Skolnik, E. Y., and Lemmon, M. A. (2000) Structural basis for discrimination of 3-phosphoinositides by pleckstrin homology domains. *Mol. Cell 6*, 373-84.
52. Lietzke, S. E., Bose, S., Cronin, T., Klarlund, J., Chawla, A., Czech, M. P., and Lambright, D. G. (2000) Structural basis of 3-phosphoinositide recognition by pleckstrin homology domains. *Mol. Cell 6*, 385-94.
53. Thomas, C. C., Deak, M., Alessi, D. R., and van Aalten, D. M. (2002) High-resolution structure of the pleckstrin homology domain of protein kinase b/akt bound to phosphatidylinositol (3,4,5)-trisphosphate. *Curr. Biol. 12*, 1256-62.
54. Graham Solomons, J. T., Zimmerly, E. M., Burns, S., Krishnamurthy, N., Swan, M. K., Krings, S., Muirhead, H., Chirgwin, J., and Davies, C. (2004) The crystal structure of mouse phosphoglucose isomerase at 1.6A resolution and its complex with glucose 6-phosphate reveals the catalytic mechanism of sugar ring opening. *J. Mol Biol. 342*, 847-60.
55. Lee, J. H., and Jeffery, C. J. (2005) The crystal structure of rabbit phosphoglucose isomerase complexed with D-sorbitol-6-phosphate, an analog of the open chain form of D-glucose-6-phosphate. *Protein Sci. 14*, 727-34.
56. Lee, D. C., Cottrill, M. A., Forsberg, C. W., and Jia, Z. (2003) Functional insights revealed by the crystal structures of Escherichia coli glucose-1-phosphatase. *J. Biol. Chem. 278*, 31412-8.
57. Oliva, G., Fontes, M. R., Garratt, R. C., Altamirano, M. M., Calcagno, M. L., and Horjales, E. (1995) Structure and catalytic mechanism of glucosamine 6-phosphate deaminase from Escherichia coli at 2.1 A resolution. *Structure 3*, 1323-32.
58. Aleshin, A. E., Zeng, C., Bourenkov, G. P., Bartunik, H. D., Fromm, H. J., and Honzatko, R. B. (1998) The mechanism of regulation of hexokinase: new insights from the crystal structure of recombinant human brain hexokinase complexed with glucose and glucose-6-phosphate. *Structure 6*, 39-50.
59. Jones, J. A., Rawles, R., and Hannun, Y. A. (2005) Identification of a novel phosphatidic acid binding domain in protein phosphatase-1. *Biochemistry 44*, 13235-45.
60. Lynch, K. R., and Macdonald, T. L. (2002) Structure-activity relationships of lysophosphatidic acid analogs. *Biochim. Biophys. Acta 1582*, 289-94.
61. Sardar, V. M., Bautista, D. L., Fischer, D. J., Yokoyama, K., Nusser, N., Virag, T., Wang, D. A., Baker, D. L., Tigyi, G., and Parrill, A. L. (2002) Molecular basis for lysophosphatidic acid receptor antagonist selectivity. *Biochim. Biophys. Acta 1582*, 309-17.
62. Wang, D. A., Lorincz, Z., Bautista, D. L., Liliom, K., Tigyi, G., and Parrill, A. L. (2001) A single amino acid determines lysophospholipid specificity of the S1P1 (EDG1) and LPA1 (EDG2) phospholipid growth factor receptors. *J. Biol. Chem. 276*, 49213-20.

Samenvatting

Biologische membranen

Biologische membranen vormen het vlies dat onze cellen omvat en beschermt tegen de omgeving. Zo houdt de membraan gevaarlijke stoffen van buitenaf tegen maar zorgt het er ook voor dat alle essentiële bestanddelen niet zo maar de cel uit kunnen. De biologische membraan bestaat uit een soort vetmoleculen, ook wel lipiden geheten, en eiwitten, de werkmachines van de cel. De lipiden vormen de basis van de membraan. Ze bevatten een hydrofiele (waterminnende) kopgroep en hydrofobe (waterafstotende) staarten. Door deze samenstelling vormen de lipiden een (platte) dubbellaag met de staarten naar binnen en de kopgroepen naar buiten. Dit is schematisch weergegeven in Figuur 1.

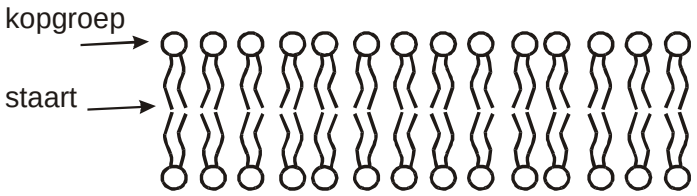

Figuur 1: Schematische weergave van een lipide bilaag.

De eiwitten die onderdeel uitmaken van de membraan zijn op te delen in twee groepen, te weten de transmembraaneiwitten, die door de lipide dubbellaag heen steken, en de periferaaleiwitten, die aan de membraan plakken. De buitenste membraan van onze cellen wordt de plasmamembraan genoemd. Naast dit plasmamembraan bevatten onze cellen, anders dan bij de bacteriën, nog een aantal gespecialiseerde compartimenten die ook met een biologisch membraan omgeven zijn. Deze compartimenten, organellen genaamd, huisvesten specifieke functies zoals eiwit en lipid synthese en sortering (endoplasmatisch recticulum, ER), eiwit afbraak (lysosomen), of DNA (de kern), wat codeert voor het grootste deel van de eiwitten die in de cel gesynthetiseerd worden. Deze organellen staan niet los van elkaar maar zijn in constant contact, bijvoorbeeld door het uitwisselen van kleine, met een membraan omgeven, (ronde) bolletjes. Op elk gegeven moment worden er van deze bolletjes gevormd in de cel en fuseren weer anderen met een membraan van bestemming. Het proces waarbij deze bolletjes worden gevormd, afsnoering genaamd, vormt de grondslag van het onderzoek zoals omschreven in dit proefschrift. Om de uiteindelijke resultaten beter te kunnen begrijpen, volgt hieronder eerst nog meer algemene informatie over lipiden in het algemeen en dit proces van afsnoering en wordt uitgelegd waarom dit zo interessant is.

Tijdens membraan afsnoering wordt afgeweken van de platte dubbellaag

Het proces van membraan afsnoering en membraan fusie zijn schematisch weergegeven in Figuur 2. Voorafgaand aan het afsnoeringsproces vervormt de platte bilaag en vormt er zich een blaasje. Dit blaasje, het uiteindelijke transportbolletje, wordt dieper en de nek vernauwt zich. Op een gegeven moment komt de binnenste lipidelaag van de sterk gebogen lipide bilaag die de nek vormt, zo dicht bij elkaar dat de kopgroepen elkaar beginnen aan te raken. Het aanraken van deze waterminnende kopgroepen is energetisch erg ongunstig en zo'n situatie kan niet lang bestaan. In plaats daarvan zal deze lipidelaag rondom de nek met zichzelf fuseren. Op dat moment is er natuurlijk geen sprake meer van een platte bilaag maar wordt er een andere structuur gevormd. Vanuit deze structuur, ook wel de afsnoeringsintermediair genoemd, zal het uiteindelijke proces van afsnoering, het loskomen van het transportbolletje, plaatsvinden. Het verrassende van dit proces is het feit dat de eiwitten (voor zover bekend) die betrokken zijn bij het afsnoeringsproces werken aan de andere kant van de membraan dan waar de lipidelaag (van de nek) met elkaar in contact komt. Voor membraanfusie, het proces waarbij een transportbolletje fuseert met een membraan van bestemming, is dit juist andersom. Bij fusie werken de betrokken eiwitten aan de kant waar de membranen van het transportbolletje en bestemmingsmembraan het eerst met elkaar in contact komen. Van membraanfusie was bij het begin van mijn promotie onderzoek al vrij veel bekend, maar membraanafsnoering was minder onderzocht. Ook was er wel aandacht voor de eiwitten die betrokken zijn bij membraanafsnoering, maar was er minder aandacht voor de lipiden. Wel waren er aanwijzingen dat specifieke lipiden betrokken zijn bij dit proces. Ook is het natuurlijk de lipide bilaag die het afsnoeringsproces ondergaat. Vandaar dat ik mij in mijn promotieonderzoek vooral heb gericht op de rol van de lipiden in de afsnoeringsprocessen. Mijn onderzoek heeft zich specifiek toegespitst op twee lipiden, te weten fosfatide zuur en lysofosfatide zuur. Voor ik nu verder in ga op de wetenschappelijke vraagstelling(en) zal ik nog iets vertellen over de vorm van membraan lipiden.

Niet bilaag lipiden bevorderen of verhinderen membraan dynamiek

Membraan lipiden die uit zichzelf een bilaag vormen als ze 'opgelost' worden in water, hebben een cylindrische vorm. Hun kopgroep is in doorsnede namelijk ongeveer even groot als de doorsnede van de staart(en). Dit is schematisch weergegeven in Figuur 1 en Figuur 3. Nu bestaan de meeste biologische membranen uit een mengsel van verschillende lipiden. Het interessante hiervan is onder andere dat niet al deze lipiden een cylindrische vorm hebben. Zo zijn er lipiden die als je ze isoleert en oplost in water andere structuren vormen dan bilagen, bijvoorbeeld micellen en de zogenaamde hexagonale H_{II} fase, zie Figuur 3. De kopgroep doorsnede van lipiden die micellen vormen in water is 'veel' groter

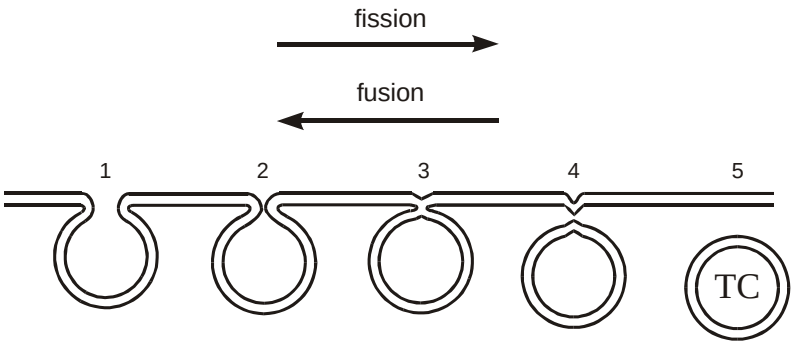

Figuur 2: Vorming en afsnoering van een transportbolletje en de fusie van een transportbolletje volgen een vergelijkbaar traject van membraan buiging. Tijdens afsnoering wordt er een blaasje gevormd op een donor membraan (1), dit wordt gevolgd door een vernauwing van de nek (2), deze vernauwing kan leiden tot de fusie van de binnenste lipid monolaag en het vormen van een afsnoeringsintermediair. (3). De uiteindelijke afsnoering is te zien in (4), hetgeen leidt tot het loskomen van het transportbolletje. Voor membraan fusie verloopt dit proces ongeveer in tegengestelde richting.

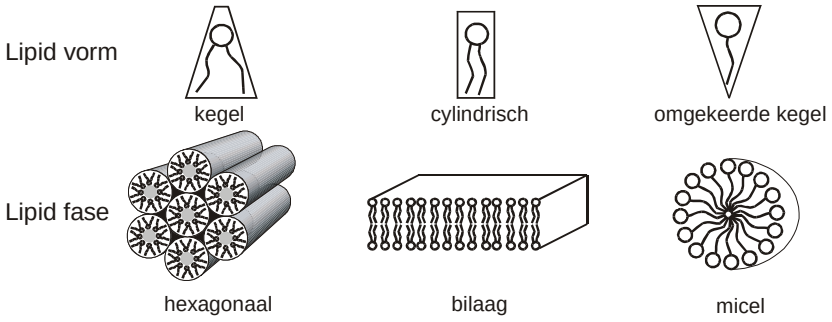

Figuur 3: Lipid vorm dicteert de organisatie vorm (fase) van lipiden in water. Lipiden met een kegel vorm, zoals het lipid fosfatidylethanolamine, vormen structuren als de afgebeelde hexagonale H_{II} fase (lipid buizen die hexagonaal gepakt zijn). Lipiden met een cylindrische vorm, zoals het lipid fosfatidylcholine, vormen bilagen, en lipiden met een omgekeerde kegel vorm zoals de lyso-lipiden (met één staart) vormen micellen.

dan de doorsnede van de staart(en), en worden wel type-I lipiden genoemd. Deze groep lipiden komt in biologische membranen echter niet zo veel voor. Daar tegen over staan de lipiden die een hexagonale fase vormen. Zij bezitten een 'veel' kleinere kopgroep doorsnede dan staart doorsnede en worden wel type-II lipiden genoemd. Zij kunnen wel relatief veel voorkomen in biologische membranen.

Tijdens membraan afsnoering en membraan fusie wordt lokaal afgeweken van de bilaag structuur. Lipiden met een cylindrische vorm "passen" niet zo goed bij deze structuren en je zou dan ook wellicht verwachten dat type-I en type-II lipiden deze processen ofwel bevorderen dan wel tegenwerken. Recent theoretisch en praktisch werk blijkt deze hypothese te bevestigen. Zo blijken type-II lipiden membraanfusie te bevorderen en type-I lipiden werken dit proces juist tegen. Voor membraanafsnoering is dit waarschijnlijk juist andersom.

Wetenschappelijke vraag

Van fosfatide zuur (Phosphatidic Acid, dus afgekort als PA) was bekend dat het betrokken is bij membraandynamiek, het vormen en/of fuseren van transportbolletjes. Wat de preciese rol van PA in deze processen is, was nog niet bekend. Twee mogelijkheden zijn aannemelijk, een directe en indirecte rol. Zo kan PA, via zijn moleculaire vorm, direct de pakking van lipiden in het membraan en dus de membraanvorm beïnvloeden. Een andere mogelijkheid is dat PA indirect membraandynamiek bevordert door specifieke eiwitten te binden die het uiteindelijke werk doen.

Een directe rol voor PA was een aantrekkelijke hypothese, omdat van PA werd aangenomen dat het een type-II lipid is. Verder waren er twee studies die lieten zien, voor twee ongerelateerde eiwitten in verschillende membraanafsnoeringsprocessen, dat de vorming van PA vanuit lysofosfatide zuur (LysoPhosphatidic Acid, dus LPA) betrokken was bij de vorming van transportbolletjes. In de conversie van LPA naar PA wordt er een hydrofobe staart aan LPA toegevoegd (zie Figuur 4 voor de chemische structuur van LPA en PA). LPA heeft er één en PA, zoals de meeste membraan lipiden, heeft er twee. Er werd verondersteld dat dit de vorm van het lipid (van LPA, type-I naar PA, type-II) in zo'n mate verandert dat dit het vormen van een transportbolletje zou bevorderen. De moleculaire vorm van PA en LPA was echter nog nooit onderzocht onder relevante fysiologische omstandigheden, dus die condities die ook in een cel voorkomen, neutrale pH en een specifieke zoutconcentratie.

PA (en LPA) is een zuur en kan dus een negatieve lading dragen. Via deze negatieve lading is het mogelijk dat PA positief geladen eiwitten kan binden. Als eiwitten aan lipiden binden, dan beïnvloedt dit vaak de functie van deze eiwitten. Zo kan het gebonden eiwit actief of juist inactief worden. Van bepaalde eiwitten betrokken bij membraandynamiek (membraanfusie) was bekend dat zij aan PA kunnen binden.

Om meer inzicht te krijgen in de rol van PA en LPA in membraandynamiek in het bijzonder, hebben wij ons gericht op het bepalen van de moleculaire vorm, zoals beschreven in hoofdstuk 2 en 3 van dit proefschrift, en de lading en ladingsinteracties, zoals omschreven in hoofdstuk 4 en 5, van deze twee lipiden. Zowel de experimentele technieken die ik gebruikt heb als de belangrijkste resultaten zal ik hieronder in meer detail bespreken.

PA en LPA hebben een bijzondere vorm

De moleculaire vorm van een lipid kan niet eenvoudig worden bepaald door er bijvoorbeeld een foto van te maken. Zelfs de allerbeste microscoop, een electronen microscoop, is niet in staat om een enkel lipid te 'fotograferen'. Toch is het wel degelijk mogelijk om op andere manieren inzicht te krijgen in de moleculaire vorm van een lipid. Zo geeft de organisatievorm van het geïsoleerde lipid opgelost in

water al veel informatie. Je kan zo onderscheid maken tussen type-I, bilaag (cylindrisch), en type-II lipiden. Echter, het gedrag (vorm) van een lipid in een lipide bilaag kan anders zijn dan als het geïsoleerd wordt opgelost in water. Om meer inzicht te krijgen in de vorm van het lipid is het interessant om de vorm te bepalen in meer complexe systemen, bilagen bestaande uit twee verschillende soort lipiden (zie hoofdstuk 2).

De organisatie van lipiden met een kopgroep die een fosfaat (een fosfor atoom) bevat, zoals PA en LPA, kan goed bepaald worden met een techniek die kern spin resonantie (Nuclear Magnetic Resonance, NMR) heet. Bij NMR wordt aan de kern van een bepaald atoom een beetje energie gegeven. Deze energie raakt de kern op een gegeven moment weer kwijt. De manier waarop dit gebeurt is karakteristek voor een bepaald atoom en kun je meten met NMR. Een voorbeeld van een 'alledaagse' medische diagnose techniek waar kern spin resonantie ook toegepast wordt, is een MRI (Magnetic Resonance Imaging) scan. Het is belangrijk om te onthouden dat het atoom fosfor gevoelig is voor kern spin resonantie en dat het daardoor mogelijk is om de organisatiestructuur van lipiden met een fosforatoom in de kopgroep te bepalen. Deze techniek wordt dan ^{31}P NMR genoemd

Naast ^{31}P NMR, kan de organisatie vorm van lipiden ook met röntgendiffractie worden bepaald. Anders dan bij de röntgen foto's in het ziekenhuis, kan met deze techniek heel nauwkeurig niet alleen de organisatievorm, maar ook de afmetingen van een bilaag (bilaagdikte) en hexagonale structuur (hexagonale pakkingsafstand) worden bepaald. Dit geeft dus ook kwantitatieve informatie over de vorm van lipiden. Op basis van deze kwantitatieve informatie kun je de spontane curvatuur van een lipid uitrekenen. De spontane curvatuur drukt de vorm van een lipid dus uit in een numeriek getal, dat kan worden gebruikt in bijvoorbeeld wiskundige modellen. In feite is de spontane curvatuur de kromming van een lipidelaag die een lipid het liefst zou willen vormen, als het niet wordt gehinderd door belemmeringen zoals de aanwezigheid van andere lipiden met een afwijkende vorm.

Met ^{31}P-NMR en röntgendiffractie hebben wij de vorm van zowel PA als LPA opgehelderd, onder fysiologisch relevante condities. PA bleek inderdaad een type-II lipid te zien. Verrassend was echter dat de vorm van PA erg gevoelig bleek voor de gebruikte condities. Bij lage pH, dus in een zuur milieu, is de vorm van PA meer type-II dan bij neutrale pH, i.e. PA heeft in een zuur milieu een kleinere kopgroep. Negatieve lading zorgt ervoor dat de effectieve kopgroep groter is omdat negatief geladen kopgroepen elkaar afstoten en daardoor meer ruimte in beslag nemen. Onder zure condities heeft PA echter minder negatieve lading dan onder neutrale condities. Dit verklaarde dus de pH-gevoeligheid van de vorm van PA. Verder was de vorm van PA gevoelig voor de aanwezigheid van zout. Tezamen betekenen deze resultaten dat de vorm van PA zal afhangen van de plek in de cel waar het zich bevind, omdat vooral de pH niet hetzelfde is voor de verschillende organellen in een cel. LPA is een type-I lipid met de meest positieve spontane curvatuur ooit gemeten voor een membraan lipid. Ook lijkt het er op dat de vorm van LPA minder gevoelig is voor zout. Met deze resultaten is het nu

mogelijk om wiskundige modellen die het afsnoerings en/of fusieproces beschrijven waarin PA een rol speelt, te evalueren.

De negatieve lading van PA en LPA word beïnvloed door een interne waterstofbrug

De lading van een lipid is, in navolging van de vorm, niet eenvoudig te meten. Zeker voor PA en LPA, die in natuurlijke bilagen maar heel weinig voorkomen, is dit verre van triviaal. Met de opkomst van een bijzondere NMR techniek, te weten magic angle spinning, of te wel magische hoek rotatie, bleek dit echter wel mogelijk. Op deze manier zijn wij er voor het eerst in geslaagd om de negatieve lading van een lage concentratie (L)PA in een platte bilaag te meten.

Uit deze ladingsbepalingen bleek heel verassend dat LPA meer lading draagt dan PA in een platte bilaag van PC (fosfatidylcholine, een veel voorkomend membraanlipid), beide gemeten onder exact dezelfde experimentele condities. Dit is te meer verrassend door het feit dat PA en LPA exact dezelfde kopgroep hebben, namelijk een fosfomonoester (een op een bepaalde manier gebonden fosfaat). Verder werd de lading van zowel PA als LPA bevorderd door het lipid PE (fosfatidylethanolamine, ook een veel voorkomend membraanlipid). Deze resultaten bleken heel goed met elkaar te rijmen. Het blijkt namelijk dat de fosfomonoester kopgroep van PA en LPA een interne waterstofbrug, dat is een verbinding via een waterstofatoom, kan vormen, zie Figuur 4. Deze waterstofbrug reguleert de lading van (L)PA. De vorming van deze waterstofbrug zorgt ervoor dat de lading van de fosfomonoester lager is dan je zou verwachten als deze verbinding er niet zou zijn.

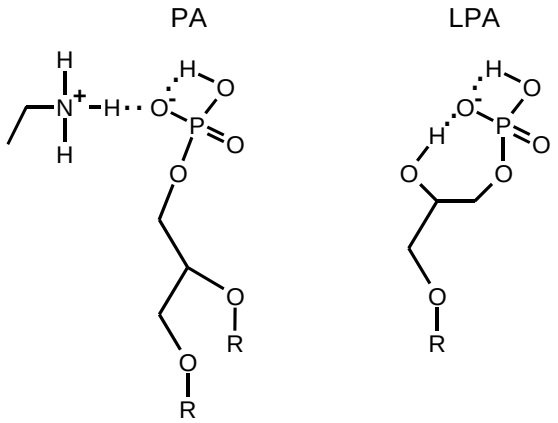

Figuur 4: Schematische cartoon van de chemische structuur van PA en LPA. De intramoleculaire waterstofbrug in de fosfaat kopgroep van PA en LPA is aangegeven met twee stippen. De additionele intramoleculaire waterstofbrug van LPA is ook aangegeven met twee stippen. De extra chemische groep (primair amine) links van PA stelt een gedeelte van de kopgroep van PE voor. De intermoleculaire waterstofbrug tussen PA en PE is ook aangegeven met twee stippen. R staat voor een hydrofobe (vetzuur) staart.

Het verschil tussen PA en LPA berust in het feit dat LPA een hydrofobe staart mist en in plaats daarvan een extra waterstof atoom (in een OH groep) vrij heeft in het stukje van het lipid die kop en staart(en) van elkaar scheidt. Dit waterstof atoom kan een waterstofbrug vormen met de kopgroep die kan competeren met de waterstofbrug die in de kopgroep zelf gevormd wordt, en verhoogt zo de lading van LPA ten opzichte van PA (zie Figuur 4). Deze interne waterstofbrug verklaart ook de resultaten met PE, aangezien de kopgroep van PE, anders dan die van PC, ook een waterstofbrug kan vormen met (L)PA, net zoals de extra waterstof van LPA zelf (zie Figuur 4). Deze intermoleculaire waterstofbrug competeert dus met de waterstofbrug in de fosfomonoester kopgroep van (L)PA en verhoogt zo de lading.

Deze bijzondere waterstofbrug en zijn effect op de lading van PA en LPA is uniek en is volgens ons nog nooit eerder beschreven. De vinding dat de lading van PA beïnvloed wordt door deze waterstofbrug heeft nog een aantal interessante biologische consequenties. Zo is bijvoorbeeld de verhouding tussen de hoeveelheid PC en PE niet gelijk voor de verschillende organellen in een cel. Deze verhouding verschilt ook voor de twee helften van sommige biologische membranen, zoals het plasmamembraan. Het feit dat deze verhouding dus verschilt tussen de onderlinge organellen of in eenzelfde organel betekend dat de lading van PA (en LPA) zal afhangen van de plek in de cel waar het zich bevindt. Ook is het mogelijk dat tijdens de omzetting van LPA naar PA de lading van de membraan verandert, aangezien de lading van LPA en PA niet hetzelfde hoeft te zijn.

Waterstofbruggen vormen de basis van de interactie tussen PA en eiwitten

De vinding van de intramoleculaire waterstofbrug in de kopgroep van PA en de intermoleculaire waterstof brug tussen PA en PE bracht ons ertoe om het effect van twee aminozuren (de bouwstenen van eiwitten) op de lading van PA te onderzoeken. De chemische groep in PE die de waterstofbrug doneert komt namelijk ook in aminozuren voor, een primaire amine (zie Figuur 4 en 5). Het aminozuur lysine heeft namelijk zo'n zijketen. Arginine, een vergelijkbaar aminozuur, kan net als lysine een waterstofbrug doneren, en daarnaast zijn zowel lysine als arginine positief geladen. Van de interactie tussen PA en eiwitten is bekend dat positieve ladingen in deze eiwitten een belangrijke rol spelen. Met magic angle spinning ^{31}P NMR hebben wij daarom het effect van lysines en arginines in peptides (een korte serie aminozuren) die met de membraan een interactie aangaan op de lading van PA onderzocht.

Uit deze experimenten kwam naar voren dat lysine en arginine inderdaad de lading van PA verhogen. Uit controle experimenten bleek verder dat het grootste gedeelte van dit effect veroorzaakt wordt door de vorming van waterstofbruggen tussen de lysine en/of arginine zijketens en de kopgroep van PA, zie Figuur 5 A voor het model. Het vormen van deze waterstofbruggen impliceert een

daadwerkelijk contact, via het waterstof atoom dat gedeeld wordt in een waterstofbrug, tussen het eiwit en PA en niet simpelweg een aantrekking tussen positieve (van het eiwit) en negatieve (van PA) ladingen. Verder zorgt het vormen van waterstofbruggen tussen eiwit en PA ervoor dat PA twee negatieve ladingen draagt (Figuur 3 en 5A).

Ons voorlopige model voor de interactie tussen PA en een PA bindend eiwit is te zien in Figuur 5B. Het PA bindende eiwit heeft eerst een electrostatische (via positieve ladingen) interactie met PA, als beide dicht genoeg bij elkaar in de buurt komen worden er waterstofbruggen gevormd waardoor PA twee negatieve ladingen draagt als het gebonden is aan het eiwit. De bijzondere vorm van PA zorgt er verder voor dat het eiwit kan inserteren in de membraan en dus steviger verankert word aan de membraan. Wij stellen voor dat kegelvorm van PA (zie Figuur 3) en de locatie van de fosfaat van PA diep in de kopgroep regio van de bilaag, gekoppeld aan de unieke waterstofbrug interactie, PA maakt tot het meest ideale lipid voor de insertie van positief geladen delen van membraan eiwitten.

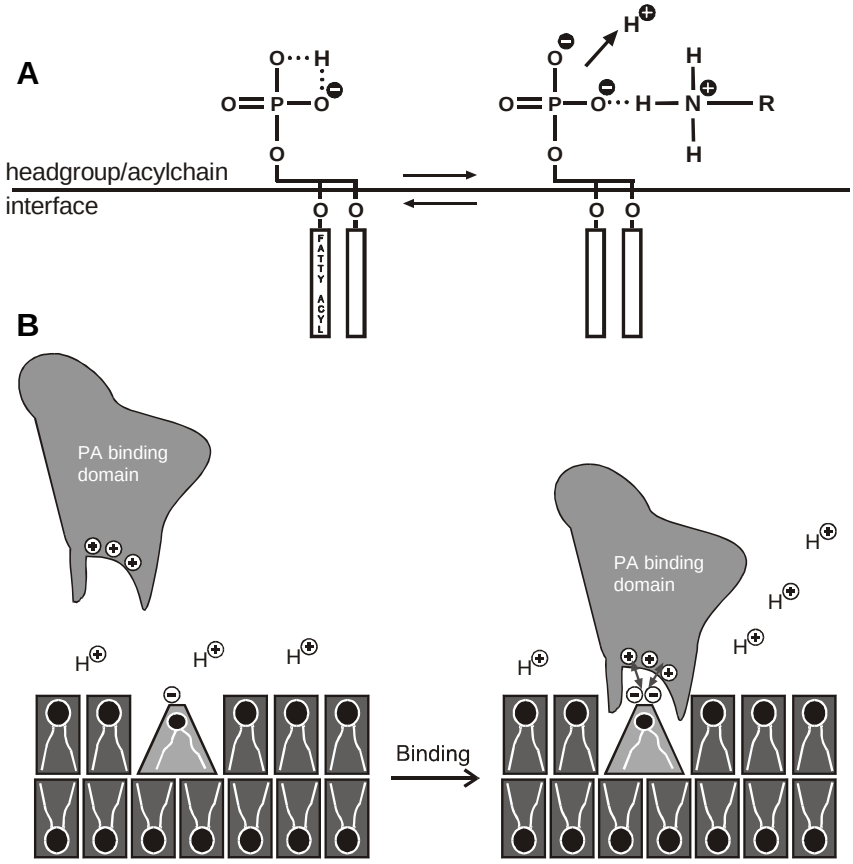

Figuur 5: Model voor PA-eiwit interactie. (A) Model voor de waterstofbrug interactie tussen aminozuren (hier de lysine zijketen) en de fosfaat van PA. (B) Model voor de interactie tussen PA en eiwitten.

Dankwoord

Menig aio zal bij het schrijven van zijn dankwoord zitten met de vraag, waar moet ik beginnen? Voor mij is het natuurlijk niet anders. Velen hebben op een of andere manier bijgedragen aan of wel het werk zoals omschreven in dit proefschrift als wel het creëren van een plezierige werk/leef sfeer. Het is ook onmogelijk om op twee kantjes iedereen bij naam te noemen en ik bied dan ook mijn verontschuldiging aan voor die gene die niet bij naam worden genoemd.

Ik zou eigenlijk willen beginnen met het bedanken van twee personen die niet direct hebben bijgedragen tot dit proefschrift maar die wel zeer belangrijk zijn geweest in mijn vorming als wetenschapper. Makis and Elizabeth thanks for believing in me and offering me the opportunity to work with you during my Masters studies.

Dan ben ik nu, via een kleine omweg, aangekomen bij de personen die het meest hebben bijgedragen aan de totstandkoming van dit proefschrift, te weten mijn promotor en co-promotor. Ben en Koert, bedankt voor jullie steun en toewijding. Koert de vele gesprekken over wetenschap en andere zaken deden mij altijd erg veel goed, ik zal ze missen. Vooral als ik weer eens mijn ei kwijt moest, leende jij altijd een luisterend oor. In het schrijven van wetenschappelijke artikelen bleek eerst jij en later ook Ben een bijzonder getalenteerde mentor. Ik heb veel geleerd over niet alleen het uitvoeren van wetenschappelijk onderzoek, maar net zo belangrijk hoe dit schriftelijk te rapporteren. Ben, jou moet ik ook bedanken voor je doorzettingsvermogen en enthousiasme voor mijn persoon en onderzoek. De werkbesprekingen liepen in het begin niet altijd op rolletjes omdat ik het meer dan eens over details wilde hebben. Jij wist de gesprekken dan altijd weer op het goede spoor te brengen. Ben en Koert, zonder jullie zou dit onderzoek nooit zo succesvol zijn geweest. Thanks!

Naast mijn promotor en co-promotor zijn er nog vele anderen geweest die mij op een of andere manier hebben geholpen bij mijn onderzoek en mijn ontwikkeling tot zelfstandig onderzoeker. Antoinette, bedankt voor de vele adviezen, experimenteel en theoretisch, die je mij de afgelopen 5 jaar hebt gegeven. De uitnodiging om in Segovia een praatje te geven, na nog geen jaar met mijn onderzoek te zijn bezig geweest, heb ik altijd erg gewaardeerd. Vladimir, bedankt voor alle hulp met de NMR. Vooral het opzetten van de MAS-NMR experimenten bleek een gulden zet. Eefjan, Mandy, Martijn en Rutger, zonder jullie praktische adviezen was ik waarschijnlijk nog steeds lipid aan het zuiveren geweest. Gonneke en Hans, bedankt voor de hulp met de elektronenmicroscoop. Helaas is het met de lipid nanotubes niks geworden, al leverde het zeker mooie plaatjes op. Frits, bedankt voor de plezierige samenwerking, jammer dat al het BARS werk niet een artikel opleverde. Maar ja wie had nou kunnen vermoeden dat de LPAAT activiteit

een artefact zou blijken te zijn. Peter and Nola, thanks for giving me the opportunity to work in your lab to measure the spontaneous curvature of PA and LPA. Jon, it was a pleasure to be your supervisor while you were an Erasmus student here in the Netherlands. Emma, bedankt voor het vele werk dat je hebt gedaan terwijl ik druk aan het schrijven was. Het leverde een mooie dataset op, en voor jouw een eerste artikel. Dave and Mischa, thanks for the numerous discussions during and after the biophysical society meeting of 2004. Dave I particularly enjoyed our dinner and discussion at the Turkish restaurant Pamukkale in Utrecht.

Naast PI's, postdocs, analisten en studenten wil ik ook mijn vele collega-aio's bedanken voor de plezierige werksfeer zowel in het lab als op de werkkamers. Eerst op Noord: Ellen en Ingrid. Later op Zuid: Bianca, Hester, Henry, Jacob, Vincent, Nick en Andrea. Suat, bedankt voor het onderhouden van de computer bij de NMR spectrometer nadat Vladimir vertrok. Zonder eerst jouw en later Thomas' inspanningen zou het met mijn laatste experimenten nooit wat zijn geworden. Els, bedankt voor de fijne gesprekken en hulp bij het schrijven van populair wetenschappelijke teksten. Leuk dat je mijn paranimf wilde zijn.

Beste Pa, Ma, broers en zussen (en aanverwanten natuurlijk), jullie zullen je wel meer dan eens hebben afgevraagd waar die zoon/broer van jullie nu allemaal mee bezig was (en is). Ik hoop dat de Nederlandse samenvatting, die ik toch vooral voor jullie heb geschreven, hier enig licht op zal werpen. Pa en Ma, bedankt voor alles dat jullie mij hebben (mee)gegeven en bijzonder bedankt voor jullie hulp in het begin toen we weer net in Nederland woonden en later als er weer eens op Arijana en later ook op Aron gepast moest worden. Edith, ook jou moet ik bijzonder bedanken voor de vele keren die je hebt willen oppassen en natuurlijk bedankt voor het feit dat ook jij mijn paranimf wilde zijn.

Lieve Dena, de afgelopen jaren zijn niet altijd een pretje geweest als ik bijvoorbeeld weer eens in het weekend of de late avonduren naar de Universiteit moest. Jij stond er dan alleen voor thuis. Bedankt voor je steun, liefde en genegenheid. Ik vond (en vind) het bijzonder fijn dat jij zo goed voor Arijana en Aron hebt gezorgd terwijl ik druk in het lab aan de slag was. Kinderen ter wereld brengen terwijl je man altijd half of geheel in het lab stond moet niet makkelijk zijn geweest, maar je deed het mooi wel, en hoe!

Lieve Arijana en Aron, papa vond het fijn dat hij jullie meer dan eens, gezellig op de fiets, mee kon nemen naar de Universiteit. Daar mochten jullie dan met de pipetpuntjes spelen, de vissen eten geven, en/of een mooie tekening maken die niet zelden op de muur van papa's kantoor belandde. Bedankt voor jullie onbevangenheid en liefde tussen alle kattenkwaad door. Zonder jullie en mama's liefde had papa het nooit klaar gespeeld, bedankt. Dit proefschrift draag ik dan ook graag aan jullie drie op!

Dan als laatste moet ik U bedanken God, voor alle kracht en moed die U mij de afgelopen jaren en daarvoor heeft gegeven. Bedankt dat u mij nooit heeft laten gaan en altijd weer tot U roept als ik weer eens van Uw pad afdwaal.

List of publications

1. Edgar E. Kooijman, Peter Tieleman, Dirk T. Rijkers, Rob Liskamp, Koert N. J. Burger and Ben de Kruijff, An electrostatic/hydrogen bond switch as basis for the specific interaction of phosphatidic acid with proteins, to be submitted.
2. Edgar E. Kooijman, Karen M. Carter, Emma G. van Laar, Vladimir Chupin, Koert N.J. Burger and Ben de Kruijff, (2005) What makes the bioactive lipids phosphatidic acid and lysophosphatidic acid so special? *Biochemistry 44*, 17007-17015.
3. Edgar E. Kooijman, Vladimir Chupin, Nola L. Fuller, Michael M. Kozlov, Ben de Kruijff, Koert N. J. Burger and Peter R. Rand (2005) Spontaneous curvature of phosphatidic acid and lysophosphatidic acid. *Biochemistry 44*, 2097-2102.
4. Lu Zou, Ji Wang, Violeta J. Beleva, Edgar E. Kooijman, Svetlana V. Primak, Jens, Risse, Wolfgang Weissflog, Antal Jakli, and Elizabeth K. Mann (2004) Langmuir monolayers of bent-core molecules. *Langmuir 20*, 2772-2780.
5. Aniol, KA, Armstrong DS, Averett T, *et al.*, (2004) Parity-violating electroweak asymmetry in (e)over-right-arrowp scattering. *Physical Review C* 69, 065501_1-35.
6. Edgar E. Kooijman, Vladimir Chupin, Ben de Kruijff and Koert N. J. Burger (2003) Modulation of membrane curvature by phosphatidic acid and lysophosphatidic acid. *Traffic* 4, 162-174.
7. Schulte, EC, Afanasev A, Amarian M, *et al.* (2002) High energy angular distribution measurements of the exclusive deuteron photodisintegration reaction. *Physical Review C* 66, 042201_1-5.
8. Wijesooriya K, Afanasev A, Amarian M, *et al.* (2002) Polarization measurements in neural pion photoproduction. *Physical Review C 66*, 034614_1-14.
9. Gayou O, Wijesooriya K, Afanasev A, *et al.* (2001) Measurements of the elastic electromagnetic form factor ratio mu(p)G(Ep)/G(Mp) via polarization transfer. *Physical Review C 64*, 038202_1-4.
10. Aniol KA, Armstrong DS, Averett T, *et al.* (2001) New measurement of parity violation in elastic electron-proton scattering and implications for strange form factors. *Physics Letters B* 509, 211-216.
11. Wijesooriya K, Afanasev A, Amarian M, et al. (2001) Polarization measurements in high-energy deuteron photodisintegration. *Physical Review Letters 86*, 2975-2979.

Curriculum vitae

Edgar Eduard Kooijman werd geboren op 19 januari 1974 te Nieuwegein. Na het behalen van zijn MAVO diploma in 1990 bracht hij een jaar door in de Verenigde Staten als uitwisselingsstudent in de staten Pennsylvania en Ohio. Bij terugkeer in Nederland begon hij in augustus 1991 met een studie procestechniek aan het Dudok college te Hilversum. Na het afronden van het theoretische gedeelte van deze studie zette hij zijn studie voort aan de rooms katholieke technische hogeschool te Rijswijk in de richting toegepaste natuurkunde. Na het cum laude behalen van de ingenieurstitel in 1998 maakte hij voor de tweede keer de sprong naar de VS, om daar te beginnen aan een studie natuurkunde aan de Kent State University, te Kent, Ohio. Onder begeleiding van Prof. Dr. Elizabeth Mann leide deze studie in 2001 tot een Masterstitel in de natuurkunde. In datzelfde jaar vertrok hij weer naar zijn geboortegrond om te beginnen met zijn promotieonderzoek bij de sectie Biochemie van Membranen, Universiteit Utrecht. Het onderzoek, zoals beschreven in dit proefschrift, werd uitgevoerd onder begeleiding van Prof. Dr. B. de Kruijff en Dr. K.N.J.Burger.